UNIVERSITÀ DEGLI STUDI DI ROMA "TOR VERGATA"

FACOLTA' DI INGEGNERIA

DOTTORATO DI RICERCA IN INGEGNERIA AMBIENTALE

XXI CICLO

Accelerated carbonation of minerals and industrial residues for carbon dioxide storage

Dott. Ing. Giulia Costa

A.A. 2008/2009

Tutor: Prof. Renato Baciocchi

Co-Tutor: Prof. Marco Mazzotti, ETH Zürich

Coordinatore: Prof. Renato Gavasci

Abstract

Carbonation of specific types of minerals and anthropogenically derived products, such as cement or lime binders, is a well known naturally occurring process which exerts several significant effects on alkaline materials, including specifically: CO_2 uptake by formation of a solid and thermodynamically stable carbonate phase, pH decrease and modifications of the leaching behaviour of the material, besides variations of some of its physical and mechanical properties. Since the kinetics of this reaction is very slow at ambient conditions, to exploit some of the above mentioned effects of chemical weathering for developing specific engineered processes, such as waste chemical stabilization and CO_2 mineral storage, carbonation processes carried out under selected and controlled operational conditions have been developed, in order to significantly increase the kinetics of the reactions involved. Depending on the application of the process and the selected material, different operating conditions have been employed and several process routes have been tested.

The main objective of this doctoral thesis was to investigate the accelerated carbonation process applied both to minerals and industrial residues in order to gain new insight on the key reaction mechanisms for each type of material.

Regarding accelerated carbonation of minerals, the effects of the presence of high pressure CO_2 (up to 100 bar) and salinity on olivine dissolution kinetics at 120 °C in a stirred flow-through reactor were specifically investigated, in order to assess whether these parameters may exert an enhancing or inhibiting effect on the kinetics of Mg dissolution.

Batch carbonation experiments on humidified material (with liquid to solid ratios < 1 l/kg) at mild operating conditions (temperature of 30-50 °C and CO_2 pressure of 1-10 bar) were specifically carried out on waste incineration residues such as bottom ash (BA) and air pollution control (APC) residues, as well as on stainless steel slag. The objectives of this study were essentially threefold: to assess the CO_2 storage capacity achievable for each type of industrial residue correlating it to the particle size and to the chemical composition of the samples; to study the influence of the main operational parameters (temperature, pressure and liquid to solid ratio) on reaction kinetics; and finally to investigate the effects of carbonation on the mineralogy and leaching behaviour of the residues.

The study on olivine dissolution kinetics showed that, under all the examined operating conditions (pH range 3-8), the only factor governing the specific dissolution rate was the

pH of the solution. Hence CO_2 pressure and salinity appeared to influence olivine dissolution kinetics only indirectly, by affecting the final pH of the solution. This is a significant finding, since it implies that carbonate precipitation, which occurs in presence of high pressure CO_2 at pH values above 6, and olivine dissolution could theoretically be carried out in the same reactor without inhibition effects on Mg dissolution kinetics.

As for the effects of accelerated carbonation on the leaching behaviour of the studied alkaline residues, significant results were obtained in particular for the BA and APC residues; for both types of materials, accelerated carbonation showed to exert a strong immobilization effect on Pb, Zn and Cu, which were among the critical elements in terms of heavy metal leaching for both types of untreated residues. For APC ash, chemical speciation modelling indicated a change in the solubility-controlling minerals from the untreated to the carbonated ash. For the latter, metal release was found to be clearly controlled by a number of carbonate minerals, indicating the potential of the carbonation process to convert the initial metal-containing minerals into generally less soluble carbonate forms, with positive implications on the environmental behaviour of the ash.

Significant CO_2 uptakes were achieved in particular for the APC ash (250 g/kg residue); however, owing due to the meagre quantities of this material generated in incineration plants compared to CO_2 emissions, accelerated carbonation of this type of industrial residues, as well as of bottom ash, does not appear to be a feasible process for CO_2 storage. Accelerated carbonation of stainless steel slag instead, appears to be an interesting technique for carrying out mineral storage of carbon dioxide in industrial facilities using part of the waste streams generated in the same plant, although more severe operating conditions than those used in this work should be applied in order to increase the CO_2 uptake of the slag.

Abstract

Le reazioni di carbonatazione di specifiche tipologie di minerali e materiali di diversa origine, come ad esempio malte cementizie o calce, costituiscono un ben noto processo naturale che produce una serie di significativi effetti sugli stessi materiali alcalini, ed in particolare: lo stoccaggio di CO_2 mediante la formazione di una fase carbonatica solida e termodinamicamente stabile, la riduzione del pH e modifiche del comportamento alla lisciviazione del materiale, oltre alla variazione di alcune proprietà fisiche e meccaniche. Dato che le cinetiche di reazione sono in genere molto lente in condizioni naturali, per sfruttare alcuni dei sopradetti effetti dell'invecchiamento chimico, come la stabilizzazione chimica di alcune tipologie di residui e lo stoccaggio minerale di CO_2, sono stati investigati e sviluppati specifici processi di carbonatazione accelerata selezionando e controllando le condizioni operative in modo tale da incrementare significativamente le cinetiche di reazione. In funzione dell'applicazione del processo e della tipologia di materiale selezionato, sono state sperimentate diverse condizioni operative e differenti tipologie di trattamento (gas-solido, ad umido, ecc.).

Il principale obiettivo della presente tesi di dottorato è stato quello di studiare sperimentalmente i processi di carbonatazione accelerata applicati sia a minerali che a residui industriali, così da ottenere nuove indicazioni relative ai meccanismi fondamentali influenzanti il processo per ogni tipologia di materiale analizzato.

Lo studio del processo di carbonatazione accelerata di minerali ha riguardato in particolare gli effetti della presenza di CO_2 ad alta pressione (fino a 100 bar) e di alcuni sali sulla cinetica di dissoluzione dell'olivina a 120 °C in un reattore agitato a flusso continuo per analizzare se queste sostanze esercitino un effetto positivo o al contrario limitante nei confronti della cinetica di dissoluzione del Mg.

Esperimenti di carbonatazione in modalità batch su materiale umidificato (con rapporti liquido/solido <1 l/kg) sono stati eseguiti in condizioni operative blande (temperatura di 30-50 °C e pressione di CO_2 pari a 1-10 bar) su residui di incenerimento di rifiuti solidi, in particolare scorie di fondo e ceneri volanti, e su scorie della produzione di acciaio inossidabile. Gli obiettivi di questo lavoro sono stati essenzialmente: la stima della capacità di sequestro ottenibile per ogni tipologia di residuo industriale correlata alla dimensione granulometrica e alla composizione chimica del campione; lo studio dell'influenza dei principali parametri operativi (temperatura, pressione e rapporto liquido solido) sulla

cinetica di reazione; e ad ultimo l'analisi degli effetti della carbonatazione sulla mineralogia ed il comportamento alla lisciviazione dei residui.

Lo studio della cinetica di dissoluzione dell'olivina ha mostrato che, per tutte le condizioni operative esaminate (pH variabile tra 3 e 8), l'unico fattore controllante il tasso specifico di dissoluzione è risultato essere il pH della soluzione. Dunque la pressione parziale dell'anidride carbonica e la salinità hanno mostrato di influenzare la cinetica di dissoluzione solo indirettamente, variando il valore finale del pH della soluzione. Questo risultato appare significativo, poiché implica che la precipitazione dei carbonati, che ha luogo in presenza di CO_2 ad elevata pressione e valori di pH maggiori di 6, e la dissoluzione dell'olivina potrebbero essere teoricamente essere eseguiti nello stesso reattore, senza effetti di inibizione sulla cinetica di dissoluzione del magnesio.

Per quanto concerne gli effetti della carbonatazione accelerata sul comportamento alla lisciviazione dei residui alcalini esaminati, significativi risultati sono stati ottenuti in particolare per i residui di incenerimento; per entrambi i materiali, la carbonatazione accelerata ha mostrato di esercitare un importante effetto di immobilizzazione nei confronti di Pb, Zn e Cu, i quali sono risultati essere elementi critici in termini di rilascio per entrambe le tipologie di residui tal quali. Per le ceneri volanti, i risultati ottenuti dalla modellazione geochimica dei dati ricavati dai test di lisciviazione condotti a pH variabile hanno mostrato una variazione nelle fasi minerali controllanti la solubilità di vari elementi tra campioni tal quali e campioni carbonatati. Per le ceneri trattate con CO_2, il rilascio di metalli è risultato chiaramente controllato da una varietà di fasi carbonatiche, indicando la potenzialità di questo processo di convertire le iniziali fasi minerali contenenti i metalli in fasi carbonatiche meno solubili, con positive implicazioni per il comportamento ambientale di questa tipologia di residui.

Significativi sequestri di CO_2 sono stati ottenuti in particolare per le ceneri volanti (250 g/kg residuo); comunque, data l'esiguità dei quantitativi di questo materiale rispetto alle emissioni complessive di CO_2 generate tipicamente negli impianti di incenerimento, il processo di carbonatazione su questa tipologia di residui, come sulle scorie di fondo, non risulta essere un processo efficace per lo stoccaggio di CO_2. La carbonatazione accelerata di scorie di acciaieria è risultata invece una tecnica potenzialmente molto interessante per il sequestro minerale dell'anidride carbonica generata dallo stesso impianto industriale, per quanto condizioni operative più severe rispetto a quelle adottate nel presente studio dovrebbero essere applicate per incrementare il sequestro di CO_2.

Table of Contents

Introduction: Aims and contents of this thesis

Climate change control and sustainable management of natural resources and waste are two of the four priority fields of intervention approved during the U.N. World Summit on sustainable development held in Johannesburg in 2002, which has set the legislative framework for European environmental policies until 2012.

The steep increase in anthropogenic emissions of carbon dioxide, which has been occurring since the beginning of the industrial revolution, has been globally recognized as the primary factor determining the ongoing global warming of the surface of the Earth.

Among the various technology mitigation options that have been proposed and investigated for achieving the stabilization of the atmospheric concentration of CO_2, carbon dioxide capture and storage (CCS) technologies have been indicated as one of the most viable and effective measures to reduce point-source emissions that could be applied in the short-medium term, at least until energy production will still rely on fossil fuels combustion (IPCC, 2005). This technology involves collection and concentration of the CO_2 generated by industrial or energy production plants and subsequent storage in safe and permanent sinks, through in situ processes such as injection into geological underground reservoirs (saline aquifers, depleted oil and gas fields or coal beds) or into the oceans, or alternatively, by an ex situ industrial process which allows to store CO_2 in a thermodynamically stable and environmentally safe solid form.

This latter process, defined mineral carbonation, mimics natural rock weathering and consists in the exothermic reaction of CO_2 with Ca and Mg oxides derived from minerals (in particular magnesium silicates such as olivine or serpentine) or industrial alkaline residues (such as steel slag for example) and produces Ca or Mg carbonates. Although these processes are thermodynamically favoured, natural carbonation of silicate materials is very slow, which means that the carbonation reaction must be accelerated considerably to make it a viable large-scale CO_2 storage method. Research in the field of mineral carbonation is currently focused on developing an energy-efficient accelerated carbonation process. Several process routes have been investigated to enhance reaction yields, including the direct gas-solid and aqueous routes, in which the dissolution of the silicate minerals and the reaction of dissolved Ca (or Mg) ions and CO_2 is carried out in a one-step process, and also indirect processes in which the minerals are first treated with specific

additives (e.g.: hydrochloric acid, acetic acid, etc.) so to optimize the dissolution of the reactive phases from the minerals and the carbonation reaction is subsequently performed at different operating conditions.

Alternatively, alkaline waste residues from thermal processes or from construction and demolition activities can be employed as a suitable alkalinity source. These materials are often associated with CO_2 point source emissions and tend to be chemically more unstable than geologically derived minerals, hence requiring a lower degree of pre-treatment and less energy intensive operating conditions to enhance carbonation yields. Furthermore, accelerated carbonation has been found to influence the mobility of inorganic trace contaminants in alkaline waste materials such as municipal solid waste incineration (MSWI) residues and steel slag, improving the chemical stability and hence the reuse potential of this waste stream. However, the influence of the accelerated carbonation reaction on the mechanisms governing the leaching behaviour of these residues, as well as the maximum CO_2 uptakes achievable for each type of material, related to the composition and mineralogy of the residues and also to the applied operating conditions, have been up to now less investigated.

The main objective of this doctoral thesis was to investigate the accelerated carbonation process applied both to minerals and industrial residues in order to gain new insight on the key reaction mechanisms for each type of material.

Regarding accelerated carbonation of minerals, the effects of the presence of high pressure CO_2 and salinity on olivine dissolution kinetics was specifically investigated, as part of a 6 months research period carried out at the Process Engineering Department of the Swiss Federal Institute of Technology (ETH) in Zürich (Switzerland). The aim of this study was to assess if CO_2 may exert an inhibiting effect on olivine dissolution kinetics, as indicated by results reported in a previous work, which would imply the necessity to carry out the olivine dissolution and Mg carbonation reactions in two separate steps. Furthermore, the effects of salinity were also assessed so to verify if specific salts (NaCl or $NaNO_3$) could enhance dissolution kinetics, as suggested by previous studies.

The experimental work carried out on alkaline industrial residues, and in particular on MSWI residues (bottom ash and air pollution control residues) as well as on a mixture of different types of stainless steel slag, was aimed at assessing the potential effects achievable for each type of material both in terms of maximum CO_2 uptakes and also of

the leaching properties of the residues. The physical, chemical and mineralogical composition of each industrial residue were analyzed in detail before and after the carbonation treatment in order to identify the reacting species and reaction products, as well as to estimate the achieved Ca conversion. The direct aqueous carbonation route was chosen (with liquid to solid ratios < 1 l/kg) and the effects of mild operating conditions (temperature of 30-50 °C and CO_2 pressure of 1-10 bar) on process kinetics were investigated. For bottom ash and steel slag, the effects of particle size were also assessed by separately investigating the effects of carbonation on different particle size fractions. For air pollution control residues, in order to elucidate the effects of accelerated carbonation on the leaching mechanisms of the material, geochemical modelling was also applied to describe the results of pH-dependence leaching tests.

The present thesis is structured as follows: in Chapter 1 a general overview on the fundamentals and main applications of accelerated carbonation processes is reported; in particular, the current state of the art on carbonation processes applied to minerals as a CO_2 sequestration option are discussed; moreover the main findings on carbonation of industrial residues, namely MSWI residues and steel slag, for improving material properties and storing CO_2, are illustrated. In Chapter 2 the study carried out on olivine dissolution kinetics is described and the main results are reported. Chapter 3 presents the results of the accelerated carbonation study carried out on air pollution control residues and bottom ash from MSWI residues, whereas in Chapter 4 the main findings of the accelerated carbonation experiments carried out on stainless steel slag are presented and discussed. Finally in Chapter 5 the most interesting findings achieved in this study are summarized, compared and discussed and perspectives on future developments of accelerated carbonation processes for the materials investigated in this study are proposed.

Chapter 1: Fundamentals and main applications of accelerated carbonation

1. 1 Natural weathering and carbonation processes

Chemical weathering of silicate minerals is one of the main mechanisms that contribute, in a million-year timeframe, to the global geochemical carbon cycle. Rock weathering involves the exchange of carbon from the atmosphere to the lithosphere, by the dissolution of atmospheric carbon dioxide (CO_2) into rainwater and the consequent leaching of alkaline earth metals from silicate-containing rocks (Brownlow, 1996). It can be viewed hence, as an acid-base reaction in which an acid (H_2CO_3/CO_2) is neutralized by a solid base (mineral) (Huijgen and Comans, 2003). As an example, the weathering reactions for wollastonite ($CaSiO_3$), forsterite (Mg_2SiO_4) and serpentine ($Mg_3Si_2O_5(OH)_4$) are shown here below respectively (as reported by Teir (2008)):

$$CaSiO_{3(s)} + 2CO_{2(aq)} + H_2O_{(l)} \rightarrow Ca^{2+}_{(aq)} + 2HCO^{-}_{3(aq)} + SiO_{2(s)} \quad (\Delta H_{(T=25°C)} = -63 kJ/molCO_2) \tag{1.1}$$

$$Mg_2SiO_{4(s)} + 4CO_{2(aq)} + 2H_2O_{(l)} \rightarrow 2Mg^{2+}_{(aq)} + 4HCO^{-}_{3(aq)} + SiO_{2(s)} \quad (\Delta H_{(T=25°C)} = -280 kJ/molCO_2) \tag{1.2}$$

$$Mg_3Si_2O_5(OH)_{4(s)} + 6CO_{2(aq)} + H_2O_{(l)} \rightarrow 3Mg^{2+}_{(aq)} + 6HCO^{-}_{3(aq)} + 2SiO_{2(s)} \quad (\Delta H_{(T=25°C)} = -349 kJ/molCO_2) \tag{1.3}$$

Subsequently, the bicarbonate, calcium and magnesium ions released to solution are transferred to rivers and eventually to the oceans, where half of the carbon is removed by precipitation of Ca and Mg carbonate minerals, while the other half is released as CO_2 to the surface of the oceans (Stephens and Keith, 2008), as shown in Equation 1.4 for wollastonite carbonation:

$$Ca^{2+}_{(aq)} + 2HCO^{-}_{3(aq)} \rightarrow CaCO_{3(s)} + CO_{2(g)} + H_2O_{(l)} \tag{1.4}$$

Natural silicate weathering processes are estimated to bind around 1.5-3.3x10^8 tons of CO_2 per year, particularly in the world's active mountain belts (where approximately 50% of the total CO_2 uptake is predicted to occur) (Hilley and Porder, 2008). The overall net

reaction for wollastonite (given by the sum of the weathering and carbonation reactions) (Equation 1.5) indicates that for every mole of weathered Ca-silicate, one mole of carbon is removed from the atmosphere forming a mineral carbonate end product that is known to be thermodynamically stable over geological timeframes (Seifritz, 1990).

$$CaSiO_{3(s)} + CO_{2(g)} \rightarrow CaCO_{3(s)} + SiO_{2(s)} \quad (\Delta H_{(T=25°C)} = -90 kJ/mol) \tag{1.5}$$

This process is recognized to have played an important role in the historical reduction of the atmospheric concentration of CO_2 after the creation of the earth. Furthermore, the precipitation and dissolution of carbonates is the primary mechanism controlling the pH of the oceans (Brownlow, 1996).

A recent study (Kelemen and Matter, 2008) has shown that in some cases natural carbonation can occur with a significantly higher rate than that generally indicated for natural rock weathering. Extensive carbonate deposits with an average age of only 26,000 years were, in fact, discovered in a tectonically exposed mantle peridotite seam in Oman, which was estimated to sequester roughly $4x10^4$ tons of CO_2 per year (Kelemen and Matter, 2008). An experimental study on rock weathering, performed to assess the CO_2 trapping potential of different types of silicates (Kojima et al., 1997), has shown that for finely ground wollastonite particles, which was indicated as the most reactive mineral analyzed in the study, the weathering reaction (Equation 1.1) took approximately 400 hours to achieve equilibrium, at ambient temperature and pressure, in a continuously stirred reactor exposed to CO_2.

The carbonation of alkaline materials is a well known process that has been exploited by man for centuries for the formation of carbonated cementitious systems. The hardening and consequent strength development of moist alkaline earth hydroxide and silicate cements and mortars is caused by the reaction of these materials with atmospheric CO_2. However, natural carbonation may exert a detrimental effect on the durability of reinforced concrete, due to corrosion of the steel structure, by deteriorating its natural chemical protection layer (Roy et al., 1999). The main hydration product of ordinary Portland cement (OPC) based materials is calcium silicate hydrate (C-S-H) gel which provides chemical protection to the steel structure by conferring it a passive oxide film, owing to the high alkalinity of the medium (pH above 12). Calcium silicate hydrate gel in contact with carbonic acid, that

may occur due to exposure of the cement based material to rainwater infiltration or humid air, tends to dissolve in the resulting acidic environment, determining the dissolution of the primary silicate and hydroxide phases and the precipitation of secondary phases, such as calcium carbonate ($CaCO_3$), owing to the decalcification of the gel phase and dissolution of portlandite ($Ca(OH)_2$) (Fernández Bertos et al., 2004a). This process is analogous to rock weathering, but characterized by significantly faster reaction rates, due to the high content of thermodynamically unstable phases, such as calcium containing oxides and hydroxides, of these materials compared to natural rocks.

During the last couple of decades natural weathering processes occurring in alkaline industrial residues, such as concrete waste, municipal solid waste incineration (MSWI) residues, cement kiln dust, coal fly ash, etc., have started to be investigated in order to assess the effects of the weathering reactions on the environmental behaviour of these alkaline waste materials (e.g.: Kirby and Rimstidt, 1994; Meima and Comans, 1997; Anthony et al., 2002; Piantone et al., 2004). The main environmental concern with respect to utilization or final landfill disposal of the above mentioned industrial residues is associated to their potential release of inorganic contaminants, including soluble salts and trace metals, as a result of leaching processes (Hjelmar, 1996).

Natural weathering upon prolonged contact with atmospheric CO_2 during temporary storage, utilization or final disposal of alkaline residues, involves a complex series of chemical and mineralogical transformations including carbonation, in addition to hydrolysis/hydration, dissociation/precipitation of hydroxides and salts of the main cations, formation of clay-like minerals from the glassy phase of the material, oxidation/reduction reactions, as well as the formation of solid solutions (Belevi et al., 1992; Zevenbergen and Comans, 1994; Meima and Comans, 1997; Meima and Comans, 1999; Bodénan et al., 2000; Sabbas et al., 2003).

The main macroscopic effects of natural carbonation of waste residues are the decrease in pH, a change in the buffering capacity of the material and the precipitation of calcite. Other possible effects include the precipitation of metal carbonates and the formation of new mineral phases (Huijgen and Comans, 2006); all of these transformations contribute in influencing the leaching behaviour of the material. The relative importance of these 'weathering' effects depends on the initial chemical composition and mineralogical characteristics of the material.

Natural weathering (alternatively referred to as ageing) is currently applied as a chemical stabilization technique prior to landfill disposal for specific types of waste materials such as MSWI bottom ash in particular, due to the positive effects it has shown to exert on decreasing the leaching of specific heavy metals, such as Cd, Cu, Pb, Zn and Mo (Meima and Comans, 1997, 1999; Chimenos et al., 2003). To enhance natural weathering processes, the residues are typically stockpiled and stored for a set period of time, ranging from a few weeks to some months, and, in some cases, periodically humidified (Rendek et al., 2007; Polettini et al., 2007).

1. 2 Accelerated carbonation processes

Carbonation processes, as previously mentioned, exert several significant effects on alkaline materials, which include specifically: CO_2 uptake in a solid and thermodynamically stable form, pH decrease and modifications of the leaching behaviour of the material, besides variations of some of its physical and mechanical properties.

Natural carbonation reactions however, are generally quite slow even for thermodynamically unstable alkaline phases, and hence the effects of chemical weathering processes on alkaline materials (minerals and anthropogenically derived products) can be assessed only in a long term scenario perspective. Hence to exploit some of the above mentioned effects of chemical weathering for developing specific engineered processes, such as for example: cement curing, waste chemical stabilization techniques and CO_2 mineral trapping, carbonation processes carried out under selected and controlled operational conditions have been developed, in order to significantly increase the kinetics of the reactions involved. Accelerated carbonation has the potential to reduce the time required for complete carbonation down to timescales of minutes or hours, by operating with pure CO_2 gas flows, controlled humidity, temperature and pressure, and solid pre-treatment stages.

Depending on the application of the process and the selected material, significantly different operating conditions have been employed and several process routes have been tested. Here below the main applications of accelerated carbonation reported in the literature are discussed.

Accelerated carbonation of compacted cement-based materials, such as mortars, has been extensively investigated to assess the effects of the process on the mechanical properties of

the material, in particular reinforced cement strength development and corrosion behaviour (e.g.: Young et al. 1974; Sorochkin et al., 1975; Papadakis et al., 1991; Roy et al., 1999; Johanneson and Utgenannt, 2001; Short et al., 2001; Van Balen, 2005; Cizer et al., 2008a; Shi and Wu, 2008). Carbonation has in fact shown to significantly accelerate the hardening of binders (lime or OPC mortars for example), modifying the mineralogy, microstructure and pore structure of the material, consequently improving strength development and durability of thin walled materials (see e.g.: Young et al., 1974; Cizer et al., 2008a,b).

In the field of waste management and contaminated soil reclamation, cement based stabilization/solidification techniques are well known and developed processes that are applied for reducing the environmental risks associated to hazardous waste and contaminated soil or sludge disposal. These techniques allow to produce chemically stable waste forms in which contaminants are chemically bound to the solid matrix or physically encapsulated, allowing for the safe disposal of the treated material. Several studies have shown that accelerated carbonation processes enhance the stabilization of cement-bound waste and improve the leaching behaviour of the treated material by lowering the pH of the solidified waste to values corresponding to the minimum solubility of several heavy metals and within the regulatory limits that define landfill acceptance criteria (e.g.: Lange et al., 1996; Bin-Shafique et al., 1998; Shtepenko et al., 2005; Van Gerven et al., 2006). Accelerated carbonation has also been applied to reduce the curing time required for stabilization of contaminated soils, sludges or sediments mixed with appropriate binders such as OPC, lime or alkaline waste products including: slag, fly ash or cement kiln dust (Fernández Bertos et al., 2004a; Antemir et al., 2008; Liu et al., 2008; Chen et al., 2009) and also for the production of secondary aggregates (Melton et al. 2008).

Accelerated carbonation processes have recently been the focus of numerous experimental studies aimed at assessing and maximizing the storage of CO_2 in a solid and stable form by accelerating natural weathering reactions of minerals and industrial alkaline residues. This process, first proposed by Seifritz (1990) and defined mineral carbonation, is one of the technological options that is being investigated and developed in the framework of CO_2 Capture and Storage (CCS) processes for reducing anthropogenic greenhouse gas emissions from point sources, such as industrial facilities and power plants (IPCC, 2005). Studies on mineral carbonation have primarily regarded minerals that are characterized by large worldwide availability and at the same time by high potential for CO_2 uptake, such as

Mg silicates, and have identified various viable process routes, which however have not yet been developed at the full scale due to the significant energy penalty associated to the overall process, and in particular to the enhancement of the reactivity of the minerals (e.g.: Gerdemann et al. 2007; Sipilä et al. 2008 and references therein).

Several alkaline industrial residues have also been investigated for mineral carbonation processes (e.g.: Johnson, 2000), steel slag in particular (e.g.: Huijgen et al., 2005; Teir et al., 2007; Lekakh et al., 2008a,b; Kodama et al., 2008) but also concrete waste (e.g.: Iizuka et al., 2004; Shtepenko et al., 2005; Stolaroff et al., 2005), cement kiln dust (Huntzinger et al., 2009) and alkaline ashes from combustion processes (Back et al., 2008; Uibu et al., 2009). These materials in fact, although quantitatively limited, prove readily reactive towards CO_2 at significantly milder operating conditions than minerals, and are hence investigated as small scale demonstration projects of the mineral carbonation technology that could be applied in particular to specific industrial facilities where processing by-products could be used to sequester part of the CO_2 emitted from the plant.

As described in the previous section, carbonation reactions can exert a significant effect on the leaching behaviour of alkaline industrial residues and hence processes to accelerate natural weathering have been investigated and applied to several types of waste residues, including MSWI residues, as a chemical stabilization technique (e.g.: Reddy et al., 1991; Meima et al., 2002; Ecke, 2003; Polettini and Pomi, 2004; Van Gerven et al., 2005b; Arickx et al., 2006). Some recent works have hence applied accelerated carbonation both as a CO_2 sequestration technique and also as a treatment strategy for improving the environmental behaviour of residues such as MSWI residues and steel slag (e.g.: Fernández Bertos et al., 2004b; Baciocchi et al., 2006a,b,c; Rendek et al., 2006; Huijgen and Comans, 2006; Li et al, 2007).

In the following sections, accelerated carbonation processes applied for CO_2 storage and for the chemical stabilization of alkaline industrial residues, the main topics of this doctoral thesis, are briefly reviewed. In Section 1.3 some of the most significant results of carbonation processes applied to Ca and Mg silicate minerals for CO_2 storage are reported, along with a description of the applied process routes and operating conditions. In Section 1.4 the results of several of the main findings of accelerated carbonation processes on industrial residues in terms of CO_2 uptake and/or the effects of the process on the environmental behaviour of the residues are reported, with particular focus on MSWI

bottom ash (Section 1.4.1), MSWI air pollution control residues (Section 1.4.2) and steel slag (Section 1.4.3).

1. 3 Accelerated carbonation of minerals

1.3.1 CCS: motivations and overview of the technology

Significant evidence on currently ongoing global warming and related climate modifications have been collected and reported by the scientific community in the last couple of decades, in particular by the U.N. International Panel on Climate Change (IPCC, 2007). An increase of almost 1 degree Celsius of the global average surface temperature of the planet since the mid 19th century, which was estimated to be the largest temperature increase occurred in the past 1300 years, has been recently confirmed (IPCC, 2007), as well as other effects correlated to climate change such as the shrinking of mountain glaciers, the increase in the frequency and intensity of draughts and tropical storms and the rise of the average sea level.

The measured global warming has been associated to a sharp increase in the greenhouse gas effect, which is a natural phenomenon related to the presence of specific gases in the atmosphere, denominated greenhouse gases (mainly carbon dioxide, water vapour and methane) which absorb and reemit part of the infrared radiation emitted by the Earth's surface, trapping heat in the atmosphere. The significant enhancement of the greenhouse gas effect has been linked to the steep increase in CO_2 atmospheric concentrations registered since the beginning of the industrial revolution (from 280 to the current concentration of 380 ppm) and is expected to increase further (about 1-2 ppm per year) (IPCC, 2007). This increase has been primarily ascribed to human activities and in particular to the combustion of fossil fuels, which are estimated to produce about three quarters of anthropogenic CO_2 emissions (IPCC, 2001b). The rest is mainly due to land use changes, especially deforestation. Several industrial processes (such as oil refining and the manufacturing of cement, lime, and steel) are also significant sources of CO_2. Annual anthropogenic CO_2 emissions are currently estimated to be ~26 Gt CO_2 (IPCC, 2007).

Significant technological developments for reducing greenhouse gas emissions have been achieved during recent years. Technological options for the reduction of emissions include more effective energy use, improved energy conversion technologies, a shift to low-carbon or renewable biomass fuels, nuclear power, zero-emissions technologies, improved energy

management, the reduction of industrial by-products and process gas emissions, and carbon capture and storage techniques (IPCC, 2001a). However, according to the IPCC, none of these options alone can achieve the required reductions in greenhouse gas emissions. Instead, a combination of these mitigation measures will be needed to achieve the stabilisation of the atmospheric concentrations of greenhouse gases (in particular CO_2). The Kyoto Protocol in 1997 has established legally binding greenhouse gas emission reduction targets to be achieved in the period 2008-2012 by signatory countries (most developed countries); the E.U. for example has committed to reduce emissions by an average of 8% compared to the year 1990, and recently passed an energy policy that includes unilateral reduction in greenhouse gases of 20% by 2020.

Carbon dioxide capture and storage (CCS) technologies have been indicated as one of the most viable and effective measures to reduce point-source emissions that could be applied in the short-medium term, at least until energy production will still rely on fossil fuels combustion (IPCC, 2005). This technology involves collection and concentration of the CO_2 generated by industrial or energy production plants (operation defined capture), transport to a suitable storage site and subsequent storage in permanent, safe disposal sites such as geological formations, including saline aquifers, oil reservoirs and coal seams, or oceans (Lackner, 2002).

The purpose of CO_2 capture is to produce a concentrated stream of CO_2 at high pressure that can be transported to a storage site (IPCC, 2005). For the energy sector, there are three main approaches to capture the CO_2 generated from the combustion of fossil fuels, biomass, or mixtures of these fuels, depending on the process or type of power plant to which CO_2 capture is applied: post-combustion, pre-combustion, and oxy-fuel combustion systems. Post-combustion systems separate CO_2 from a flue gas stream, which generally contains 3-15% vol. CO_2, typically using a liquid solvent such as monoethanolamine. This technique is currently used to absorb CO_2 from part of the flue gases generated from a number of existing power plants. It is also commercially used in the natural gas processing industry. Pre-combustion systems remove CO_2 before combustion by employing gasification, water-shifting, and CO_2 separation. This technology is widely applied for fertiliser manufacturing and hydrogen production. Oxy-fuel combustion systems use oxygen, instead of air, for the combustion of the primary fuel to produce a flue gas that consists mainly of water vapour and CO_2. This relatively new technology requires the

production of pure oxygen from air and results in a flue gas with high CO_2 concentrations from which water vapour is removed by condensation. The main challenge for the development of CO_2 capture technology is to reduce the energy requirements of the capture processes. The energy needed for capturing 90% of the CO_2 generated by a power plant increases the fuel consumption per unit of electricity produced by 11-40%, using the best current technology compared to power plants without capture; which in other words means that to produce the same amount of energy and capture the related CO_2 emissions from three power plants a fourth one would be needed, implying an increase in the cost of electricity production of 35-85% (IPCC, 2005).

The separated CO_2 must, in most cases, be transported to the storage site, since suitable storage sites are seldom located near CO_2 emission sources (IPCC, 2005). Transportation by pipelines is a mature technology which has been in use for enhanced oil recovery since the 1970s. To avoid pipe corrosion the gas must be dehydrated before transportation. Transportation by ship or road and rail tankers is also a possibility. Gaseous CO_2 is typically compressed for transportation to a pressure above 80 bar in order to avoid two-phase flow regimes and increase the density of the CO_2, thereby making it easier and less costly to transport. The cost of pipeline transport is dependent on various parameters, such as: the flow rate, the type of transport: offshore/onshore and the distance. For a nominal distance of 250 km the cost is typically 1-8 US$/t$CO_2$ (IPCC, 2005).

In order for CCS to be a useful option for reducing CO_2 emissions, the captured CO_2 has to be stored for geological timeframes (at least thousands of years) in isolation from the atmosphere (IPCC, 2005). Currently, the only technology that has reached demonstration level for accomplishing this objective on a sufficiently large scale is in situ underground storage in geological formations. Nearly depleted or depleted oil and gas reservoirs, deep saline formations, and unminable coal beds have been indicated as the most promising options for the geological in situ storage of CO_2. Suitable storage formations can occur in both onshore and offshore sedimentary basins. In any case, CO_2 is injected in compressed form into a rock formation at depths greater than 800 m, where the CO_2 is in a liquid or supercritical state due to the local pressures. To ensure that the CO_2 remains trapped underground, a well-sealed cap rock over the selected storage reservoir is necessary. The geochemical trapping of CO_2 (i.e. fixation into carbonates) will eventually occur as CO_2 reacts with the fluids and host rock in the reservoir, but as previously mentioned, this

happens on a time scale of hundreds to millions of years (IPCC, 2005). Currently, there are several projects running that demonstrate this technology. The injection of CO_2 into geological formations in fact involves many of the same technologies that have been developed in the oil and gas exploration and production industry. 30 Mt of CO_2 are being injected annually for enhanced oil recovery (EOR) in Texas (USA), where EOR has been used since the early 1970s for economic reasons. However, most of the injected CO_2 is obtained from natural CO_2 reservoirs. Currently three industrial-scale projects are all together annually storing 3-4 Mt of CO_2 in saline aquifers (Sleipner in Norway, Weiburn in Canada and In Salah in Algeria). Besides enhanced gas and oil recovery, another technology that is being recently investigated within the framework of geological storage of CO_2 is enhanced coal bed methane recovery (ECBM). The scope of this process is to inject CO_2 into coal seams in order to displace and recover methane. One of the greatest challenges of geological storage remains the risk of leakage from the reservoir, which implies the need for accurate and continuous monitoring of the storage sites for thousands of years. It has been estimated in fact that if only 1% of the remaining geologically stored CO_2 were to leak every 1000 years, in 200,000 years there would be a 87% loss, resulting in a larger CO_2 release than the emissions that would have been released without CCS, owing to the energy penalty associated to CCS technology (Sipilä et al., 2008). The estimated total CO_2 storage capacity for geological formations worldwide is 2,000-10,000 Gt of CO_2, while the costs of storage in saline formations and depleted oil and gas fields have been estimated to be 0.5-8 US$/t CO_2 injected, with an additional cost for monitoring of 0.1-0.3 US$/t CO_2 (IPCC, 2005).

Another option that has been indicated for large-scale storage of CO_2 is direct injection into the ocean at depths greater than 1000 m. This option is not a mature technology but has been under research for several decades. CO_2 can be transported via pipelines or ships to an ocean storage site, where it is either injected directly into the ocean or deposited into a CO_2 lake on the sea floor. The analysis of direct observations or modelling results both indicated that injected CO_2 could remain isolated from the atmosphere for at least several hundreds of years, and that the fraction retained tends to be higher increasing the depth of the injection. The cost of injecting CO_2 into the oceans at a depth of 3000 m has been estimated to be roughly 5-30 US$/t CO_2 (IPCC, 2005). However, actively injecting CO_2 may exert harmful effects on the ocean environment, about which little is known.

Experiments showed that adding CO_2 can harm marine organisms, but it is still unclear what effects the injection of several million tonnes of CO_2 would have on ocean ecosystems.

1.3.2 Ex situ mineral carbonation

As an alternative to underground geological storage or ocean storage, long-term (or actually permanent) storage of CO_2 may be achieved by an industrial ex situ process by which CO_2 is stored in the form of solid inorganic carbonates by means of chemical reactions. The accelerated carbonation process for the storage of CO_2 is commonly referred to as mineral carbonation. Carbonation of alkaline minerals mimics natural rock weathering and involves the permanent storage of CO_2 under the thermodynamically stable form of calcium or magnesium carbonates (IPCC, 2005). This process, as previously described, is based on acid-base reactions in which an acid (H_2CO_3/H_2O) is neutralized by a solid base (alkaline minerals).

Although oxides or hydroxides of alkaline or alkaline earth metals can be carbonated, calcium and magnesium silicate minerals are usually preferred, since they are available worldwide in large amounts. Magnesium-rich silicates such as olivine, serpentine and talc can be found in ultramafic rocks such as dunites, peridotites and serpentinites, whereas one of the preferred calcium containing silicates is wollastonite due its high content in CaO (Huijgen and Comans, 2003); a complete list of the minerals investigated up to now for mineral carbonation is reported in Sipilä et al. (2008). These minerals, Mg oxide-based silicates in particular, are available worldwide in large amounts and have the potential of sequestering the total amount of CO_2 emitted from the combustion of all the available fossil fuel reservoirs (Lackner, 2003), which, according to updated calculations, would amount to approximately 8,000 Gtons (Ziock et al., 2000). Furthermore, the final products of mineral carbonation (carbonates and silica) are environmentally stable and can therefore be disposed of as mine filler materials or used for construction purposes (Lackner, 2002). Hence, unlike underground geological storage, there would be little or no need to monitor the disposal sites and the environmental risks would be very low (IPCC, 2005). In Figure 1.1 the estimated capacities and storage times associated to different sequestration techniques is represented; as can be noted, mineral carbonation in particular shows the

largest potential both in terms of capacity (similar to underground injection in saline aquifers) and of storage timeframes.

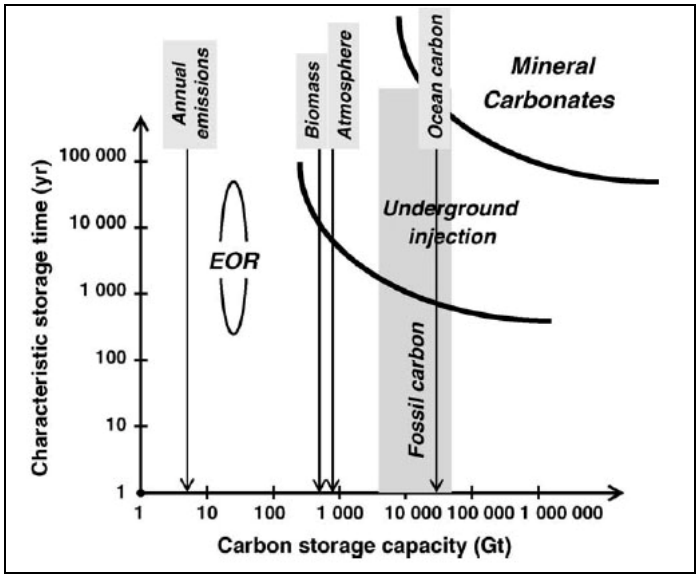

Figure 1.1 Estimated storage capacities and relative timeframes for various sequestration methods (Zevenhoven et al., 2006).

The overall carbonation reaction for magnesium or calcium silicates can be expressed as follows (Teir, 2008):

$$(Mg,Ca)_xSi_yO_{x+2y+z}H_{2z(s)}+xCO_{2(g)}\rightarrow x(Mg,Ca)CO_{3(s)}+ySiO_{2(s)}+zH_2O \quad (1.6)$$

Apart from the large and safe storage capacity, the exothermic nature of the overall carbonation reaction is another benefit of mineral carbonation which motivates further research. In the case of Mg-bearing silicates the following exothermic chemical reactions take place, for forsterite and serpentine respectively (wollastonite carbonation is reported in Equation 1.4):

$$Mg_2SiO_{4(s)}+2CO_{2(g)}\rightarrow 2MgCO_{3(s)}+SiO_{2(s)} \quad (1.7)$$

$$(\Delta H_{(T=25°C)}=-89 \text{ kJ/mol } CO_2)$$

$$Mg_3Si_2O_5(OH)_{4(s)}+3CO_{2(g)}\rightarrow 3MgCO_{3(s)}+2SiO_{2(s)}+2H_2O \quad (1.8)$$

$$(\Delta H_{(T=25°C)}=-64 \text{ kJ/mol } CO_2)$$

Since these reactions release heat, the formation of carbonate phases is thermodynamically favoured at low temperature, whereas at high temperature (above 900 °C for calcium

carbonate and above 300 °C for magnesium carbonate, at a CO_2 partial pressure of 1 bar) the reverse reaction (calcination) is favoured (Lackner et al., 1995).

The natural carbonation of silicate materials is very slow, which means that the carbonation reaction must be accelerated considerably to make it a viable large-scale CO_2 storage method. Therefore, research in the field of mineral carbonation is currently focused on developing an energy efficient accelerated carbonation process.

Additional requirements for a commercial CO_2 storage process by mineral carbonation are the mining, crushing, and milling of the mineral-bearing ores and their transportation to a processing plant that has access to a concentrated CO_2 stream from a capture plant. Accelerated carbonation technology is still in the development stage and is not yet ready for implementation. The best case studied so far is the wet carbonation of natural silicate olivine, for which the estimated process costs are 50-100 US$/t net CO_2 carbonation, excluding CO_2 capture and transport costs (O'Connor et al., 2005; Gerdemann et al., 2007). The energy requirements of this carbonation process are typically 30-50% of the output of the power plant from which CO_2 is captured. In combination with the power requirements of the capture facility, up to 60-180% more energy input would be required per kWh produced than for a power plant without CCS. The carbonation process would require 2-4 t silicates/t CO_2 to be mined and would produce 3-5 t material/t CO_2 stored to be disposed of as carbonates, which could exert a similar environmental impact to current large-scale surface mining operations (IPCC, 2005).

1.3.3 Main process routes investigated for ex situ mineral carbonation

The major challenge hindering the large-scale application of silicate minerals for CO_2 sequestration is their slow reaction kinetics. Therefore, most research in this field has focused on identifying faster reaction pathways, by characterisation of the mineral reactants and reaction products, as well as bench-scale experiments for determining reaction rates (Teir, 2008). Although the raw materials required are relatively cheap and the net carbonation reactions are, as earlier shown, exothermic, the process conditions (high pressures and temperatures) and additional chemicals for speeding up the carbonation reactions, all contribute to excessive process costs, as compared to other storage techniques such as geological sequestration. However, due to extensive research in

this field, several encouraging findings have led to the definition and development of different potentially promising process routes that will be here below briefly outlined.

First of all, an important aspect of mineral carbonation is the need to activate the surface of the mineral to increase its effective carbonation yield. This can be done by applying a variety of physical pre-treatment methods, including size reduction, magnetic separation, thermal treatment (to eliminate chemically-bound water, in particular for serpentine) or steam activation (O'Connor et al., 2005). Chemical pre-treatment methods (Maroto-Valer et al., 2006) involving sulphuric acid were shown to be effective for serpentine as they increased the surface area from 8 to 330 m^2/g.

Upon activation, the mineral may be carbonated applying one of the several carbonation process routes, which are schematically reported in Figure 1.2 and described in detail in a recent review by Sipilä et al., (2008).

In direct processes, the mineral carbonation reaction takes place in a single process step, whereas in indirect processes, calcium or magnesium are first extracted from the mineral and subsequently carbonated so that each reaction may be optimized by separately setting its optimal operating conditions.

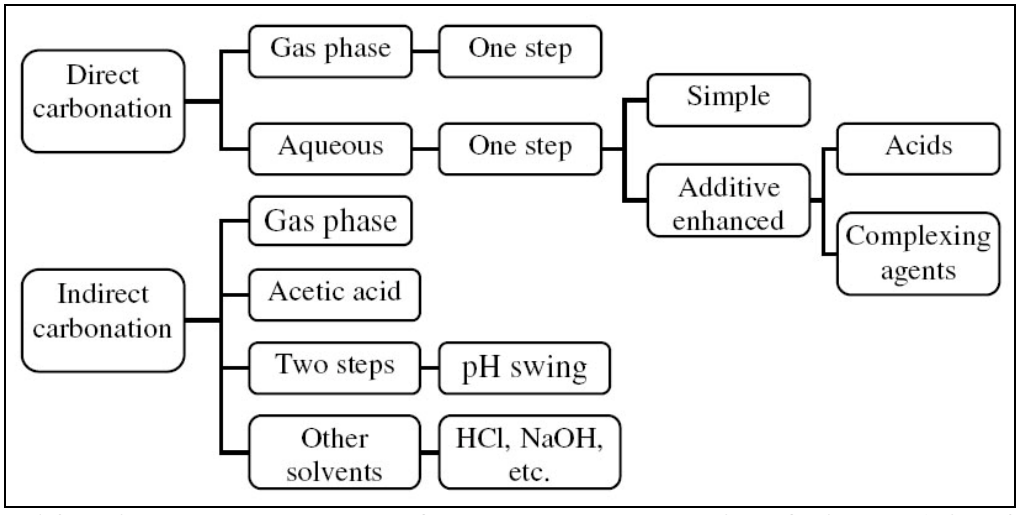

Figure 1.2 Main process routes tested for accelerated carbonation of minerals (Uibu, 2008).

Direct carbonation

The direct carbonation route may be applied either in an aqueous solution (three phase system) or directly at the gas-solid interface.

The **direct gas-solid carbonation process** first studied by Lackner et al. (1995) consists in converting oxide or silicate minerals directly to carbonates using gaseous or supercritical CO_2. The advantages of this approach are its simplicity and the possibility of recovering heat at high temperature. The reaction proceeds very slowly at room temperature, but the rate can be accelerated by increasing the temperature. However, above a certain temperature the reaction equilibrium shifts and favours free CO_2 instead of carbonates, i.e. the calcinations reaction, as previously mentioned. This temperature limit can be raised by increasing the CO_2 pressure.

Gas-solid carbonation reactions for lime (Equations 1.9 and 1.10) are rapid and completion can be achieved in minutes at optimum temperature. Although $Mg(OH)_2$ carbonation is fast enough for industrial use, under dry conditions the rate of MgO carbonation is too slow for significant amounts of CO_2 to be sequestered (Lackner et al., 1997).

$$Ca(OH)_{2(s)} \rightarrow CaO_{(s)} + H_2O_{(g)} \quad (1.9)$$

$$(\Delta H_{(T=25°C)} = +65 \text{ kJ/mol } CO_2)$$

$$CaO_{(s)} + CO_{2(g)} \rightarrow CaCO_{3(s)} \quad (1.10)$$

$$(\Delta H_{(T=25°C)} = -178 \text{ kJ/mol } CO_2)$$

In an early study, Bhatia and Perlmutter (1983) investigated the kinetics of the dry carbonation of lime in a modified TGA apparatus at different temperatures in a 100% CO_2 atmosphere and obtained a maximum calcium conversion of 70% at 500°C and atmospheric pressure. The rate of the dehydroxylation reaction (Equation 1.9) and the carbonation reactions (Equation 1.10) diminished in time as a thin layer of calcite formed on the reagent material and acted as a barrier for both the outward diffusion of H_2O and the inward diffusion of CO_2 (Huijgen and Comans, 2003).

For silicate minerals which, as previously observed, are the only interesting minerals for large scale implementations, the reaction rates of such a process have been shown to be too slow and thermodynamic limitations have been observed (Zevenhoven et al., 2006). The highest reported conversion by direct gas-solid carbonation of silicates appears to be 25% of the stoichiometric maximum, which was achieved by exposing 100 μm serpentine particles to a CO_2 pressure of 340 bar and a temperature of 500 °C for 2 h (Lackner et al., 1997).

In the **direct aqueous process**, carbonation occurs in a three-phase system (gas-water-solid medium), which considerably increases the reaction rate compared to the direct gas-solid route. Aqueous mineral carbonation experiments carried out in an autoclave reactor on a slurry phase aqueous suspension of wollastonite ($CaSiO_3$) found a maximum CO_2 conversion yield of 70% with a reaction time of 15 min at 200 °C, 20 bar CO_2 partial pressure and particle size < 38 μm (Huijgen et al., 2006b).

Carbonation through the aqueous route occurs mainly in three steps; as an example, in the case of $CaSiO_3$ the process involves: 1) the leaching of calcium from the wollastonite matrix (Equation 1.11), 2) the contemporary dissolution of CO_2 and conversion of carbonate species to bicarbonates (Equations 1.12 and 1.13), 3) the formation of calcium carbonate (eq. 1.13).

$$CaSiO_{3(s)} + 2H^+(aq) \rightarrow Ca^{2+}{}_{(aq)} + H_2O_{(l)} + SiO_{2(s)} \quad (1.11)$$

$$CO_{2(g)} + H_2O_{(l)} \rightarrow H_2CO_{3(aq)} \rightarrow HCO^-_{3(aq)} + H^+{}_{(aq)} \quad (1.12)$$

$$Ca^{2+}{}_{(aq)} + HCO^-_{3(aq)} \rightarrow CaCO_{3(s)} + H^+{}_{(aq)} \quad (1.13)$$

The first step is considered rate-limiting for the whole carbonation reaction (O'Connor et al., 2005); enhancement though was found when the specific surface area was increased or when additives such as NaCl or $NaHCO_3$ were used. In studying the kinetics of the process, Huijgen and co-workers (2006b) identified two temperature regimes influencing the overall reaction rate. At temperatures below the optimum reaction temperature, they hypothesized that the reaction rate was limited by calcium leaching from $CaSiO_3$ (Equation 1.11), due to the formation of a calcium depleted silicate rim on the mineral which limited Ca diffusion towards the water phase. At higher temperatures they found the nucleation and growth of calcite (Equation 1.13) to be the rate-limiting step, due to reduced bicarbonate activity, resulting from the lower solubility of CO_2 at higher temperatures. CO_2 partial pressure was instead found to have an influence on the optimum reaction temperature (Huijgen et al., 2006b).

Similar results were also reported for Mg-containing silicates like olivine (O'Connor et al., 2005) concerning the influence of both reaction temperature and CO_2 partial pressure. Due to the relatively limited availability of wollastonite, work has focused mainly on the carbonation of Mg-bearing minerals, such as olivine (see Equations 1.14 and 1.15) or

serpentine (see Equation 1.16). Preliminary tests conducted at ambient temperature and sub-critical CO_2 pressures (below 74 bar) resulted in very slow carbonate formation. In later tests, using an aqueous solution of sodium bicarbonate ($NaHCO_3$) and sodium chloride (NaCl) at elevated temperatures and pressures, several silicate minerals were successfully carbonated to a large extent in one hour (O'Connor et al., 2005).

$$2Mg_2SiO_{4(s)}+CO_{2(g)}+2H_2O_{(l)} \rightarrow Mg_3Si_2O_5(OH)_{4(s)}+MgCO_{3(s)} \quad (\Delta H_{(T=25°C)}=-157 \text{ kJ/mol } CO_2) \quad (1.14)$$

$$Mg_2SiO_{4(s)}+2CO_{2(g)}+2H_2O_{(l)} \rightarrow 2MgCO_{3(s)}+H_4SiO_{4(aq)} \quad (\Delta H_{(T=25°C)}=-80 \text{ kJ/mol } CO_2) \quad (1.15)$$

$$Mg_3Si_2O_5(OH)_{4(s)}+3CO_{2(g)}+2H_2O_{(l)} \rightarrow 3MgCO_{3(s)}+2H_4SiO_{4(s)}+2H_2O \quad (\Delta H_{(T=25°C)}=-37 \text{ kJ/mol } CO_2) \quad (1.16)$$

In the case of olivine, the optimized conditions determined for aqueous carbonation were 180 °C and 15 bar in a 1M NaCl and 0.64M $NaHCO_3$ solution for a reaction time of 1 hour and finely milled olivine grains (<37 μm) (O'Connor et al., 2005; Gerdemann et al., 2007), which led to a 80% conversion yield.

Multiple factors (temperature, pressure, liquid to solid (L/S) ratio, stirring speed, additives, material, particle size distribution) have shown to affect the outcome of aqueous mineral carbonation, as indicated by several studies (e.g.: Bearat et al. 2006; Chen et al, 2006; Huijgen et al., 2006b; Alexander et al., 2007). One of these studies, conducted by Chen et al. (2006), investigated some of the key parameters affecting the carbonation process by analysing literature results. The process was divided into two principal steps: 1) magnesium ion dissolution and 2) magnesite precipitation and it was concluded that enhancing either one of the two-steps often means limiting the other. Therefore, in order to improve the overall carbonation process, finding a balance between these two steps is essential (Chen et al., 2006). Hänchen et al. (2006; 2007; 2008) have also extensively studied the chemistry of aqueous mineral magnesium carbonation. This research group has provided a model for the dissolution of olivine in water (Hänchen et al. 2006; 2007) as well as a better understanding of magnesium carbonate precipitation (Hänchen et al., 2008). By investigating olivine precipitation from a $H_2O–CO_2–Na_2CO3–MgCl_2$ system at different temperatures and CO_2 pressures (25 °C and 1 bar, 120 °C and 3 bar, 120 °C and 100 bar), Hänchen et al. (2008) confirmed that magnesite or hydromagnesite ($(MgCO_3)_4 \cdot Mg(OH)_2 \cdot 4H_2O$)) precipitation at ambient temperature does not occur, instead

nesquehonite ($MgCO_3 \cdot 3H_2O$) precipitation is favoured. At higher temperatures magnesite precipitated and the initial kinetics were determined by supersaturation with respect to brucite (3 bar) and hydromagnesite (100 bar). Only the high temperature and high pressure precipitation experiments were sufficiently rapid for industrial applications, but only if supersaturaturation with respect to hydromagnesite was achieved (Hänchen et al., 2008).
The lowest costs reported from a case-specific feasibility study regarding aqueous carbonation applied using the above reported operating conditions were 54 US$/t CO_2 with olivine as feedstock, 78 US$/t$CO_2$ using serpentine as feedstock and 64 US $/t$CO_2$ with wollastonite as feedstock (O'Connor et al., 2005; Gerdemann et al., 2007); it must be highlighted though that in these estimations the costs for CO_2 capture and transport were not taken into account.

Indirect carbonation

In indirect carbonation processes a reactive magnesium or calcium compound is first extracted from the mineral, after which the intermediate magnesium/calcium products are carbonated. Most of these processes usually provide a faster carbonation route than direct processes, but demand additional energy or chemicals.

Gas-solid carbonation of Ca and Mg oxides obtained by the dissolution of the silicate minerals with HCl has been investigated by several studies (Sipilä et al., 2008). The direct gas-solid carbonation of calcium/magnesium oxides/hydroxides as previously mentioned in fact, proceeds much faster than the gas-solid carbonation of calcium/magnesium silicates, although a high temperature and CO_2 pressure are required. 100% conversion of magnesium hydroxide was achieved in less than 2 h using a CO_2 pressure of 340 bar and a temperature of 500 °C (Lackner et al., 1997). Zevenhoven et al. (2006) suggested a staged gas-solid process for the carbonation of serpentine. The process involved the extraction of reactive magnesium as magnesium oxide or hydroxide at atmospheric pressure, followed by carbonation at a higher temperature (>500 °C) and at elevated pressures (>20 bar) that allowed for reasonable carbonation reaction kinetics under conditions where magnesium carbonate was thermodynamically stable (Zevenhoven et al., 2006).
Metal dissolution from the silicate minerals is the rate-controlling step of the whole process and may be achieved by adding an acid, such as hydrochloric or acetic acid, (e.g.: Lackner et al., 1997; Kakizawa et al., 2001; Park et al., 2003), or also high pressure CO_2 (Hänchen et al., 2006) to the reaction system. However, irrespective of the type of process

used for mineral dissolution, the acidic conditions required do not allow for quantitative precipitation of the alkaline metals in the carbonate form. The degree of supersaturation required for an efficient and effective carbonate precipitation is so high that a pH shift to basic conditions is required. This is especially true when carbonation of Mg-bearing minerals is pursued, because magnesium carbonate formation is more difficult to achieve than calcium carbonate. This requires the addition of other amendments, such as NH_4OH (Park and Fan, 2004), whose recycling is once again a critical issue.

Several studies have investigated Mg-silicates **dissolution using HCl** (Lackner et al. 1995; 1997; Butt et al., 1998). In these processes the silicates were first decomposed in hydrochloric acid (HCl) at ~100 ºC, forming magnesium chloride in the solution and a silica gel that was recovered by filtration. Any excess acid and water was boiled off at 150 ºC, at which conditions the formed solid magnesium chloride ($MgCl_2$) decomposed regenerating HCl and forming magnesium hydroxide chloride which in turn decomposed in water yielding magnesium hydroxide and magnesium chloride. The magnesium hydroxide was hence separated, while the magnesium chloride was recycled through the acid recovery step. The drawback of the process is its high energy demand for the evaporation of the aqueous solution and the large variations in free energy resulting from the necessary formation of intermediate products. Costs up to 233 US$/t CO_2 sequestered were estimated. The same process route was also used for carbonating calcium silicates (Lackner et al., 1995). By this route calcium silicate was dissolved in hydrochloric acid at 80 °C producing calcium chloride. After silica filtering, $CaCl_2$, reacting with Mg(OH)Cl, produced $Ca(OH)_2$ and $MgCl_2$. The calcium hydroxide was then separated, dissolved in water, and then reacted with CO_2 to produce calcium carbonate. The $MgCl_2$ was instead decomposed at 150 °C to regenerate Mg(OH)Cl. Major drawbacks reported for this process were the energy demand for the acid recycling stage and a very large water demand to hydrate the $Ca(OH)_2$ for the carbonation stage: 840 t H_2O/t $Ca(OH)_2$.

A similar process for the carbonation of calcium silicate was studied by Kakizawa et al. (2001). The chemical reactions in this process occurred in two steps. The first step consisted in the extraction of calcium ions from calcium silicates (e.g. wollastonite) using **acetic acid** (CH_3COOH) (Equation 1.17). The solid SiO_2 precipitated and was separated using a thickener. Gaseous CO_2 was hence injected into the solution, causing calcium carbonate to crystallize and deposit (Equation 1.18).

$$CaSiO_{3(s)} + 2CH_3COOH_{(aq)} \rightarrow Ca^{2+}_{(aq)} + 2CH_3COO^-_{(aq)} + SiO_{2(s)} + H_2O_{(l)} \quad (1.17)$$
$$(\Delta H_{(T=25°C)} = -105 \text{ kJ/mol})$$

$$Ca^{2+}_{(aq)} + 2CH_3COO^-_{(aq)} + SiO_{2(s)} + H_2O_{(l)} \rightarrow CaCO_{3(s)} + 2CH_3COOH_{(aq)} \quad (1.18)$$
$$(\Delta H_{(T=25°C)} = +16 \text{ kJ/mol})$$

At 25 °C, the theoretical conversion that could be achieved is 40% at 1 bar and 75% at 30 bar. The acetic acid was recovered in this step and recycled for use in the extraction step. Kakizawa et al. (1991) conducted extraction experiments with wollastonite (particle size <37 μm) at 60 °C and atmospheric pressure in a batch reactor. The extraction of calcium reached 48% in 250 minutes using an aqueous solution of acetic acid (acetic acid/water = 13.7 g/50 g). Crystallization experiments were conducted at 5-50 bar in a batch reactor of 200 ml. The best carbonation conversion achieved was about 20% in 60 min under a total pressure of 30 bar using CO_2. However, the conversion was calculated from the total amount of precipitate produced, and the chemical composition of the precipitate was not reported.

Blencoe et al. (2003) developed a carbonation process that used **caustic soda** (NaOH) to dissolve silicate minerals. First, serpentine reacted with a concentrated solution of caustic soda, which formed crystalline brucite and an aqueous solution rich in dissolved silica. Injecting CO_2 into the solution caused magnesite and a silica gel to form. According to Blencoe et al. (2003), both olivine and (hydroxylated) serpentine were rapidly decomposed by an aqueous solution of caustic soda (30-80 wt-% NaOH) at relatively low temperatures (at 200 °C and below), and the pressure required to achieve rapid and efficient carbonation was about 15 bar. The process was also used for carbonating calcium silicates (Blencoe et al., 2004). According to Blencoe et al. (2004), 90% pure carbonate could be produced in 72 h under these process conditions. However, the reaction times reported seem too long for industrial applications, and large amounts of NaOH are consumed in the process.

Park et al. (2003) studied the dissolution of serpentine in aqueous solutions of HCl, acetic acid, ethylenediaminetetraacetic acid (EDTA), orthophosphoric acid, and oxalic acid for subsequent carbonation. The authors found that a mixture of orthophosphoric acid, oxalic acid, and EDTA gave the best extraction of magnesium from serpentine. However, when an acidic solvent was used for aqueous mineral carbonation, the overall carbonation rate was limited by the dissolution of CO_2 and dissociation of carbonic acid, rather than the dissolution rate of the mineral. Park and Fan (2004) proposed a **two-step pH swing**

process for the carbonation of serpentine. First, ground serpentine was dissolved at 70 ºC and under ambient pressure using either a) an aqueous solution of 1% vol. orthophosphoric acid, 0.9% wt. oxalic acid, and 0.1% wt. EDTA or b) 1.4 M ammonium bisulphate. Experiments showed that after 1 h, 65% of the magnesium in the serpentine had been extracted using solvent a), while 42% had been extracted using solvent b). After this stage, solid SiO_2 was separated by filtration. By raising the pH of the filtrate to ~ 8.6 using NH_4OH, iron, dissolved from the serpentine ore, precipitated as amorphous iron oxide. After the precipitated iron oxide had been removed by filtration, CO_2 was bubbled through the solution at 1 atm. The pH of the solution was further increased to pH ~ 9.5 using NH_4OH, which caused relatively pure $MgCO_3 \cdot 3H_2O$ to precipitate.

In conclusion, several studies on mineral carbonation have investigated the possibility of enhancing the overall reaction rate by speeding up the extraction of magnesium or calcium using acetic acid (or some other solvent). However, the problem of effectively recycling the extraction agent remains unsolved and more research is warranted before this route can be considered feasible for long-term CO_2 storage.

1. 4 Accelerated carbonation of alkaline industrial residues

One way of bypassing some of the drawbacks of accelerated carbonation of minerals is to employ alkaline waste by-products of thermal processes or construction and demolition activities, as a feedstock. As these materials are often associated with CO_2 point source emissions and tend to be chemically more unstable than geologically derived minerals (Huijgen et al., 2006b), they require a lower degree of pre-treatment and less energy intensive operating conditions to enhance carbonation yields (Huijgen and Comans, 2003; Huijgen et al., 2006b). Furthermore, after stabilisation by accelerated carbonation, the leaching behaviour, with respect to specific heavy metals, of alkaline waste materials such as bottom ash (e.g.: Van Gerven et al., 2005b) and air pollution control residues (Baciocchi et al., 2006a,b,c; Li et al., 2007) generated by MSW incineration, steel slag (Huijgen and Comans, 2006) and oil shale ash (Reddy et al., 1991) among others, has shown to improve, and may allow to reuse the treated residues in selected civil engineering applications or at least to fulfil landfill acceptance criteria.

Table 1.1 provides the average oxide composition of some of the waste residues that have been tested for CO_2 sequestration as compared to typical ordinary Portland cement (OPC).

Accelerated carbonation has been applied to many of the solid residue streams produced by coal fired power stations, including pulverized fly (PF) ash (Reddy et al., 1994; Johnson, 2000; Montes-Hernandez et al., 2008), clean coal technology (CCT) ash (Tawfick et al., 1995) and fluidized bed combustion (FBC) ashes (Jia and Anthony, 2000). Various by-products of oil shale combustion, such as PF and circulating fluidized bed combustion (CFBC), have been also tested (Reddy et al., 1991, 1994; Uibu et al., 2009), as well as lignite combustion fly ash (Back et al., 2008), specifically to assess CO_2 storage potential, owing to the higher CaO contents of these types of residues, e.g. 37% CaO and 15% MgO for lignite fly ash (Back et al., 2008) and around 50% CaO and 10-15% MgO for different types of oil shale ash (Uibu, 2008), compared to coal combustion fly ash, and in particular PFA (see Table 1.1).

The carbonation potential in terms of CO_2 uptake of several other types of combustion residues has also been investigated, including de-inking ash, paper mill ash (Johnson et al., 2000; Pérez-López et al., 2008) and ash from MSW and special waste incineration. It has been applied primarily as a treatment technique before reutilization or final disposal of MSW bottom ash (MSW-b) with the purpose of producing a chemically stable material with improved leaching behaviour (Meima et al., 2002; Polettini and Pomi, 2004; Van Gerven et al., 2005b; Arickx et al., 2006; Rendek et al., 2006a), see Section 1.4.1. In the case of residues with high free Ca oxides and hydroxide contents, such as MSWI air pollution control (APC) residues and fly ash (MSW-f), cement kiln dust (CKD), deinking ash and paper mill waste, accelerated carbonation has been proposed as a possible CO_2 capture and storage (CCS) technology, due to the typically high reactivity of these materials with CO_2 even at mild operating conditions. For APC residues, which are further discussed in 1.4.2, see in particular: Fernández-Bertos et al., 2004b; Baciocchi et al., 2006a; Li et al., 2007; Prigiobbe et al., 2009a, for CKD: Huntzinger et al., 2009, and for paper mill waste carbonation: Pérez-López et al., 2008.

Slag produced as a by-product of steel manufacturing has also shown potential for CO_2 uptake, due to its high CaO content, prevalently in the form of Ca and Mg silicates, including ground granulated blast furnace slag (GGBS), produced by the rapid cooling of molten slag and stainless steel slag (SSS), which is generally characterized by high contents of Ca and Mg oxides as a result of steel refining processes in specific converter units. Depending on the type of steel processing plant, slags with quite different

compositions can be generated (Teir et al., 2007). The characteristics of the main types of steel slag and the results of the principal accelerated carbonation investigations carried out on these materials is reviewed in more detail in Section 1.4.3. Recently, accelerated carbonation has been applied also to alumina manufacturing residues, generally known as red mud, which are highly alkaline residues containing around 8% CaO and 1% MgO, to assess their CO_2 sequestration capacity (Bonenfant et al., 2008b).

The CO_2 sequestration potential of concrete demolition waste has also been studied, owing to the high contents of both free lime and calcium silicates of this material (Iizuka et al., 2004; Shtepenko et al., 2005; Stolaroff et al., 2005).

Table 1.1 Typical bulk compositions of some of the calcium silicate containing waste residues tested for accelerated carbonation (% in weight of each oxide) (Johnson, 2000).

Sample	CaO	SiO_2	MgO	Al_2O_3	Fe_2O_3
OPC	65.04	20.71	1.03	4.83	2.77
PFA	3.36	46.96	1.76	23.71	11.33
Deinking Ash	37.69	33.76	3.72	20.12	0.03
MSWI-b	22.62	10.32	1.61	5.30	0.95
MSWI-f	35.89	15.29	1.29	6.25	1.11
GGBS	41.38	34.59	6.84	14.02	1.51
Stainless Steel Slag	46.66	27.92	9.75	2.91	1.22

Besides bulk chemical composition, important factors affecting the reactivity of industrial residues towards CO_2 are mineralogy and particle size distribution. As previously mentioned, free oxide and hydroxide phases such as lime, portlandite and periclase (MgO) are very reactive with CO_2 even at mild operating conditions, while the reactivities of many of the different Ca and Mg containing silicates detected in alkaline industrial residues vary greatly in dependence of the types of crystal phases and of the presence of inclusions of various elements, such as Al, Cr and Fe etc., in the crystal lattice. Particle size, as indicated in the previous section, is one of the controlling factors of the dissolution kinetics of any kind of mineral or anthropogenically derived material. For the residues generated as by-products of flue gas treatment units, cement kiln dust and other ashes or particular products of industrial refining processes, average grain particle sizes (generally <100-150 μm) are already in the optimum range for carbonation treatment, whereas slag residues from combustion processes or scraps from construction and demolition activities present a wider particle size distribution curve and a significant percentage of coarse particles.

Hence, unlike carbonation processes applied to geologically derived minerals, one of the fundamental aspects of accelerated carbonation investigations on alkaline industrial waste materials is the physical, chemical and mineralogical characterization of the residues for the identification and quantification of the reactive phases. Other factors of primary importance are the relative abundance of each waste stream, which determines the overall potential impact of the accelerated carbonation technique as a CO_2 mitigation strategy, and the environmental behaviour of the industrial residues.

Both these issues may vary from country to country as a function of many factors including: the main features of the industrial and energy sectors, available natural resources, implemented waste management strategies, adopted waste residue disposal and flue gas treatment technologies, as well as landfill disposal criteria. Thus, for this reason accelerated carbonation has been applied to such a variety of residues as a technique to achieve different objectives in different countries. For example, in Estonia most of the energy demand is supplied by oil shale combustion, which emits significant amounts of CO_2 (emission factor of 29.1 tC/TJ) along with large amounts of alkaline oil shale ash, thus making CO_2 sequestration via carbonation of oil shale ash a very attractive process (Uibu, 2008); in Flanders instead, stringent legislative landfill acceptance criteria related to the leaching of specific heavy metals (such as Cu, Zn and Pb, in particular) do not allow MSWI residues to be directly landfilled even after natural weathering periods, hence accelerated carbonation studies have been specifically undertaken to improve the chemical stability of these residues (Van Gerven et al., 2005a,b; Arickx et al., 2006).

Accelerated carbonation of alkaline solid waste has been up to now primarily investigated through the direct aqueous route (see e.g. Reddy et al., 1994; Fernández-Bertos, 2004b; Van Gerven et al., 2005b; Huijgen and Comans, 2006; Li et al., 2007; Back et al. 2008; Uibu et al., 2009), or to a lower extent by means of the direct gas-solid reaction, applied only to materials with high lime and portlandite contents (Jia and Anthony, 2000; Baciocchi et al., 2006a; Prigiobbe et al., 2009a). Carbonation of residues does not generally require the extraction of alkaline metals from the solid matrix, since the main reactive species are Ca-containing silicates, oxides and hydroxides. These minerals, as earlier mentioned, behave differently from those containing Mg, as hydration, solvation and carbonation of Ca-bearing phases can be carried out under the same operational conditions in a one stage operation.

Aqueous accelerated carbonation studies have been performed in two different modes, either in slurry phase with liquid to solid (L/S) ratios above 5 w/w (Stolaroff et al., 2005; Huijgen et al., 2005; Back et al., 2008; Bonenfant et al., 2008a,b; Lekakh et al., 2008a,b; Pérez-López et al., 2008; Montez-Hernandez et al., 2009), in particular for waste materials of low solubility in which CaO is generally bound as a silicate, or humidifying the material with small amounts of water so to set the L/S ratio below 1.5 w/w, by (Reddy et al., 1991; 1994; Tawfic et al., 1995; Fernández-Bertos, 2004b; Polettini and Pomi, 2004; Rendek et al., 2006; Li et al., 2007; Huntzinger et al., 2009; van der Laan et al., 2008; Uibu et al., 2009). This latter type of treatment in which the CO_2 and Ca and Mg ions dissolution, as well as carbonation reactions, occur in the thin liquid film in direct contact with the solid residues, has been originally applied for cement curing processes (see e.g.: Young et al. 1974; Papadakis et al., 1991) and has hence been used as a carbonation route also for industrial residues that present high contents of soluble elements such as salts and heavy metals, so to avoid the treatment and disposal of the processing liquid, as well as to favour dissolution kinetics at moderate operating conditions.

Accelerated carbonation of specific waste residues, characterized by high contents of silicate phases, such as various types of steel slag or cement waste residues, has been also tested applying the indirect aqueous route to slurry suspensions, separating the dissolution and precipitation steps so to optimize each set of reactions by operating on the pH, dosing specific additives, similarly to the previously described pH swing process, (Kodama et al., 2006 and 2008; Teir et al., 2007; Eloneva et al., 2008a,b) or by varying some of the operating parameters, such as CO_2 pressure (Iizuka et al., 2004).

Depending chiefly on the main composition of the residues, the chosen process route, and also the final aim of the study (CO_2 sequestration or chemical stabilization), a variety of operational conditions have been applied and quite different results in terms of CO_2 uptake have been achieved.

The effects of accelerated carbonation on the leaching behaviour of pulverized coal fly ash and oil shale ash was first analyzed by Reddy et al. (1991; 1994). Treating the humidified samples (20% moisture) with 100% CO_2 at around 3 bar for 120 hours, lowered the pH of the residues from 12.3-12.8 to 8.8-9.7 and caused calcite precipitation (Reddy et al., 1994). Carbonation also showed to decrease the leaching of Mn, Cd, Pb and Zn for the fly ash and oil shale samples tested by Reddy et al., 1994. In an earlier study the leaching of F and Mo

was indicated to decrease as a result of accelerated carbonation treatment (Reddy et al., 1991). Tawfick et al. (1995) studied the effects of accelerated carbonation on the pH and heavy metal leaching of humidified CCT fly ash. Results showed that significant pH reductions (of up to 5 units) could be attained in 24 hours by operating on reaction parameters, such as temperature, CO_2 pressure and sample humidity. XRD analyses of fresh and treated ash showed the decrease in Ca oxide and silicate phases and an increase in calcite and gypsum ($CaSO_4 \cdot 2H_2O$) after the treatment with CO_2; a decrease in the leaching of As, Cd, Pb and Se was also reported (Tawfick et al., 1995).

Carbonation of coal and petroleum coke FBC fly ash was also studied applying the gas-solid route (Jia and Anthony, 2000). The experiments were carried out in a pressurized thermogravimetric analyzer (PTGA) at 1 or 11 bar of CO_2; hydrated ash was found to react faster with CO_2 than nonhydrated ash, presenting also a higher final CaO to $CaCO_3$ conversion ratio (60% compared to 27.4% respectively), owing to the effects of hydration on increasing the ash surface area (Jia and Anthony, 2000). Carbonation reactions showed to occur in the temperature range 300-600 °C for hydrated ash and in the range 400-700 °C for the unhydrated ash, while CO_2 pressure did not show to exert a significant effect on carbonation kinetics or the final calcium conversion yield (Jia and Anthony, 2000).

Recent slurry phase carbonation experiments carried out on fly ash from coal combustion power plants showed a high reactivity of the lime content of the ash (over 80%) with pure CO_2 at 30 ºC and atmospheric pressure for 2 hours; owing to the limited amount of CaO in the ash though, a CO_2 sequestration capacity of only 26 g CO_2/ kg ash was reported (Montes-Hernandez et al., 2009).

For oil shale ash carbonation, 89-100% and 48-73% extents of carbonation were reported for experiments conducted on CFBC ash and PFA respectively, introducing pure CO_2 into an aqueous solution at atmospheric pressure and room temperature for 20-40 minutes (Uibu, 2008). Lime was found to be the main CO_2 binding component, but also periclase and Ca-silicates ($CaSiO_3$ and Ca_2SiO_4) were taken into account for calculating the maximal binding potential of oil shale ash (Uibu, 2008).

For lignite fly ash, a significantly higher uptake of CO_2 (230 g CO_2/ kg ash, with a Ca conversion yield of 75%) was measured in a slurry system at 75 ºC, 0.1 bar of 100% CO_2, for over 4 hours (Back et al., 2008); the authors assessed that this result could account for a

CO_2 sequestration capacity of 3.5 million tons of CO_2, corresponding to around 2% of the CO_2 emissions from lignite power combustion in Germany (Back et al., 2008).

The CO_2 sequestration capacity of cement kiln dust (CKD) treated with humidified CO_2 was recently assessed in batch and column tests at ambient temperature and pressure (Huntzinger et al., 2009). The predominant reactive phase was $Ca(OH)_2$ and the extent of carbonation with time was found to follow the unreacted core model theory (Shih et al., 1999), in which reaction kinetics is controlled at early times by a first order rate constant, which indicates kinetics control by the chemical reaction, and at longer times by a zero order constant, so that the extent of carbonation tends to a maximum value (70-80% of the maximum Ca conversion yield to calcite) induced by diffusion control, due to the coverage of the reacting particle surface by the reaction product, i.e. calcite (Huntzinger et al., 2009). A sequestration extent of over 60% was observed within 8 hours and the authors estimated that applying this process a 6.5% emission reduction in U.S. cement related emissions could be attained (Huntzinger et al., 2009).

Compositions similar to those indicated in the previous study for cement kiln dust (around 50% $Ca(OH)_2$) were indicated also for paper mill waste, which allowed to achieve a CO_2 net uptake of 218 g CO_2/kg paper waste, with pure CO_2 at 30 ºC and atmospheric pressure for 2 hours. A sequestration potential of round 15,000 tons of CO_2 for an average size cellulose pulp factory was estimated (Pérez-López et al., 2008).

Studies on the CO_2 sequestration capacity of bauxite residues (red mud) showed a CO_2 uptake of 40 g CO_2/ kg residues for red mud slurries with L/S = 10 kg/kg at 20 ºC and ambient pressure, bubbling 15% vol. CO_2 with a flow rate of 5 ml/min for up to 24 hours, which was attributed to the complete carbonation of the Ca and Na (hydr)oxides contents of the residues (Bonenfant et al., 2008b).

Iizuka et al. (2004) proposed to apply pressurised CO_2 for carbonating waste cement. The proposed process consists in a first step in which calcium is extracted from waste cement in an aqueous solution using pressurised 100% CO_2, and a second step after the extraction in which the pressure is reduced causing the extracted calcium to precipitate as calcium carbonate. Experiments showed that up to 50% of the calcium in waste cement could be extracted with a CO_2 pressure of 9-30 bar (Iizuka et al., 2004).

Stolaroff et al. (2005) studied an indirect route by which the $Ca(OH)_2$ and CaO contents of steel slag or concrete waste could be dissolved in water and carbonated with atmospheric

CO_2. Experimental results showed that a major part of the available calcium dissolved in a time scale of hours, which was taken to be sufficiently fast for use in an industrial process. No carbonation experiments were performed. The authors however proposed a carbonation process in which an aqueous solution is sprayed over a bed of slag or concrete waste to dissolve CaO and $Ca(OH)_2$ from the alkaline solids and then drops into a pool underneath the bed, from which the solution is recycled through the sprayers. The saturated solution absorbs CO_2 from the air, producing $CaCO_3$ that precipitates and allows more CaO and $Ca(OH)_2$ to dissolve. The operating cost of this scheme was estimated to be 8 US$/tCO2 sequestered (excluding the transportation costs of the slag). However, using steelmaking slag as raw material would increase the total costs by 25 US$/t$CO_2$ (calculated using a market price of 8 US$/t steelmaking slag) (Stolaroff et al., 2005).

Accelerated carbonation tests were also applied to dicalcium silicate and Portland cement to examine the effects of the process on the microstructural properties of the material (Shtepenko et al., 2006). Carbonation experiments were carried out in a batch reactor contacting the humidified material (L/S = 0.1 l/kg) with 100% CO_2 at 2 bar and ambient temperature for 1 hour. After the treatment, the material was dried at 40 °C, milled for 2-3 minutes and then recarbonated. This procedure was repeated 5 times, so to mechanically activate the material by reducing the product layer (defined also as passivating layer) which coats the particles of the reacting material and acts as a diffusion barrier, inhibiting the advancement of the carbonation reaction. CO_2 uptakes of 480 and 370 g CO_2/kg residue were measured for Ca_2SiO_4 and PC respectively, with corresponding conversion efficiencies of 96 and 76% (Shtepenko et al., 2006). XRD spectroscopy analyses showed that, upon exposure to CO_2, the original crystalline structures decomposed and calcite and aragonite formed, whereas no crystalline silicate reactions products were detected. A polymerized silicate product was instead identified by NMR analysis, particularly for dicalcium silicate (Shtepenko et al., 2006).

1.4.1 Accelerated carbonation of MSWI bottom ash

[1]MSWI bottom ash (BA) can be characterized as a heterogeneous mixture of slag, ferrous and non ferrous metals, ceramics and other non-combustible materials (IAWG, 1997). Excluding oversized material (>10 cm), particle size is generally quite uniform and BA can be classified as well gradated sand and gravel. Porosity and specific surface area are very high, due to the expelling of gas from the material in a molten state, whereas moisture contents can vary quite considerably depending on quenching procedures.

BA is alkaline in nature, with pH values ranging from 9.5 to 11.5, and contains alkaline and alkaline earth elements and metal oxides which form hydroxides during hydrolysis. The elemental composition of BA depends primarily on the composition of the feed stock and on the type, capacity and operational temperature of the furnace. The major elements (> 10 g/kg) in MSWI BA are O, Si, Fe, Ca, Al, Na, K, Mg and C. Trace elements commonly detected in BA include Ba, Cr, Sn, Ni, Mn, V, Co and Sb (Hjelmar, 1996). The more volatile trace elements (Cd, Hg, As, Pb and Zn) are generally present in relatively low concentrations in BA and are rather concentrated in fly ash and air pollution control (APC) residues, although some exceptions have been reported, e.g. a study on metal distribution in Japanese ash residues reported that two thirds of the total waste content of Pb and Zn were found in BA (Jung et al., 2004).

Mineralogical studies indicate that the main crystalline phases of BA are silicates (quartz, gehlenite, augite, etc.), sulphates (mainly anhydrite, ettringite and gypsum), carbonates (calcite, metal carbonates), to a lower degree metal oxides and hydroxides (magnetite, hematite, etc.) and chlorides (Kirby and Rimstidt, 1993; IAWG, 1995; Eusden et al., 1999; Speiser et al., 2000). The overall solubility of BA is relatively low when compared to the other residue streams and is mostly due to calcium and sodium salts, i.e. NaCl, $CaCl_2$ and $CaSO_4$ (IAWG, 1997). BA is typically classified as a non-hazardous waste according to the European Waste Catalogue, and has therefore a high recycling potential. It is currently being used as an aggregate substitute in road bases and bituminous pavements in several European countries (e.g., the Netherlands, Denmark) (IAWG, 1997; Astrup at al., 2007). BA has potential to be used in concrete bricks to replace sand and gravel, but its wider use is controlled by the leaching of heavy metals, which must not exceed regulatory limits.

As previously mentioned, the carbonation of BA has been investigated to produce mineralogical changes similar to those occurring as a result of natural weathering and to

[1]Most of this section was published in Costa et al., 2007.

induce a reduction in trace metal mobility (Meima et al., 2002; Polettini and Pomi, 2004; Van Gerven et al., 2005b). Some studies have also focused on the principal carbonation mechanisms and controlling operating parameters, such as temperature, CO_2 partial pressure, water content, residence time as well as particle size (Fernández-Bertos et al., 2004b; Rendek et al., 2006a). Rendek and co-workers showed that, due to the presence of unburned organic material, microbial activity can be detected in MSWI BA and they hypothesized that atmospheric CO_2 augmented by the CO_2 produced during biodegradation processes, might account for the stabilization of BA during carbonation (Rendek et al., 2006b).

Table 1.2 gives a summary of the main operating conditions applied in the accelerated carbonation studies reported in the literature. The exclusively adopted carbonation route was the direct aqueous process, however different water contents were used, with values of the water-to-solids ratio either in the low range (typically 0.05-0.6 w/w), or in the range corresponding to slurry-phase conditions (typically 5-20 w/w). Other operating parameters were typically: pressure, from atmospheric to 17 bar, temperature, between ambient and 50 °C, CO_2 percentage, from 0.03 to 100%, and residence times, from a few hours to a few weeks.

Pre-treatment of materials consisted mainly of drying, sieving and grinding. Generally only the size fraction from 0.1-4 mm was investigated, since presumably larger particles are less reactive towards CO_2 on account of their chemical composition (lower CaO and higher SiO_2 content) (Speiser et al., 2000; Rendek et al., 2006a) and lower specific surface area.

The mechanisms involved in the carbonation of MSWI BA have not been completely elucidated so far; however on the basis of the mineralogical characteristics of the ash prior to and after accelerated carbonation, it is possible to hypothesise the reactive phases involved and their carbonation pathways.

Table 1.2 Summary of the operating conditions applied for accelerated carbonation experiments on MSWI BA reported in the literature.

Material type	Carbonation conditions					Reference
	CO_2 conc.	Pressure	Temperature	Duration	Water content	
MSWI BA	10% vol.	atmospheric	50°C	1 h, 2 h, 3 h, 6 h, 1 d, 2 d, 3 d, 1 w, 2 w , 3 w, 4 w	natural moisture content (initial)	Arickx et al., 2006
MSWI BA	100% vol.	not specified (slight overpressure)	ambient	20 min, 40 min, 1 h, 3 h, 6 h	not specified	Bodénan et al., 2000
MSWI BA	100% vol.	atmospheric	ambient	not specified	not specified	Bone et al., 2003
MSWI BA	20% vol.	not specified	37°C	2 h, 6 h, 1 d, 7 d	6.4%	Cornelis et al., 2006
MSWI BA	20% vol. (CO_2-enrich. air)	atmospheric	not specified	24 h	not specified	Dijkstra et al., 2006
MSWI BA	100% vol. (R.H. 65%)	3 bar	ambient	0-400 min	0-60 %.	Fernández Bertos et al., 2004b)
MSWI BA	0.03% (atmosp. air)	atmospheric	ambient	3–4 d	slurry phase (L/S 5 w/w)	Meima et al., 2002
MSWI BA	100% vol. (water-satur. CO_2 flow)	atmospheric	ambient	24 h, 48 h	not specified	Polettini and Pomi, 2004
MSWI BA	100% vol.	atmospheric	ambient	24 h, 48 h	slurry phase (L/S 10)	Polettini et al., 2005
MSWI BA	100% vol.	2, 3, 5, 7, 11, 17 bar	ambient	0–180 min	5-25% (initial)	Rendek et al., 2006a
MSWI BA	100% vol.	atmospheric	ambient	27 d (+49 d)	natural moisture content (initial)	Todorovic and Ecke, 2006
MSWI BA	10% vol., 20% vol.	not specified	30°C, 37°C, 50°C	1 h, 2 h, 3 h, 1 d, 2 d, 3 d, 6 d/7 d,	2.3%, 6%, 13%, 25%, 37%, 50% (initial)	Van Gerven et al., 2005b
MSWI BA	0.03% (atmosp. air)	atmospheric	40°C	1 h, 2 h, 3 h, 1 d, 2 d, 3 d, 6 d/7 d	6% (initial)	Van Gerven et al., 2005b

Effects of carbonation on BA mineralogy

Speiser et al. (2000) studied the mineralogical composition of deposited MSWI BA and argued that hydrated calcium silicate may form as a result of the reaction between $Ca(OH)_2$ and SiO_2. A number of other potential reactive phases for carbonation, including olivine, wollastonite, feldspar and dicalcium silicate were also detected (Kirby and Rimstidt, 1993;

Eusden et al., 1999; Fernández-Bertos et al., 2004b). XRD analyses of carbonated MSWI BA (Fernández-Bertos et al., 2004b; Polettini and Pomi, 2004) showed an increase in the amount of calcite and quartz, a decrease in corundum and the disappearance of ettringite upon carbonation. The formation of quartz as a result of carbonation can be explained by the dissolution of calcium silicate and consequent precipitation of calcite, thus increasing the availability of silicate ions, which form quartz or amorphous aluminosilicates (Meima et al., 2002).

The fate of Al-containing minerals as a result of the decreased pH of carbonated BA was discussed by Zevenbergen and Comans (1994). Under the pH conditions pertaining, Al can be precipitated into a number of mineral phases, which may include amorphous Al (hydr)oxides, with lower amounts of aluminosilicate minerals (Meima et al., 2002). The dissolution of ettringite upon carbonation has been observed by several authors (Zevenbergen and Comans, 1994; Meima and Comans, 1997; Meima et al., 2002; Polettini and Pomi, 2004) and may result in increased sulphate leaching (Bodénan et al., 2000; Polettini and Pomi, 2004). However, the fate of sulphates during the carbonation process has not been fully explained. Fernández-Bertos et al. (2004b) reported an increase in gypsum detected during XRD analyses; Meima et al. (2002) did not find any evidence of gypsum precipitation in carbonated BA and Polettini and Pomi (2004) showed a decrease in the amount of anhydrite in accelerated carbonated BA.

Effects of carbonation on BA leaching behaviour

A number of workers have focused on the effects of accelerated carbonation on the leaching of trace metals from bottom ash. In general the multiple reaction mechanisms occurring during carbonation are accompanied by surface interactions between trace contaminants and neo-formation minerals and these will impact on the mobility of trace metals. The specific properties of individual trace metals, their solubility curves, and behaviour as a function of pH and Eh and their affinity for such minerals as calcite and Al and Fe (hydr)oxides are important.

The fate of major elements during accelerated carbonation is of particular relevance in that the chemistry of major species of BA has been shown to be capable of affecting the behaviour of trace contaminants in fresh, naturally weathered and accelerated aged BA (Zevenbergen and Comans, 1994; Meima and Comans, 1997 and 1999). Ca leaching at alkaline pH values has generally been found to decrease for carbonated BA as a result of

solubility control by calcite (Zevenbergen and Comans, 1994; Meima and Comans, 1997 and 1999; Bone et al., 2003; Polettini and Pomi, 2004; Polettini et al., 2005), which is less soluble than ettringite and portlandite.

Carbonation has also been variously reported to result in increasing the amount of amorphous Al (hydr)oxides (Dijkstra et al., 2006) or to have little effect (Cornelis et al., 2006). The same investigators found no appreciable effect of carbonation on precipitation of Fe (hydr)oxides.

Among the heavy metals which are immobilised by accelerated carbonation, Pb and Zn are particularly relevant. A strong reduction in both Pb and Zn release from carbonated BA has been reported by Fernández-Bertoz et al. (2004b). Zn released from two BA samples during the EN 12457 leaching at L/S 10 l kg^{-1} decreased from around 10 mg kg^{-1} to less than 1 mg kg^{-1}, while the release of Pb from the same samples decreased from initial values of about 50 and 100 mg kg^{-1} to less than 1 mg kg^{-1}. A significant decrease in Zn and Pb leaching, by one and two orders of magnitude respectively, was observed by Bone et al. (2003) under the same leach testing conditions, by Arickx et al. (2006) using the EN 12457-2 and NEN 7343 (column test) leaching procedures, and by Bodénan et al. (2000) using the NF X31-210 test (L/S = 10 l kg^{-1} deionized water leaching in three steps each 16 hours-long). In studies on slurry-phase carbonation of BA, Polettini et al. (2005) measured Pb leachate concentrations below 50 μg kg^{-1}, applying the EN 12457 tests with L/S = 2 l kg^{-1} and L/S = 10 l kg^{-1}, while Zn concentrations were below 0.4 mg kg^{-1} as opposed to 0.9 mg kg^{-1} for the fresh BA. Leaching as a function of pH showed that the reduction in Zn was pH dependent, whereas for Pb, this resulted from a modified leaching curve, as compared to that of the fresh material. Geochemical modelling indicated strong undersaturation in eluates for both $Pb(OH)_2$ and Pb carbonate species, and the authors concluded that, as a consequence of slurry-phase carbonation, Pb was probably sorbed onto newly precipitated phases. Different results for Pb and Zn release were obtained by Van Gerven et al. (2005b) in L/S = 10 l kg^{-1}, 24-h deionized water leaching tests, for which carbonation did not show to affect Pb release, while Zn leaching increased with carbonation time. The application of the NEN 7345 diffusion leaching test on two accelerated carbonated BA samples by Todorovic and Ecke (2006) showed mobilization of both Pb and Zn.

The leaching behaviour of Cu is affected by accelerated carbonation, with most literature indicating immobilisation, although with different leaching characteristics. Van Gerven et al. (2005b) measured a change in Cu leaching (EN 12457, L/S =10 l kg^{-1}) from about 3.3 mg kg^{-1} for untreated BA to between 1.0 and 2.0 mg kg^{-1} at the end of the carbonation period (7 days), while the reduction found by Arickx et al. (2006) was from about 29 mg kg^{-1} to about 8 mg kg^{-1}. Meima et al. (2002) found that Cu concentrations in BA suspensions were reduced by about 50% upon carbonation. Similar shaped leaching curves for Cu were found by Van Gerven et al. (2005b) and Meima et al. (2002) (see Figure 1.3a and b), with a poor pH dependency of Cu release from carbonated BA. In other work, Arickx et al. (2006) indicated a stronger pH dependent leaching for Cu in 4-week old carbonated BA, with a one order of magnitude decrease in Cu concentration at the point of minimum solubility if compared to the untreated material (see Figure 1.3c); however, in the acidic pH range, the leaching from fresh and carbonated BA were coincident. In their study, Meima et al. (2002) also analyzed the composition of the precipitates formed during carbonation of filtered BA leachates and concluded that the reduction in Cu leaching was due to the precipitation of amorphous Al species, that typically display a very high affinity for this metal.

The findings by Polettini and Pomi (2004) and Polettini et al. (2005) indicated a very similar pH dependence of Cu leaching for fresh and carbonated BA (using both direct and slurry-phase carbonation) for pH values below the natural pH of the carbonated material (pH around 8.3) (see Figure 1.3 d). Since the natural pH of fresh bottom ash was around 10 units (i.e., already in the range of minimum solubility), the reduction to about 8.5 as a consequence of carbonation resulted in an enhanced Cu release, although there may have been other mechanisms potentially controlling Cu leaching in the pH range 8.5-10. Further indications on the mechanisms of Cu release from carbonated BA were provided by Dijkstra et al. (2006), who observed similar shapes of the leaching curves for the untreated and carbonated material in the acidic to neutral pH range, while a consistently lower Cu leaching from carbonated BA between pH 7.5 and 10, thus confirming the results obtained by Arickx et al. (2006).

Speciation modelling calculations involving Cu complexation by Fe and Al (hydr)oxides and humic substances, showed that at pH > 7 the leaching of Cu is controlled by sorption on humic acids and that the positive effect of carbonation on Cu release in the alkaline pH

range is mainly related to the change in leaching of such species, augmented by an enhanced adsorption onto Fe/Al (hydr)oxides (Dijkstra et al., 2006).

A contrasting Cu leaching behaviour of BAs from different incineration plants was found by Todorovic and Ecke (2006), who reported both the effects of mobilization and immobilization of Cu as a result of carbonation.

In the absence of detailed information on the mineralogy of BA prior and after carbonation treatment, the inconsistencies in the literature cannot be explained. However, the different initial composition of the materials investigated may be important, as are the particular carbonation process conditions (Van Gerven et al., 2005b) which were found to result in decreased Cu leaching by 2-3 times, as compared to carbonation with atmospheric air.

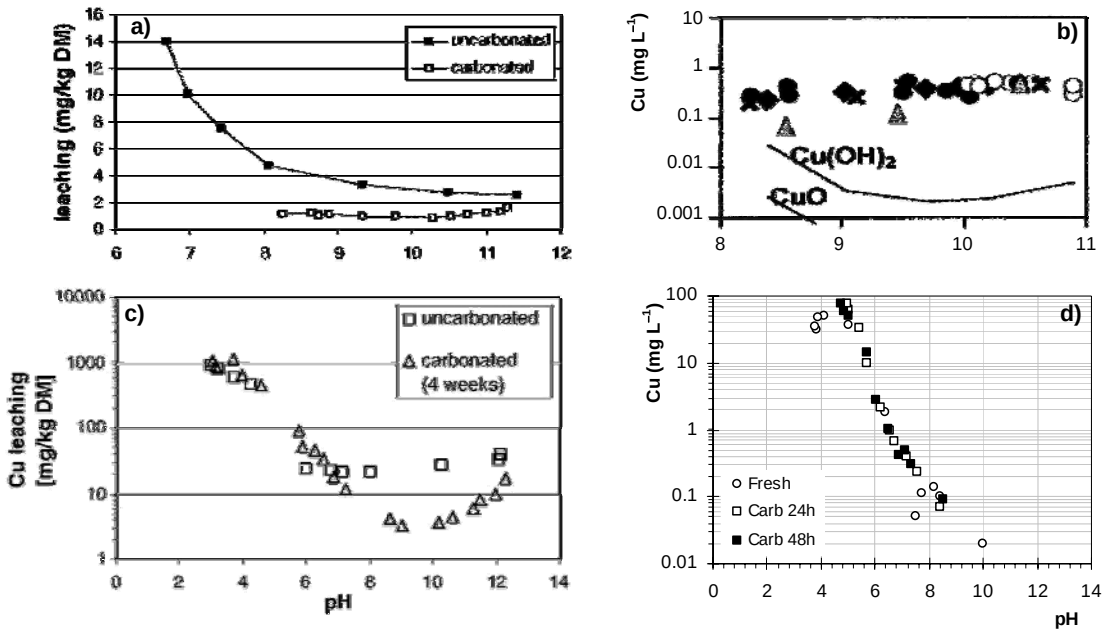

Figure 1.3 Cu leaching from carbonated BA as a function of pH reported in different literature studies: a) Van Gerven et al. (2005b); b) Meima et al. (2002) (○ = uncarbonated BA; ◆/● = carbonated BA suspensions; ✕ = carbonated filtered BA leachates, ▲ = 1.5-y old BA); c) Arickx et al. (2006); d) Polettini et al., (2005)

The leaching behaviour of typical oxyanion-forming metals such as Cr has been investigated by several workers. Bone et al. (2003) report that, while Cr leaching from fresh BA was in the order of 1 to 10 μg l^{-1}, Cr concentrations in the eluate from carbonated BA ranged from 10 to 100 μg l^{-1}. A mobilization effect of Cr was also indicated by Van Gerven et al. (2005b), although the maximum release appeared to occur after 6 h of

carbonation, and for longer treatment durations Cr leaching was shown to decrease again. A similar result was obtained by Polettini et al. (2005) for slurry-phase carbonation of BA, where Cr leaching was found to increase by two to three times after the application of the process, although the mobilization effect was reduced by prolonged carbonation times. Rendek et al. (2006a), however, reported immobilization of Cr, with a decrease in leachate concentration (deionised water, L/S = 10 l kg^{-1}, 24 h) from 0.022 to 0.005 mg l^{-1}, whereas Arickx et al. (2006) reported a very weak or even absent carbonation effect on Cr immobilization.

An attempt to explain the mechanisms of Cr leaching from carbonated as opposed to fresh BA was given by Van Gerven et al. (2005b) in their study on pH-dependent Cr leaching. They found that in the pH range 8-11.5, Cr leaching was lower for carbonated with respect to untreated BA. This was linked to the acidic pH range resulting from carbonation which leads to sorption of anionic species including chromates onto the surface of Al and Fe (hydr)oxides precipitates in BA. The influence of the operating conditions on Cr leaching showed that an increase in CO_2 concentration yielded higher Cr release, while an increase of the treatment temperature improved Cr leaching (Van Gerven et al., 2005b).

The other oxyanionic metals Mo and Sb were shown to be affected by carbonation in different ways. Van Gerven et al. (2005b) found that while Mo leaching remained approximately constant during carbonation and appeared not to be appreciably affected by changes in pH (as also reported by Meima et al., 2002 and Bone et al., 2003), Sb was mobilized, with eluate concentrations increasing by a factor from two to three as the carbonation degree increased. Conversely, the study by Todorovic and Ecke (2006) indicated a slight reduction in Sb release during diffusion leaching of carbonated BA.

The pH-dependent leaching behaviour of Mo (see Figure 1.4) was investigated by Van Gerven et al. (2005b) and Dijkstra et al. (2006) and showed a large decrease in Mo release from carbonated BA between pH 6 and 10, with a positive effect of carbonation in the pH range 8-11 associated to increased amounts of Fe and Al (hydr)oxides as a result of carbonation.

The leaching behaviour of Sb was studied in detail by Cornelis et al. (2006). In untreated BA, Sb can be incorporated in ettringite formed after quenching. The effect of carbonation on the dissolution of ettringite was thought to cause the mobilization of Sb, whose solution concentrations become controlled by calcium antimonate, $Ca[Sb(OH)_6]_2$, at pH > 9. The

same authors noted that, in the pH range 6-8.6, Sb solubility was likely controlled by sorption onto amorphous Fe (hydr)oxides for both untreated and carbonated BA.

Dijkstra et al. (2006) investigated the fate of organic matter during carbonation. They indicated a consistent reduction in DOC leachate concentration over a wide pH range. The speciation of organic matter in the eluates showed a strong decrease in concentrations of fulvic acids over the entire pH range investigated (2-12). Since the total amount of fulvic acids was not shown to be affected by carbonation and the degradation process of such substances has been shown to occur within timeframes of thousands of years (Petterson et al., 1994) it was hypothesized that adsorption onto the active surfaces of BA (presumably Fe and Al (hydr)oxides) could be the reason for decreased release of fulvic acids. Modelling studies using tentative equilibrium constants values for the surface complexation reactions involving fulvic acids with Fe (hydr)oxides indicated that the assumption was reasonable.

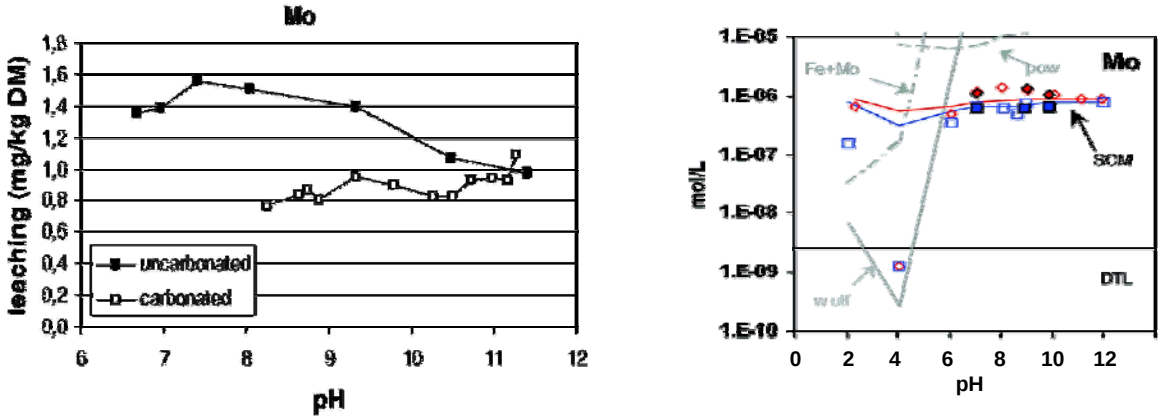

Figure 1.4 Mo leaching from carbonated BA as a function of pH as reported by: a) Van Gerven et al. (2005b); b) Dijkstra et al. (2006) (◆/◇ = fresh BA; ■/□ = carbonated BA; Fe+Mo = ferrihydrite + $Fe_2MoO_{4(s)}$; SCM = complexation to Fe/Al (hydr)oxides; pow = powellite; wulf = wulfemite).

Effects of BA carbonation on CO_2 uptake and influence of operating conditions

The sequestration potential of accelerated carbonation of BA is influenced by the main operational parameters governing the carbonation process. CO_2 uptake potential is generally measured as the weight gain in treated BA after oven-drying, or as the decrease in CO_2 partial pressure in the reactor. Because of the possibility of hydration reactions occurring (Van Balen, 2005), TG is an appropriate method to quantify the increase in the calcium carbonate content of the material upon carbonation. Due to the metastability of

many mineral phases in BA, the temperature range at which calcium carbonate decomposes can be quite wide (600-900 °C) leading to inaccuracies in calcium content calculations. Therefore, coupling TG devices with gas chromatographic measurements of the evolved CO_2 could provide advantages (Baciocchi et al., 2006b). For BA, maximum values of weight gain upon carbonation w/w dry weight range from around 3% to 6.5% (Johnson, 2000; Fernández-Bertos et al., 2004b; Rendek et al., 2006a), but these are dependent on particle size and the source of BA.

The mechanisms involved in the carbonation of BA are not yet well known, due to the material's complex chemistry and mineralogy. However, it is likely that more than one alkaline oxide-containing mineral (including Ca and Mg silicates) reacts with CO_2 in addition to calcium hydroxide. Most of the studies hitherto reported have considered a simplified approach for the carbonation of $Ca(OH)_2$ via the aqueous route (Arickx et al., 2006; Rendek et al., 2006a).

The rate limiting steps of the carbonation reaction involve the dissolution of calcium from the solid matrix into the liquid phase and the diffusion of CO_2 into the pore system. Arickx et al. (2006) proposed a model for the diffusion of CO_2 from air to a porous solid and the reaction with Ca^{2+} in the liquid phase to calculate the change in pH occurring after accelerated carbonation (assuming pH control by the dissolution of $Ca(OH)_2$) .

The kinetics of CO_2 uptake, as previously reported discussing the results of accelerated carbonation tests on other industrial residues, is generally characterized by two reaction steps: 1) a first steep increase in the rate of CO_2 uptake with time, followed by 2) a decrease in the rate until an approximately constant value of CO_2 uptake is attained (Fernández-Bertos et al., 2004b; Van Gerven et al., 2005b; Rendek et al., 2006a). Huijgen et al. (2005) observed this trend for steel slag and assumed that the first reaction stage may involve 'faster' reacting minerals such as $Ca(OH)_2$; whereas the second stage may involve other, less reactive, minerals. Although a similar trend was found also for the carbonation kinetics of 'pure' materials such as $Ca(OH)_2$ or Ca_2SiO_4 (e.g: Shih et al., 1999; Shtepenko et al., 2006). Hence the specific surface of the reacting particles appears to be the controlling mechanism also for BA carbonation, so that the observed second reaction step may be due to diffusion control by product layer coating of the reactive surface of the particles. The degree of carbonation achieved (or process efficiency) should be calculated as the conversion to calcium carbonate of all Ca-reacting species found in the feed-stock,

although it should be recognised that some uncertainty remains as to which silicate mineral phases contribute to CO_2 binding.

Fernández-Bertos et al. (2004b) found that, under specific reaction conditions, 75% of the carbonation reaction took place in the first 2.5 hours and therefore they selected this time interval as the optimum reaction time. However, the main process-related parameters were found to be: sample water content, particle size, temperature and CO_2 partial pressure.

Particle size has been identified as an important process parameter, since the fine fractions are often enriched in Ca. Rendek and co-workers (2006a) found that 4mm-sieved material had double the CO_2 uptake when compared to the unsieved material. Fernández-Bertos et al. (2004b) found similar results but related the higher CO_2 uptake to the increased surface area of the smaller particles, indicating 710 μm as the optimal size fraction for carbonation (weight gain around 3% w/w).

The efficacy of accelerated carbonation via aqueous-based processes is dependent upon the water content employed. As water content increases, a critical liquid to solid ratio, characteristic of the material, is reached and then carbon dioxide uptake diminishes. Although water is necessary to hydrate and solvate CO_2 and Ca^{2+}, when it exceeds the pore capacity of a material it forms an inter-granular film and hinders CO_2 diffusion. For BA carbonation, optimum L/S values of 0.18 and 0.3-0.4 l kg^{-1} have been reported (Rendek et al., 2006a; Fernández-Bertos et al., 2004b, respectively).

The effect of other process parameters such as temperature and CO_2 partial pressure has not been extensively examined up to now; however Rendek et al. (2006a) noted that the time required for achievement of complete carbonation decreased from over 2 days to 3.5 hours when the partial pressure of CO_2 increased from 2 to 17 bar.

Van Gerven and co-authors (2005b) have studied the influence of process parameters on leaching behaviour and found that an increase in CO_2 from atmospheric levels to 20% decreased Cu leaching, but increased, for example, Cr and Sb leaching. Whereas, increasing temperature from ambient levels to 50 °C reduced or stabilized the leaching of contaminants from the material. They also concluded that moisture contents of 13 and 25% gave the lowest leaching concentrations.

Authors agree (Van Gerven et al., 2005b; Baciocchi et al., 2006c; Rendek et al., 2006a) that the CO_2 uptake potential of MSWI BA could reduce CO_2 emissions by only 0.4-1% (0.4, 0.5 and 0.5-1% respectively). However, with the primary aim of accelerating BA

natural weathering, incinerator stack gas emissions, which normally contain around 10% CO_2, could be blown into BA stockpiles (Steketee et al., 2006) or supplied to BA in a counter-current mode (Arickx et al., 2006) or in a closed reactor with mixing equipment (Sakita et al., 2006). One of the main problems that occur when stack gas is carbonated via the aqueous process (temperatures ranging from ambient to approximately 50 °C) is, as reported by Arickx and co-workers (2006), the condensation of the water contained in the gas which leads to the soaking of the BA media and hence to a reduction in process efficiency. Sakita and co-workers (2006) solved this problem by using a heat exchanger to decrease the water content of the stack gas prior to carbonation.

1.4.2 Accelerated carbonation of MSWI air pollution control residues

[1]Solid residues generated from flue gas treatment consist in a heterogeneous mixture of the excess sorbent material injected into the stack gas (mainly activated carbon and lime), flue gas condensation and reaction products and, when not captured upstream, combustion fly ash. Fly ash particles are generally larger (40-200 μm) than treatment sorbent particles (10-40 μm). The particle size is usually lower for semi-dry scrubber systems involving fabric filters (IAWG, 1997).

The porosity of APC ash is very high when excess amounts of activated carbon are injected into the stack gas as during, for example, hazardous waste incineration. The pH of residues from dry and semi-dry APC systems is typically >12, due to the significant lime excess additions used for flue-gas treatment; APC ash is hence typically characterized by a high buffering capacity.

The major elements found in APC residues are Ca, Cl, Si, Al, Na, K, S, Mg, Fe, O. High levels of volatile elements, such as Cd, As, Hg, Pb and Zn, may be present (Hjelmar, 1996) together with soluble salts (mainly chloride and sulphate salts), therefore APC residues are classified as hazardous waste according to the European Waste Catalogue.

Calcium and chloride containing compounds make up around 75-95% w/w of APC residues, whereas the remaining species are H_2O, organic carbon, iron oxides, silicates and quartz. The main crystalline phases detected by XRD are $Ca(OH)_2$, $CaSO_4$, silicates and alluminosilicates, carbonates (calcite, metal carbonates) and salts (mainly NaCl, KCl, CaClOH and Na_2SO_4) (IAWG, 1997; Bodénan et al., 2003; Fernández-Bertos et al., 2004b). Mineralogical investigations have shown that CaClOH is the main crystalline

[1]Most of this section was published in Costa et al., 2007.

calcium and chloride containing phase (Bodénan et al., 2003). This is regardless of the type of flue gas treatment process, filtration mode and specific surface of the Ca-based sorbent and shows that, in both dry and semi-dry systems $Ca(OH)_2$ does not react completely with HCl, thus explaining why $CaCl_2$ is generally not readily detected by XRD analysis on APC ash (Bodénan et al., 2003; Li et al., 2007). From thermogravimetric analysis (TGA) of fresh APC residues two main weight changes have been generally identified between 25 °C and 1000 °C (see Figure 1.5a), a first on between 300 and 500 °C attributed to the dehydroxilation of phases such as $Ca(OH)_2$ and CaClOH and/or the combustion of organic compounds and a second one between 450-500 °C and 800 °C linked to $CaCO_3$ decomposition (Baciocchi et al 2006b; Li et al., 2007; Prigiobbe et al., 2009a).

APC residues from dry and semi-dry acid gas scrubbing units are characterized by a high soluble salt content (30-40% w/w) (Hjelmar et al, 1996), and thus require careful management to limit their environmental impact during final disposal; several treatment techniques have hence been applied to improve the chemical stability of APC ash, including physical/chemical separation, thermal processing and solidification and/or stabilization (Sabbas et al., 2003; Quina et al., 2008).

The application of accelerated carbonation to APC residues before landfilling may also be beneficial as carbonation has been shown to decrease the pH of alkaline materials to values corresponding to minimum solubility levels of specific metals and within defined regulatory limits (pH < 9.5) (Ecke, 2003; Fernández Bertos et al., 2004a). Furthermore, APC residues can have a high content of CO_2-reactive minerals (see Table 1.1) such as $Ca(OH)_2$ and CaClOH and therefore may have a useful CO_2 uptake potential (Fernández Bertos, 2004b; Baciocchi et al., 2006a,b; Prigiobbe et al., 2009a).

The accelerated carbonation of APC residues has been investigated via the aqueous route similarly to BA, with water contents ranging from 5 to 60% w/w (Johnson, 2000; Bone et al., 2003; Ecke, 2003; Fernández Bertos, 2004a; Li et al., 2007) and also via the direct gas-solid route (Baciocchi et al., 2006a,b; Prigiobbe et al., 2009a). The high content of soluble compounds of APC residues entails that slurry-phase carbonation is not considered viable.

Table 1.3 summarises the operating conditions adopted for the accelerated carbonation of MSWI APC residues; as it can be noted operating parameters varied quite considerably. For aqueous-based experiments, ambient temperature and atmospheric or slightly higher CO_2 pressure were generally used. For the dry route, atmospheric pressure or CO_2 partial

pressures typical of flue gas (0.1 to 0.5 bar) and temperatures ranging from 300 to 500 °C were adopted (Baciocchi et al, 2006a,b; Prigiobbe et al., 2009a). Residence time depended on the aims of the investigation, varying from a few minutes (for assessing process kinetics) to a few weeks, when the long-term effects of carbonation were being studied. APC ash was not normally pre-treated in any way.

Effects of carbonation on APC ash mineralogy

The content of the main CO_2 reacting species in APC residues ($Ca(OH)_2$ and CaClOH) was found to be significantly reduced upon carbonation (Fernández Bertos, 2004b; Li et al., 2007). During the advancement of the carbonation reactions, TG analysis showed an increase in sample weight loss in the temperature range corresponding to calcite decomposition (500-850 °C) (Baciocchi et al., 2006b; see Figure 1.5b).

Li et al. (2007) detected Si-Al-Ca compounds, such as gehlenite ($Ca_2Al_2SiO_7$), in carbonated APC residues, and considered this fact as an indication that hydration of the samples could have been occurring at the same time as carbonation.

As a result of the higher content of CO_2-reactive mineral species in APC ash, physical changes were generally reported as being more evident for these residues with respect to BA carbonated under similar conditions. Particle size has been indicated to increase due to particle agglomeration, while porosity, tortuosity and total pore size to decrease, probably due to $CaCO_3$ precipitation into the pore space (Fernández Bertos, 2004b;). Microstructural analysis also revealed notable differences in the morphology of carbonated and non-carbonated APC ash samples (Fernández Bertos, 2004b; Prigiobbe et al., 2009a). Untreated APC ash showed a complex microstructure in which the size and shape of individual grains was quite variable and in which the characteristic layer-like structure of Ca (hydr)oxide phases was generally evident; whereas for carbonated APC ash, larger grains and a reduced pore space were observed, with a more regular and "rounded out" particle morphology, typical of calcium carbonate particles (Prigiobbe et al., 2009a).

Table 1.3 Summary of the operating conditions applied for accelerated carbonation experiments on MSWI APC reported in the literature.

Material type	Carbonation conditions					Reference
	CO_2 conc.	Pressure	Temperature	Duration	Water content	
MSWI APC residue	0.03% (atmosp. air)	atmospheric	ambient	2–4 w	not specified	Astrup et al., 2005
MSWI APC residue	0.03% (atmosp. air)	atmospheric	ambient	4 w	not specified	Astrup et al., 2006a; Astrup et al., 2006b
MSWI APC residue	100% vol.	atmospheric	200 °C, 300 °C, 400 °C, 500 °C	6 h	0%	Baciocchi et al, 2006a
MSWI APC residue	100% vol.	atmospheric	300 °C, 400 °C, 450 °C 500 °C	0,5–48 h	0%	Baciocchi et al, 2006b
MSWI APC residue	100% vol.	atmospheric	ambient	not specified	25% (initial)	Bone et al., 2003
MSWI APC residue	0.03%, 50% vol.	atmospheric	20 °C, 60°C	4 d, 40 d	50% (initial)	Ecke, 2003
MSWI APC residue	100% vol. (65% R.H.)	3 bar	ambient	0–400 min	0-60 %.	Fernández Bertos et al., 2004b
MSWI APC residue	10%, 25%, 50%, 60%, 80%, 100% vol. (65% R.H.)	3 bar	10 °C, 23 °C, 43°C, 62 °C	0–200 min	30 %.	Fernández Bertos et al., 2006
MSWI APC residue	100% vol.	3 bar	ambient	24 h	not specified	Johnson, 2000
MSWI APC residue	100% vol. (75% R.H.)	3 bar	ambient	3 h	10-80 %	Li et al., 2007
MSWI APC residue	10%, 22%, 50% vol.	1 bar	350 °C, 400 °C, 450 °C 500 °C	2 h	0%	Prigiobbe et al., 2009a

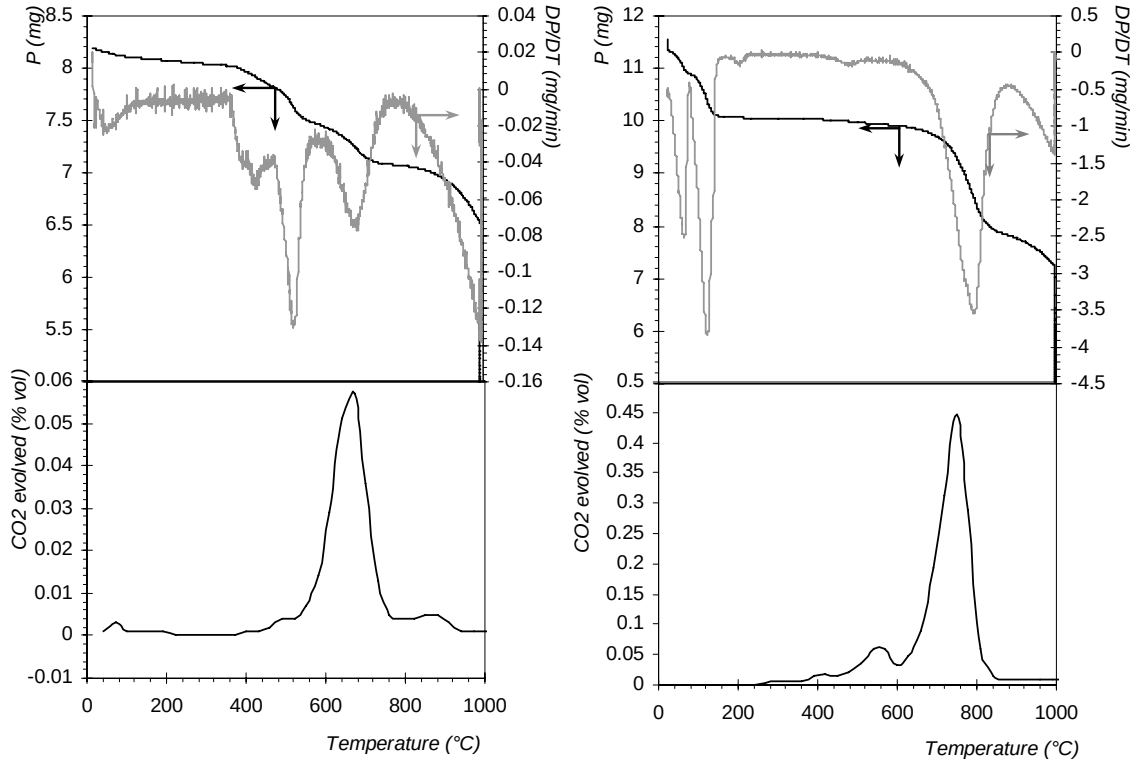

Figure 1.5 TGA/DTG results (top) and CO_2 evolved (bottom); (a) as received fly ash; (b) fly ash treated in CO_2 flux at 400°C (Baciocchi et al. 2006b).

Effects of carbonation on APC ash leaching behaviour

The changes in the physical, chemical and mineralogical properties of carbonated APC residues may influence leaching behaviour. Studies on the stabilisation of APC ash by carbonation have in fact recorded the modification of the leaching properties of these residues upon carbonation (Ecke, 2003; Fernández Bertos, 2004b).

In regard to the mechanisms controlling the leaching of trace metals from carbonated APC residues, the behaviour of major cations can help to understand the processes governing solution chemistry and pH conditions (Astrup et al., 2006b); for this reason, elements such as Al, Ca, Si, as well as S, have been investigated (Bone et al., 2003; Astrup et al., 2006a; Baciocchi et al., 2006a).

A comparison of the results obtained reveals that the change in contaminant leaching can be affected by the L/S ratio (which is a parameter that provides a measure of the leaching timeframe). It is also well established that pH is a key parameter determining metal release, so by evaluating pH dependent leaching properties, the processes controlling leaching at

various pH values, as well as the potential solubility-controlling phases for each contaminant of interest, can be elucidated.

Accelerated carbonation, as earlier described, induces mineralogical change in APC residues. For example, hydroxides conversion into carbonates results in a consequent lowering of pH which affects the solubility and leachability of many elements and enhances the acid neutralization capacity of the material. Thus, carbonation is likely to promote the retention of metals which are mainly mobilized at high pHs and to lead to a faster release of metals leached at moderate or low pHs (Astrup et al., 2006b).

Accelerated carbonation was found to reduce the release of Zn and Pb during the EN 12457 leaching test (Bone et al., 2003; Fernández Bertos et al., 2004b; Baciocchi et al., 2006a). Zn release from APC residues was equal to 100 mg kg^{-1} (Baciocchi et al., 2006a) and 20-100 mg kg^{-1} (Fernández Bertos et al., 2004b) before carbonation, while it decreased to 10 mg kg^{-1} (Baciocchi et al., 2006a) and to below 2 mg kg^{-1} (Fernández Bertos et al., 2004b) after carbonation. In the case of Pb, EN 12457 leaching test results indicated that, while Pb leachate concentrations ranged from 100 to 1000 mg kg^{-1} for fresh APC ashes, these were reduced by two or three orders of magnitude to, in some cases, below 1 mg kg^{-1} after carbonation (Fernández Bertos et al., 2004b; Baciocchi et al. 2006a).

Geochemical modelling (Astrup et al., 2006a) revealed that the U-shaped pH-dependency for Zn could not be attributed to smithsonite ($ZnCO_3$), which was undersaturated by more than one order of magnitude in the eluate, for both fresh and carbonated APC residues. A similar behaviour was observed for lead, even though cerrusite ($PbCO_3$) appeared to act as a solubility controlling mineral in the pH range 6-12.

For Cu, the shape of the leaching curve was not modified by carbonation The possibility that copper carbonate (malachite) precipitated in the eluates of carbonated APC ash was indicated. During EN 12457 leaching, Cu was reduced from approximately 0.6 mg l^{-1} for fresh ash to below 0.2 mg l^{-1} for carbonated ash (Baciocchi et al. 2006a), although in this case Cu release was ascribed to the reduction of pH towards the range of minimum solubility.

Cr leaching is more complex when compared to other metals in the case of both fresh and carbonated APC ashes; this may be explained considering mechanisms other than solubility control (Astrup et al., 2006a). The decrease in Cr concentration observed at high pH values can be due to hexavalent chromium incorporation into low-solubility minerals,

such as ettringite and Ba(S, Cr)O_4 (Astrup et al., 2006a). At pH values in the range 4.5-8.5, lower chromium leaching might be explained by the reduction of Cr(VI) to the less soluble form of Cr(III) by the Al(0) present in the APC ash (Astrup et al., 2005).

Effects of APC ash carbonation on CO_2 uptake and influence of operating conditions

The CO_2 uptake potential of APC residues is considerably greater than that of other MSW combustion residues. Values ranging from 7% (Fernández Bertos et al., 2004b) to 12-13% (Johnson, 2000; Baciocchi et al., 2006a) have been reported. Differences in values, however, probably depend on the carbonation conditions used in each study and the incineration facilities from which the APC residues were collected.

The mechanisms governing APC carbonation are more straightforward than those for BA carbonation, since in the former case the reactive species are almost entirely composed of portlandite and CaClOH. The kinetics of CO_2 uptake for APC residues show the same trend as for BA, though with higher weight gains, which are related to higher lime contents, specific surface area and microporosity (Fernández-Bertos et al., 2004b).

During carbonation of APC residues via the aqueous route, water content, particle size, temperature, CO_2 partial pressure and concentration have been indicated as the most important parameters affecting reaction kinetics and the final CO_2 uptake. Fernández-Bertos et al. (2004b) selected the 212 μm size fraction and L/S ratios of 0.2-0.3 w/w as the optimal values.

Fernández-Bertos and co-workers (2006) studied the influence of CO_2 concentration and temperature on CO_2 uptake in APC residues and showed that as the % CO_2 increased, higher CO_2 uptakes were recorded, although the conversion achieved at a 50% v/v CO_2 was only 5% lower than that measured for a 100% CO_2 v/v. Thus, during industrial-scale carbonation at combustion facilities, CO_2 could be directly sequestered from the flue gas, reducing the operational costs and complexity of the system. An increase in carbonation reaction temperature was shown to have a dual effect on the carbonation of APC residues. Initially it enhanced the kinetics of the carbonation reaction, while later it reduced the final conversion values (Fernández-Bertos et al., 2006; Li et al., 2007); this was related to an initial increase in Ca^{2+} dissolution from residues at higher temperatures, followed by a reduction in CO_2 solubility/diffusion due to the enhancement in the production of the passivating product layer.

Ecke (2003) studied the influence of temperature, water content, CO_2 partial pressure and reaction time on the leaching behaviour of APC residues using multivariate data analysis and a two-level factorial design. The results showed that at high CO_2 concentrations and long treatment times, the stabilization of APC residues (in terms of lower pH and Pb and Zn leaching) was enhanced. Temperature and sample water content instead, were found to exert minor influence on the process (Ecke, 2003).

Baciocchi and co-workers (2006b) and recently Prigiobbe et al. (2009a) have shown that the main mechanisms governing dry carbonation of $Ca(OH)_2$ apply to the gas-solid carbonation of APC residues. In similarity with the aqueous route process, the kinetics of gas-solid carbonation was found to consist of two distinct stages: 1) the rapid conversion of calcium to carbonate and 2) a much lower rate phase involving diffusion of CO_2 into the porous material (see Figure 1.6). The first stage was described by Bhatia and Perlmutter (1983) as being characteristic of a kinetics controlled regime, whereas the second one was linked to the reduction of the global process rate by the diffusion of CO_2 through the product layer.

To further investigate the kinetics of carbonation in the first stage of the reaction and to obtain kinetic parameters, Baciocchi and co-workers (2006b) used the random pore model (Bhatia and Perlmutter, 1983) to correlate the reaction behaviour of the material with the internal pore structure. From their results they concluded that the process could be fast enough to enable fluidized bed processing of APC directly using flue gases. Recent experimental results confirmed that indeed high Ca conversion to calcite yields (over 60%) can be achieved for 10%, 22% CO_2 gas flows for temperatures above 400 °C in only a few minutes (see Figure 1.5) (Prigiobbe et al., 2009a).

The results reported so far in the literature indicate maximum CO_2 uptake potentials of 250-300 g CO_2/kg of APC residues for the gas-solid carbonation route (Baciocchi et al., 2006a) and lower values via the aqueous carbonation route (Ecke et al., 2003; Fernández-Bertos et al., 2006; Li et al., 2007). The sequestration potential of APC residues indicates that carbonation technology is a technically viable option to reduce CO_2 emissions from point sources, such as waste incinerators or power plants. Baciocchi and co-workers (2006a) have estimated that the use of all the APC residues annually produced from the existing plants in the EU would have the same CO_2 sequestration capacity as one of the largest pilot-scale CO_2 geological storage facilities running today (IPCC, 2005),

corresponding to roughly 0.02-0.05% of the total CO_2 European storage capacity required to comply with the Kyoto protocol objectives (Prigiobbe et al., 2009a).

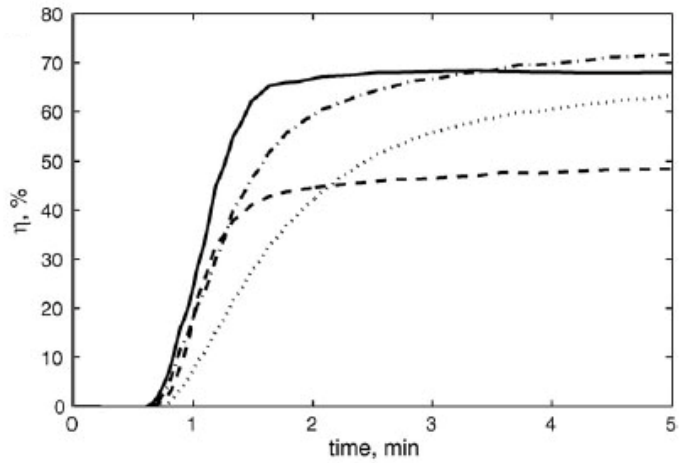

Figure 1.6 Calcium conversion versus time in the first 5 minutes of reaction for experiments with 22% CO_2 at different temperatures: 350°C (– –), 400 °C (——), 450 °C (·····) and 500 °C (– · –) (Prigiobbe et al. et al. 2009a).

1.4.3 Accelerated carbonation of steelmaking slag

During steel manufacturing, a significant amount (10-15% by weight of the produced steel) (Proctor et al., 2000) of various types of slag is generated. It has been estimated that the world output of iron (blast furnace slag) and steel slag in 2006 was of about 218-262 Mt and 124-186 Mt respectively (van Oss, 2007). Iron and steel slags (generally denominated steelmaking slags) are alkaline materials consisting principally of calcium, magnesium and aluminium silicates, with significant amounts of iron, manganese, or other elements such as chromium, nickel or titanium. The percentage of each constituent varies depending on the feedstock and processing conditions applied for iron or steel production. The main processes currently adopted for iron and steel production (see Figure 1.7) and the major slag by-products generated by each unit are here below briefly summarized.

Crude or pig iron is produced in a blast furnace, in which lime and limestone are used to remove oxygen and other impurities of the iron and adjust the viscosity of the molten iron product. At high temperatures, CaO (as additioned or produced by limestone decomposition) reacts with impurities, in particular SiO_2 and Al_2O_3 to form a liquid melt called iron or blast furnace slag, which is hence separated from the molten iron and removed from the blast furnace. The crude iron removed from the blast furnace is

transported to a steel converter, generally a basic oxygen furnace (BOF) where the residual carbon content of the iron is reduced (from 4 to 0.5 w/w %) along with other impurities (such as silicon, phosphorous, manganese and iron as liquid oxides) reacting with lime and forming a slag (BOF slag), similarly to the process occurring in the blast furnace (Shi, 2004; Teir, 2008). Pig iron, but prevalently scrap metals, can be also processed in steel furnaces such as electric arc furnaces (EAF), in which oxygen is added to reduce steel impurities and eventually other metals (ferro-alloys) are added to confer the steel its required chemical composition (as in the case of stainless steel production); a slag (EAF slag) floating on the surface of the molten steel is produced also in this case and subsequently separated from the molten steel by tilting the EAF unit (Shi, 2004).

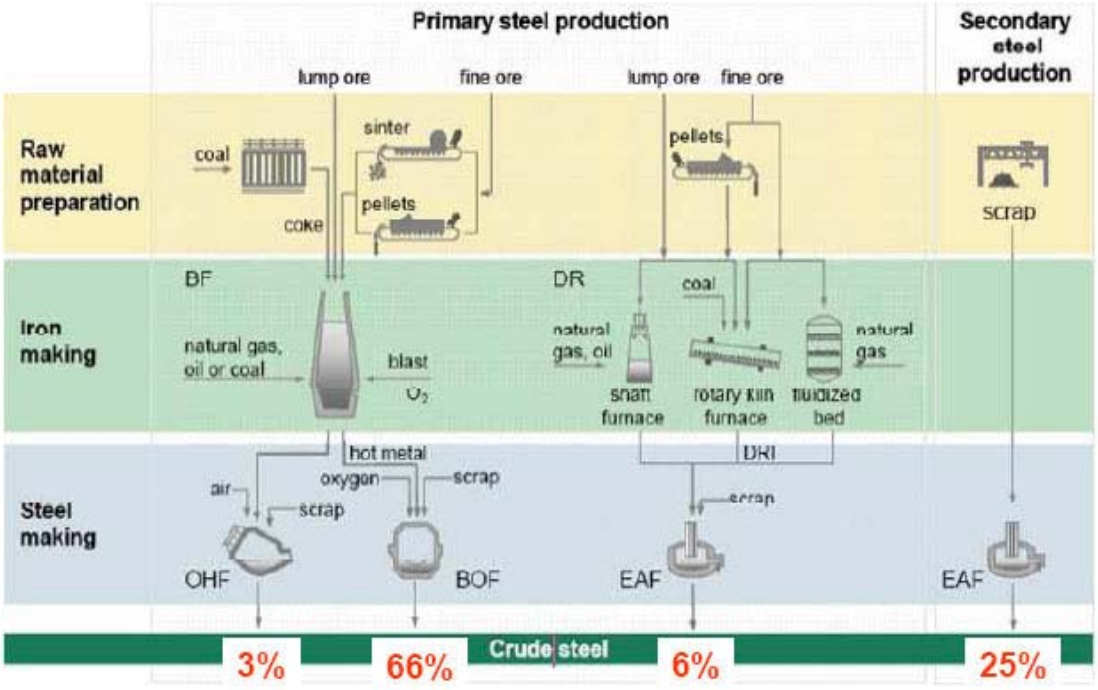

Figure 1.7 Main iron and steel production processes currently in use and world production shares in 2007, in which BF: blast furnace; OHF: open hearth furnace; BOF: basic oxygen furnace; EAF: electric arc furnace, DR: direct reduction (Birat, 2009).

Molten steel is then transferred into a ladle for further refining to remove additional steel impurities or to add alloys. During this process, defined ladle refining, additional steel slags are generated by adding fluxes such as CaO to the melt (Shi, 2004).

Stainless steel grades obtained by adding ferro-alloys (in particular Cr, Mn and Ni) such as stainless steel slag are generally produced in an induction or electric arc furnace. Stainless

steel refining is hence carried out in specific argon-oxygen decarburization (AOD) units, the by-products of which are defined AOD slags.

Steelmaking slags are mainly made up of CaO, SiO_2, MgO, and FeO (Motz and Geiseler, 2001). The proportion of these oxides and the concentration of minor compounds are highly variable and may change from batch to batch even for the same plant, depending on raw materials, type of steel produced and other factors (Shi, 2004). Table 1.4 lists examples of the average composition of some of the main types of steelmaking slag. EAF slag as a by-product of carbon steel production is similar to BOF slag, however EAF slag from stainless steel production is quite different. Alloy steel slags, such as Stainless Steel Slag (SSS) contain in general less FeO, more SiO_2 and high contents of Cr (2-5%) and some Ni (0.02-0.55%) (Shen and Forssberg, 2003). Also ladle slag has a lower FeO content compared to steel furnace slag. In some cases, as for example AOD refining of stainless steel slag, CaF_2 is added and the slag consists mainly of CaO and SiO_2 (Shi, 2004).

While steelmaking slag chemical characteristics depend primarily on the type of manufacturing and refining processes applied for steel production and on the type of raw materials used (natural ore or scrap material), the physical characteristics of the solidified slags depend chiefly on the cooling techniques applied, which usually determine the final use of the slag. Natural air cooling, water spraying, water quenching, air cooling and shallow box drying are the main methods (Shi, 2004). From these processes air-cooled, granulated (water cooled) and pelletized (or expanded) slags can be obtained (Teir, 2008). In air cooled slags β-Ca_2SiO_4 convert to γ-Ca_2SiO_4 at around 675 °C, with a volume increase of about 10% which results in the shattering of the crystals into a fine dust (Shi, 2004). This phenomena does not usually occur for water cooled slag, which breaks into grains during rapid cooling, making slag handling and metal recovery more feasible (Shi, 2004).

The main mineral phases detected in steel slag are dicalcium and tricalcium silicates, calcium-aluminium silicates, calcium oxides and periclase (MgO); SSS contain in addition Mg and Ni chromites (Shen and Forssberg, 2003). Free lime in steel slag comes from two sources: residual free lime from the raw material and precipitated lime from the molten slag; periclase derives instead from the use of dolomite as a flux additive and also from the refractory used for the lining of the steel furnace (Shi, 2004).

Steel slag is generally regarded as a non hazardous waste owing to low leachability of trace compounds (Proctor et al., 2000); however, SSS may be classified as hazardous, due to high Cr release (Shen and Forssberg, 2003; Shi, 2004).

Depending on its characteristics and particle size, steelmaking slag can be employed for various uses, e.g. as an aggregate or as a filler in cement production (Motz and Geiseler, 2001), owing to the cementitious properties that are conferred to this material by its content of dicalcium and tricalcium silicates (Shi, 2004). The most important factor for the utilisation of steel slag in engineering applications is its content of free CaO and MgO, since, due to hydration and natural carbonation, the slag volume increases causing disintegration of the material and hence strength loss (Motz and Geiseler, 2001).

Table 1.4 Typical bulk compositions of some of the calcium silicate containing waste residues tested for accelerated carbonation (% in weight of each oxide).

Sample	CaO	SiO_2	MgO	Al_2O_3	FeO	MnO	Cr
Blast converter[1]	41	35	10	9.2	0.8	0.5	0
GGBS[3]	41.4	34.6	6.8	14	0.7	n.a.	n.a.
Steel converter[1]	46	13	2.1	1.7	23.2	3.2	0.2
BOF[2]	30-55	8-20	5-15	1-6	10-35	2-8	0.1-0.5
EAF (carbon steel)[2]	35-60	9-20	5-15	2-9	15-30	3-8	0.1-1
EAF(alloy/stainless)[2]	39-45	24-34	8-15	3-7.5	1-6	0.4-2	0.1-20
AOD[1]	56	30	8.3	1.2	0.8	0.4	0.3
Ladle[2]	30-60	2-35	1-10	5-35	0.1-15	0-5	0-0.5
Chrome converter[1]	39	36	17	3.5	0.4	0.3	1
Ferrochrome[1]	1.4	28	23	28	5.9	n.a.	8.5
Stainless steel slag[3]	46.7	27.9	9.8	2.9	1.2	n.a.	n.a.

[1](Teir, 2008), [2](Shi, 2004), [3](Johnson, 2000).

In recent years, accelerated carbonation of steelmaking slag has been progressively tested to assess the CO_2 sequestration potential of this material (Johnson, 2000; Johnson et al., 2003a,b; Stolaroff et al., 2005; Huijgen et al., 2005; Chen et al., 2007; Teir et al., 2008; Bonenfant et al., 2008; Eloneva et al., 2008a,b; Kodama et al., 2008; Lekakh et al., 2008a,b; van der Laan et al., 2008). Lekakh et al. (2008a) calculated in fact that assuming full stoichiometric conversion of CaO and MgO to carbonates, BOF slag would have the potential of sequestering 6 to 10% of BOF CO_2 emissions (considering 75-150 kg BOF slag and 519 kg CO_2 produced per ton of manufactured steel) and 35 to 45% of EAF CO_2 emissions (considering 65-80 kg EAF slag and 119 kg CO_2 produced per ton of manufactured steel).

Accelerated carbonation of steelmaking slag has been also applied to enhance the mechanical properties of the residues for reuse in specific civil engineering applications (Johnson, 2000; Johnson et al., 2003a; Chen et al., 2007). A few studies have in addition assessed the effects of carbonation on the leaching behaviour of the slag (Johnson et al., 2003b; Huijgen and Comans, 2006; Chen et al., 2007; van der Laan et al., 2008). Accelerated carbonation of steelmaking slag has recently been additionally investigated as a technique for producing precipitated calcium carbonate (PCC) to use in industrial applications, e.g.: as a filler and coating pigment in plastics, rubbers, paints and paper manufacturing (Teir et al., 2007; Eloneva et al., 2008a,b). PCC is currently produced by carbonating calcined natural limestone; during calcination more CO_2 than that which is sequestered during the carbonation process is emitted to the atmosphere (Teir et al., 2005); hence the use of calcium silicates for PCC production could contribute in reducing both CO_2 emissions (theoretically 340 kg CO_2/t PCC produced, considering wollastonite carbonation (Teir et al., 2005)) and the consumption of natural resources such as limestone (Eloneva et al., 2008b).

Accelerated carbonation of steel slag, similarly to the process described for geologically derived minerals, consists of two sequential reactions: the dissolution of alkaline elements (Ca and Mg) from the silicate minerals, and the precipitation of the corresponding carbonate phases (Huijgen et al., 2005). The two processes can be performed in the same reactor (single-stage process), or in two in-series reactors (two-stage process).

Single-stage carbonation of steelmaking slag

The single-stage process has been carried out either in slurry phase systems (with L/S $\geq$ 2 kg/kg) or on partially humidified slag (with L/S < 1 kg/kg).

Slurry phase accelerated carbonation was performed under high temperature (25-225 °C), moderate CO_2 pressures (10-30 bar) and a reaction time of up to 30 minutes (Huijgen et al., 2005), or alternatively at ambient temperature, atmospheric pressure with 15% or 100% vol. CO_2 and long reaction times of (up to 72 or 24 hours) (Bonenfant et al., 2008a) and (Lekakh et al., 2008a) respectively.

'Fast' slurry phase carbonation experiments on ground BOF slag (also indicated as Linz Donawitz slag) were performed in an autoclave reactor to assess the maximum CO_2 uptake of the material, as well as the corresponding Ca conversion yield and the influence of operating conditions on process kinetics (Huijgen et al., 2005). A maximum CO_2 uptake of

about 180 g CO_2/kg BOF slag, corresponding to a carbonation conversion of 74% of the Ca content of the slag, was achieved in 30 minutes at 19 bar CO_2 pressure and 100 °C for a slag particle size < 38 μm. The reactive phases in the slag were found to be portlandite and Ca-(Fe)-silicates and the only reaction product detected by XRD and SEM/EDX analysis was calcite (Huijgen et al., 2005). Slag particle size was found to exert the most significant effects on the reaction, smaller grain sizes proving more reactive towards CO_2, while temperature, which enhanced silicate dissolution up to 200 ºC, reaction time and CO_2 partial pressure showed milder effects on Ca conversion yields. The diffusion of calcium through the solid matrix toward the surface of the slag particles appeared to be the rate-limiting reaction step, which was found to be hindered by the formation of a $CaCO_3$-coating and a Ca-depleted silicate layer on slag particles during the carbonation process (Huijgen et al., 2005). The energetic efficiency and cost evaluations of this process applied to BOF slag and wollastonite ore were investigated and compared (Huijgen et al. 2006a; 2007). The authors concluded that the energetic CO_2 sequestration efficiency of BOF slag aqueous carbonation was lower (69%) than that of wollastonite (75%) at the same operating conditions, owing to the lower Ca content of the feedstock. To achieve higher CO_2 sequestration efficiencies, a reduction of the amount of process water (which decreases the L/S ratio) and further grinding were indicated as the most effective operations; however the main energy-consuming process steps were found to be feedstock grinding and CO_2 compression (Huijgen et al., 2006a). A total sequestration cost of 64€/t CO_2 sequestered or 77€/t CO_2 avoided (considering the additional costs associated to the energy penalty of the process) was evaluated by Huijgen et al. (2007) for the aqueous carbonation of finely grinded BOF slag (d < 38 μm) carried out at 200 ºC, 20 bar CO_2, L/S = 2 kg/kg for 15 minutes, as reported in their previous paper (Huijgen et al., 2005), taking into account CO_2 compression and slag grinding.

Recently another similar slurry phase process for steelmaking slag carbonation (particle size of 50 μm, reaction temperature of 90 ºC, 100 bar CO_2 and a process time of 90 minutes) was indicated to provide a CO_2 storage capacity of 250 g CO_2/kg slag with a conversion yield of 70% (Birat, 2009).

The CO_2 sequestration potential of steelmaking slag at milder operating conditions has also recently been tested. Slurry phase (L/S = 10 kg/kg) carbonation of EAF and ladle slag carried out at 20 ºC and ambient temperature with 15% vol. CO_2 flows of 5 ml/min

resulted in a CO_2 uptake capacity of 17 g/kg EAF slag in 24 hours and 247 g/kg ladle slag in 40 hours, which was ascribed to the higher content of portlandite of the ladle slag suspension (Bonenfant et al., 2008a). The leachates of fresh and hydrated slag obtained after three consecutive leachings also showed CO_2 uptake potential, EAF slag leachate in particular (Bonenfant et al., 2008a).

Slurry phase batch tests were also performed on different size fractions of EAF and ladle steel slag at ambient temperature and atmospheric pressure to separately investigate the Ca leaching rate of the slag and the carbonation reactions (Lekakh et al., 2008a). Dissolution experiments, carried out at constant pH under an Ar atmosphere, indicated the chemical reaction as the initial rate-limiting step and diffusion through the developed porous layer as the final mechanism controlling the kinetics of Ca leaching from the slag, in accordance with the shrinking particle core model described in Section 1.4. Particle size exerted the most significant effect on Ca dissolution (over 90% and less than 40% Ca dissolved in 24 hours from 45-75 and 150-250 μm sized ladle slag respectively); temperature also exhibited an enhancing effect but only during the first 3 hours of the dissolution reaction (18% compared to 8% Ca dissolved from 150-250 μm ladle slag at 20 and 60 ºC respectively) (Lekakh et al., 2008a). Carbonation, performed with 100 % CO_2 and a L/S = 8.3 l/kg, showed significantly slower reaction kinetics, which was strongly affected by slag particle size. The shrinking pore model was used also to describe the overall carbonation reaction and diffusion through the calcium carbonate product layer was indicated as the rate limiting step; a maximum uptake of 120 g CO_2/kg slag was achieved in about 22 hours for the 150-250 μm particle size fraction of ladle slag (Lekakh et al., 2008a). Experimental results were hence used by the same authors to simulate different processing options of a two-stage carbonation system in which slag dissolution in water and the carbonation of the leachates would be carried out in two different reactors (Lekakh et al. 2008b); a continuous system with fresh water additions for slag dissolution was shown as the most effective process, although presenting a high water demand; alternatively decreasing the L/S ratio, or increasing the residence time or the slag surface area were indicated as possible reaction enhancement strategies (Lekakh et al., 2008b).

Partially humidified steelmaking slag with L/S ratios between 0.1 and 1 l/kg have also been carried out at mild operating conditions (30-50 °C and 1-10 bar) to investigate the potential CO_2 uptake of different types of slag as well as the effects on the leaching

behaviour and on the mechanical properties of the material (Johnson, 2000; Johnson et al., 2003a,b; Chen et al., 2007; van der Laan et al., 2008). Johnson (2000) indicated stainless steel slag to be significantly more reactive than GGBS slag with 100% CO_2 at 3 bar and ambient temperature, owing primarily to the differences in the composition of the two slags, see Table 1.4; for stainless steel slag an optimum L/S of 0.125 l/kg and a maximum CO_2 uptake of 180 g/kg residue for grinded (<125 μm) slag were reported (Johnson, 2000; Johnson et al., 2003a). 28-day compressive strength tests carried out on different size fractions of slag carbonated for 2 hours at the optimum L/S, indicated that both grinded fine particle size fractions (<125 μm) and grinded bulk stainless steel slag showed a significant compressive strength increase upon carbonation (around 10 MPa compared to below 0.6 MPa) (Johnson et al., 2000; Johnson et al., 2003a).

Similar operating conditions (ambient temperature, 100% CO_2 at 3 bar and L/S = 0.15 l/kg) were applied to compare the extent of carbonation and the leaching behaviour of different types of steelmaking slag with OPC, in order to assess if concrete durability could be increased mixing OPC with alkaline residues (Chen et al., 2008). For 72 hour carbonated samples the estimated degrees of carbonation reported were: 62% OPC, 50-52% converter steel slag and 44% GGBS, and calcite and aragonite were identified as the reaction products (Chen et al., 2008).

Column carbonation experiments on two types of converter steel slag were also recently reported (van der Laan et al., 2008). These experiments were carried out at atmospheric pressure, feeding 900 g of wetted steel slag with a water-saturated CO_2/Ar mixture at a flow rate of 400 ml/min for reaction times ranging from 8 to 200 hours and temperatures between 5 and 90 °C. The aim of this particular study was to assess the leaching behaviour of the slag more than the CO_2 storage potential of the material, hence relatively large (2-3.3 mm) steel slag grains were used and consequently lower carbonation degrees were achieved compared to other studies (e.g.: Huijgen et al., 2005). CO_2 uptakes of 15 or 6 g/kg slag were reported for the two different types of converter steel slag in dependence of the free lime content of the material. Reaction kinetics was shown to be enhanced by increasing temperature and humidity (van der Laan et al., 2008).

Two-stage carbonation of steelmaking slag

Two-stage steelmaking slag carbonation processes have been investigated by some researchers in order to separately optimize slag dissolution and carbonate precipitation by selecting the optimum pH and operating conditions for each reaction, so to achieve higher conversion yields and a pure calcium carbonate reaction product (PCC), which could be sold for specific industrial applications, as earlier mentioned (Kodama et al., 2006 and 2008; Teir et al., 2007; Eloneva et al., 2008a,b).

Kodama et al. (2006) developed a process for CO_2 sequestration from Ca-silicate industrial residues using the pH swing of a weak base-strong acid solution. In particular an ammonium chloride solution was chosen to extract Ca^{2+} ions from calcium silicate, as shown in Equation 1.19. As the reaction proceeds, due to NH_3 production, the solution becomes alkaline and hence when CO_2-containing gas is introduced in the extraction solution, $CaCO_3$ precipitates and NH_4Cl is regenerated, as shown in Equation 1.20. To avoid ammonia leakage with the flue gas, a NH_3 recovery tower was added after the CO_2 absorption unit (Kodama et al. 2008). Dissolution experiments of various size fractions of crushed converter steel slag were carried out with a 1N NH_4Cl slurry solution for 1 hour at atmospheric pressure and temperature between 60 and 90 ºC. A Ca extraction yield of 60% was achieved at 80 ºC for the finest particle size fraction (< 63 μm) with a very high Ca selectivity (> 99%), due to a final solution pH of of 9.4, which allowed only Ca^{2+} to be dissolved, differently from other extracting agents (i.e. HCl and CH_3COOH). Calcium carbonate precipitation conversion showed a maximum conversion of 80% at 40 ºC which decreased to 70% at 80 ºC, owing to lower CO_2 solubility. A $CaCO_3$ purity of 98% was obtained, with the formation of calcite at lower temperature (plate-like morphology) and aragonite at higher temperature (needle-like morphology) (Kodama et al., 2008). The total energy consumption of the process, including slag grinding, and assuming direct treatment of flue gas (CO_2 concentration of 13% vol.), was estimated to be 300 kWh/t CO_2, the main drawback of the process being the need to remove NH_3 emissions downstream of the CO_2 absorption tower (Kodama et al., 2006 and 2008).

$$4NH_4Cl_{(aq)} + 2(CaO)\cdot SiO_{2(s)} \rightarrow 2CaCl_{2(aq)} + SiO_{2(s)} + 4NH_{3(aq)} + 2H_2O \quad (1.19)$$

$$4NH_{3(aq)} + 2CO_{2(aq)} + 2CaCl_{2(aq)} + 4H_2O \rightarrow 2CaCO_{3(s)} + 4NH_4Cl_{(aq)} \quad (1.20)$$

Another research group investigated the feasibility of enhancing steelmaking slag dissolution with acetic acid solutions and other chemicals (Teir et al., 2007; Eloneva et al., 2008a,b,c), similarly to the process developed by Kakizawa et al. (2001) for wollastonite carbonation. Thermodynamic equilibrium calculations showed that at atmospheric pressure calcium extraction is exothermic and feasible at temperatures below 156 ºC, whereas calcite carbonate precipitation may be obtained at temperatures above 45 ºC (Teir et al. 2007). A high Ca extraction yield was achieved with 33.3% weight of acetic acid for different types of steelmaking slag (BF, AOD, EAF and converter slag) at 50 ºC, however due to the low pH values, other elements dissolved as well, including Mg, Al, Fe and Si; at 70 ºC silicon was found to form a gel phase which could be separated by mechanical filtration and hence this temperature was chosen as the optimum reaction temperature for calcium extraction from steelmaking slag with acetic acid (Teir et al., 2007). Carbonation experiments performed at 30-70 ºC and 1-30 bar CO_2 on aqueous solutions of calcium extracted from blast furnace slag (Eloneva et al., 2008a) and steel converter slag (Eloneva et al., 2008b) with acetic acid, showed that in order for significant calcite precipitation to occur, the addition of a strong base, such as NaOH, is needed to increase the pH of the solution. With NaOH addition, calcium carbonate phases (calcite, aragonite and calcite magnesium) were produced at 30 ºC and atmospheric pressure from blast furnace slag (Eloneva et al., 2008a). Preliminary process calculations showed that approximately 4.4 kg blast furnace slag, 3.6 l of acetic acid (100% weight) and 3.5 kg NaOH would be required to bind 1 kg CO_2, resulting in 2.5 kg of 90% calcium carbonate (Eloneva et al., 2008a). Higher purity was achieved with carbonation tests carried out on aqueous solutions of calcium extracted from converter steel slags dissolved with weak acetic acid solutions (30% or less of the acid stoichiometrically required to dissolve all of the calcium) (Eloneva et al., 2008b). In this case a maximum calcium conversion to carbonate of 86%, with a precipitate purity of up to 99.8%, was achieved at 30 ºC with 10% vol. CO_2. Solution temperature as described also by Kodama et al. (2008) showed to affect calcium carbonate morphology, the precipitate formed at low temperature showing rhombohedral particle shape and small particle size, hence appropriate characteristics for commercialization as PCC (Eloneva et al., 2008b). The main limits of this process are the high costs and requirements of additives such as NaOH and CH_3COOH; hence other solvents have been tested for Ca^{2+} extraction from steel making slag (Eloneva et al., 2008c). Ammonium salt

solutions were found to be particularly selective in terms of Ca^{2+} dissolution and operational parameters showed a similar effect as that described by Kodama et al. (2008).

Effects of carbonation on steelmaking slag leaching behaviour

The leaching behaviour of carbonated steelmaking slag has been up to now less investigated in comparison to that of other industrial residues such as MSWI bottom ash for example, owing to the fact that this material, except for some types of stainless steel slag or ladle slag, presents generally a lower release of soluble salts and heavy metals. Some researchers though have compared the results of leaching tests performed on fresh and carbonated steelmaking slag in order to identify the solubility-controlling processes of major elements so to elucidate carbonation mechanisms, as well as studying trace elements' mobility (Huijgen and Comans, 2006).

Different methodologies have been applied to assess the leaching behaviour of steelmaking slag. Batch compliance tests performed with distilled water and a L/S = 10 l/kg were applied by some authors (Huijgen and Comans, 2006; Chen et al. 2007), whereas others have used also pH dependence leaching tests (Johnson et al. 2003b; Huijgen and Comans, 2006), or alternatively column percolation tests according to the CEN/TS 14405 procedure (van der Laan et al., 2008). In some cases the results of the leaching tests were analyzed by geochemical modelling (Huijgen and Comans, 2006).

All types of the analyzed fresh steelmaking slag showed a very alkaline pH (above 12) which decreased significantly, depending on the extent of carbonation, of even a couple of units, although in some cases the acid neutralization capacity curves reported for fresh and carbonated steel slag did not show to differ significantly, e.g. in the case of stainless steel slag as described by Johnson et al. (2003b).

For fresh steel slag, Huijgen and Comans (2006) reported that pH dependent Ca^{2+} leaching curves showed to depend on the solubility of the different Ca phases making up the slag. Two pH intervals in particular showed increased Ca leaching: a first step between pH 11 and 9.6 at which almost 30% of the total Ca was leached from portlandite and hydrated Ca silicate phases, and a second step between pH 5 and 3.5 at which another 32% of the Ca was leached, supposedly from dicalcium silicate phases, whereas the rest of the Ca was assumed as non-available, possibly bound as Ca-Fe-oxides (Huijgen and Comans, 2006).

Upon carbonation, leaching tests carried out at the natural pH of the slag, showed a significant decrease in Ca leaching, due to the formation of less soluble phases such as

calcite, and an increase in Mg and Si leaching, consistent with the pH decrease (for Mg leaching) and with the at least partial dissolution of the calcium silicate phases (Huijgen and Comans, 2006; Chen et al., 2007). For trace elements such as V a significant mobilization effect for carbonated samples was reported (Huijgen and Comans, 2006; van del Laan et al., 2008), whereas for Cr a decrease in mobility was indicated for some kinds of steel making slag, i.e. for stainless steel slag (Johnson et al., 2003b), and instead a slight mobilization effect was reported for GGBS (Chen et al., 2007).

Geochemical modelling of the results of pH-dependent leaching tests showed for fresh steel slag solubility control by portlandite at pH = 12.5, and by hydrated calcium silicate phases (as also indicated by Si leaching) at pH values > 10, (however in alternative solubility control by ettringite in the same pH interval was not excluded), (Huijgen and Comans, 2006). For carbonated slag, Ca leaching was reduced in the pH interval 6-12.5 and the results of the leaching tests showed a similar trend to the calcite solubility curve, even though the leachates remained significantly oversaturated with respect to calcite, as indicated by other authors for MSWI bottom ash (e.g.: Meima and Comans, 1997).

The increasing Si concentrations measured in the eluates of carbonated samples at high pH proved to be consistent with the solubility pattern of amorphous SiO_2 instead of hydrated Ca silicates, thus indicating at least partial dissolution of these phases as a result of the carbonation treatment (Huijgen and Comans, 2006). The leaching curves of other elements such as Al, Fe and Mn did not seem to be significantly modified by carbonation, and solubility control by diaspore (AlOOH), ferrihydrite ($Fe(OH)_{3am}$) and MnO_2 were found to adequately describe the solubility of these metals in a wide pH interval respectively (Huijgen and Comans, 2006).

For trace compounds, such as Cr, Ni, Co and Zn at pH > 9.5 solubility control was attributed to metal (hydr)oxides, whereas at lower pH values the adsorption of these metals to reactive Al-, Fe- and Mn-(hydr)oxide surfaces was postulated to likely control leaching; significant variations associated to the carbonation reaction were not reported for these elements and Cr in steelmaking slag was hypothesized to be in its reduced oxidation state (Cr(III)) (Huijgen and Comans, 2006). The leaching of another oxyanion forming element, V, was instead found to be significantly modified by carbonation (Huijgen and Comans, 2006; vab der Laan et al., 2008). V leaching for fresh steel slag was found to be quite low, but increased by 2-3 orders of magnitude after carbonation, probably due to initial

incorporation in dicalcium silicate phases and hence consequent release after the dissolution of these phases caused by carbonation (Huijgen and Comans, 2006). Column percolation experiments also showed a correlation between the carbonation degree of the compacted steel slag and V concentrations in the eluates, which resulted higher than Dutch compliance criteria for reuse of the slag as building material (van der Laan et al., 2008).

Chapter 2: Mineral carbonation: olivine dissolution kinetics

[2]This chapter reports the results of an experimental study on the dissolution kinetics of olivine ($Mg_{1.82}Fe_{0.18}SiO_4$) at operating conditions relevant to the mineral carbonation process for the permanent storage of CO_2. In particular, the effects of CO_2 fugacity and of salinity on the kinetics of olivine dissolution, which is assumed to be the rate-limiting step of the overall carbonation process, were investigated. Dissolution experiments were carried out at 120 °C in a stirred flow-through reactor. Different pH values (between 3 and 8) and solution compositions were investigated by varying CO_2 fugacity and by dosing LiOH (only for pH control), NaCl, and $NaNO_3$. Specific dissolution rate values were estimated from the experimental data using a population balance equation (PBE) model coupled with a mass balance equation. The logarithms of the obtained dissolution rate values were regressed with a linear model as a function of pH and compared to the model reported earlier by Hänchen et al. (2007) for experiments with neither CO_2 nor salts. The results confirmed that, at a given temperature, olivine dissolution kinetics depends on pH only, and that CO_2 fugacity and the concentrations of NaCl and $NaNO_3$ affect it exclusively through their effect on pH.

2.1 Introduction

Aqueous mineral carbonation, as discussed in the previous chapter, is a technology that is being currently particularly investigated and developed in the framework of carbon dioxide capture and storage (CCS) processes (IPCC, 2005). This technology aims at binding CO_2 into stable carbonates, using metal oxides via a high-pressure and high-temperature ex situ process, which mimics natural rock weathering. For a large scale implementation of this process, the most suitable sources of metal oxides are magnesium silicate minerals, such as olivine and serpentine, due to the large worldwide availability of these minerals (e.g., in ophiolite belts) (Goff et al., 2000).

Aqueous mineral carbonation of olivine involves CO_2 dissolution in water, the dissolution of the silicate minerals, and the precipitation of Mg-carbonates. In particular, the

[2]Most of this Chapter is under publication as Prigiobbe et al., 2009b.

dissolution of the silicate minerals is considered to be the rate-limiting step of the entire aqueous mineral carbonation process.

In the case of the dissolution of forsterite, the magnesium end-member of olivine, the chemical reaction in a CO_2-free solution is:

$$Mg_2SiO_{4(s)} + 4H_2O \rightarrow 2Mg^{2+}_{(aq)} + H_4SiO_{4(aq)} + 4OH^-_{(aq)} \quad (2.1)$$

This reaction has been extensively studied at ambient pressure and temperature and its kinetics has been found to depend primarily on pH (see e.g. Rosso and Rimstidt, 2000).

Two different mechanisms for olivine dissolution have been postulated at 25 °C, corresponding to a pH-dependence for pH < 8, and to no pH-dependence for higher values (e.g.: Wogelius and Walther, 1991; Pokrovsky and Schott, 2000; Rosso and Rimstidt, 2000). The first mechanism is governed by the adsorption of one H^+ ion onto two olivine cells leading to a preferential release of magnesium over silicon and to the formation of a thin Mg-depleted, and Si-rich (altered) layer. At higher pH values, the dissolution is controlled by the formation of $Mg(OH)_2^+$ complexes and exhibits a preferential release of silicon into solution, thus creating a Si-depleted and hence Mg-rich surface layer. Hänchen et al. (2006) studied olivine dissolution at temperatures between 90 and 150 °C and at pH values between 2 and 12.5 (tuned using HCl and LiOH), and observed the same behaviour, and hence postulated that the same mechanism described for lower temperatures applied also in this case. In particular, the specific dissolution rate (r), in the pH range from 2 to 8.5, was expressed as function of pH by the following equation (that corresponds to a linear dependence of the logarithm of r on pH at a given temperature):

$$r = a^n_{H^+} A e^{-\frac{E_a}{RT}} \quad (2.2)$$

In which r is the specific dissolution rate (mol cm^{-2} s^{-1}), T is the temperature (K), R is the gas constant (8.3145*10^{-3} kJ K^{-1} mol^{-1}), a_{H+} is the hydrogen ion activity (dimensionless), and A is a pre-exponantial factor (mol cm^{-2} s^{-1}). In the above mentioned study (Hänchen et al., 2006) the parameters A, E_a (activation energy), and n (reaction order of H^+) were estimated by fitting all the experiments to Equation 2.2, thus resulting in the following values: A =0.0854 mol cm^{-2} s^{-1}, E_a = 52.9 kJ mol^{-1}, and n = 0.46.

Moreover, to assess the influence of CO_2 on olivine dissolution kinetics, in the same work a few experiments were also carried out at 120 °C under a CO_2 partial pressure (from 15 to

180 bar) and in a pH range between 3 and 6 (adjusted by LiOH addition) (Hänchen et al., 2006). The measured dissolution rates were the same as, or slightly higher than, those without CO_2 up to a pH value of 5, and markedly lower beyond this value. Although earlier studies have reported and justified such dissolution inhibition (Wogelius and Walther, 1991; Pokrovsky and Schott, 2000), others have questioned this conclusion (Golubev et al., 2005). There is, however, agreement concerning the importance of the formation of Mg-carbonate complexes on the surface of olivine particles in determining the dissolution behaviour. It is worth noting that the pH effect on silicate dissolution can in principle be exploited to control the mineral carbonation process, namely by dissolving silicates at low pH and by precipitating carbonates at high pH, i.e. through a so called pH-swing process, as described in chapter 1 (see e.g. Park et al., 2004).

Inorganic salts such as NaCl, $NaHCO_3$, and $KHCO_3$ have been used in different works to enhance the carbonation of silicates (Geerlings et al., 2002; O'Connor et al., 2005; McKelvy et al., 2005). However, in a thorough study on forsterite dissolution in a CO_2-free solution at 25 °C in a pH range from 1 to 4, it has been shown that the dissolution rate was not affected by the presence of the inorganic salts KNO_3, $Mg(NO_3)_2$, Na_2SO_4, and $MgSO_4$ at an ionic strength of up to 12 M (Olsen, 2007).

Nevertheless, specific studies regarding the dissolution kinetics of Mg-silicates at high CO_2 fugacity, salinity, and temperature, the operating conditions typically reported for the mineral carbonation process (see chapter 1) (e.g.: O'Connor et al., 2005; Gerdemann et al., 2007) are still missing. Hence, the effects of CO_2 and salinity on olivine dissolution kinetics are not clear enough, both qualitatively and quantitatively, at the conditions of interest for mineral carbonation. Thus, the main scope of this work was that of achieving a deeper understanding of these effects on olivine dissolution kinetics in order to gain insight on the most effective strategies to employ so to optimize the mineral carbonation process.

Olivine dissolution was studied at 120 °C in a H_2O-CO_2-LiOH-NaCl/$NaNO_3$ system, for different values of CO_2 fugacity (in the range 0.4 to 123 bar), of pH (2 to 8), and of salinity (salt concentration up to 2.5 mol kg^{-1}). For each experiment, the values of r were estimated by fitting the experimental data (olivine concentration versus time) with a population balance equation (PBE) model coupled with a mass balance equation as described in Hänchen et al. (2007). Finally, the obtained values of the specific dissolution rate were regressed using the model reported in Equation 2.2.

2.2 Materials and methods

The dissolution kinetics of natural San Carlos gem-quality olivine grains ($Mg_{1.82}Fe_{0.18}SiO_2$), with a particle size between 90 and 180 μm and a specific surface of 797 ± 55 cm^2 g^{-1}, was studied in a LiOH-CO_2 aqueous system.

Selected experiments were also carried out in NaCl/$NaNO_3$-LiOH-CO_2 aqueous solutions. Small amounts of LiOH were added to the solution in order to achieve pH values higher than 4 in the presence of CO_2. This hydroxide was chosen since Li^+ concentrations of the solution could be accurately monitored online, as described below.

In Figure 2.1 the experimental set up used to perform olivine dissolution kinetics experiments is schematically illustrated. A flow-through high-pressure, high-temperature stirred titanium reactor with a volume of 300 ml, as described in (Hänchen et al., 2006) was used for all experiments. All runs were performed at a temperature of 120 °C, with a liquid volume of 170 ml and a gas headspace of 130 ml. Carbon dioxide 99.995% vol. purity (PanGas, Werk Dagmersellen, Switzerland), fed to the reactor from a high-pressure buffer tank and via a front-pressure regulator, was used to pressurize the solution at specific values, ranging from 2 to 100 bar. The gas was fed to the solution through the stirrer to facilitate the achievement of gas-liquid equilibrium. The stirrer was operated at 700 rpm to avoid mixing limitations and particle sedimentation.

For the entire duration of each experiment, the feed solution was purged with N_2 with a purity of 99.999% vol. (PanGas, Werk Dagmersellen, Switzerland), fed directly from a gas cylinder. Such a solution, consisting of ultrapure water only, or of ultrapure water with electrolytes, i.e. LiOH, NaCl, and $NaNO_3$, was introduced into the reactor at a constant flow rate of either 2 or 5 ml min^{-1}, after being pre-heated up to 90 °C with a heat exchanger, in order to minimize the temperature drop at the entrance of the reactor. A second HPLC pump was used to withdraw liquid at exactly the same flow rate as the inlet pump, in order to maintain a constant liquid level in the reactor. Before passing through the second pump, the outlet stream was cooled down to ambient temperature by a copper-tubular heat exchanger, then it's flow rate was measured with a flow meter and finally it was depressurized to ambient pressure by using a hydraulic disconnection. For each experiment, the reactor was initially filled with a known amount of olivine, closed, and flushed with CO_2 to purge O_2 from it. Then a known amount of solution was pumped into

the vessel and heated up to 120 °C. Once the system stabilized, the reactor was pressurized and kept at these conditions for the entire run.

The Mg^{2+} and Li^{+} concentrations in the outlet solution were measured online by means of an ion chromatograph (CS12A column, Dionex). Solution samples were taken with a fraction collector at regular intervals and their silicon concentration was measured with a spectrophotometer using the Molybdate Blue method (Grasshoff and Anderson, 1999; ICRAM, 2001). The standards for the Mg^{2+} and Si^{4+} measurements were prepared with the feed solution to take into account the effects of salinity on the analysis.

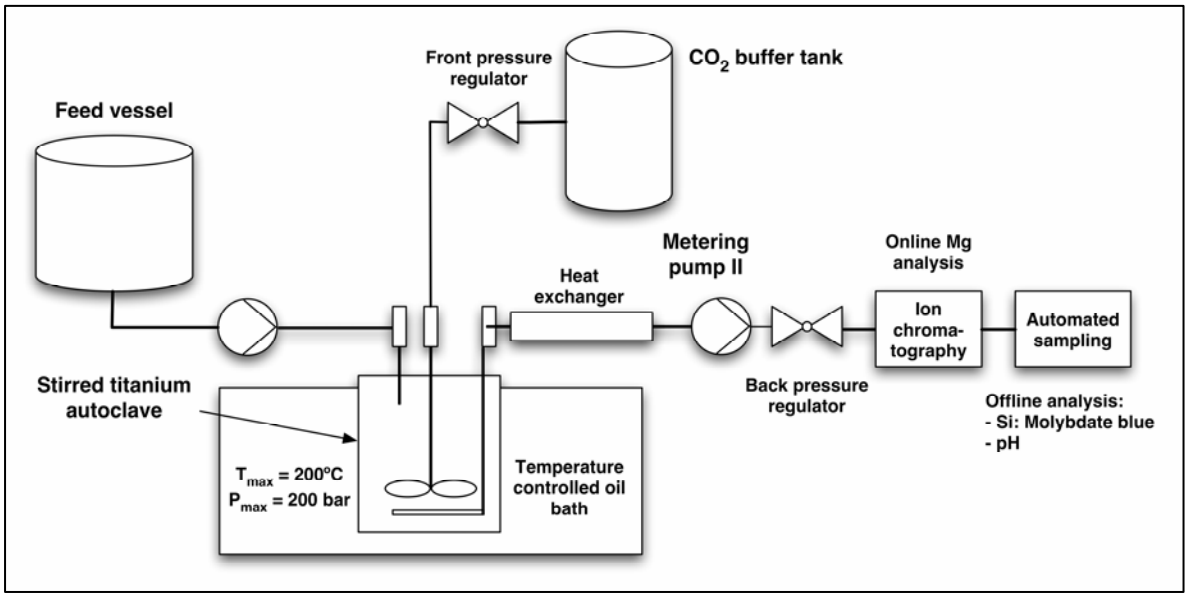

Figure 2.1 Scheme of the experimental set up, as reported also in Hänchen et al. (2006).

In order to estimate the pH, the geochemical software package EQ3/6 version 8.0 (Wolery and Jareck, 2003) was used to model the composition of the solution, assuming that the time scale for achieving equilibrium was smaller than the residence time (30-90 min).

A database employing Pitzer equations to estimate the activity coefficients of the aqueous species at high ionic strengths was used. Based on the measured temperature and pressure, the CO_2 fugacity was calculated by using a noniterative procedure developed by Spycher et al. (2003), based on the Redlich-Kwong equation of state for the CO_2-H_2O mixture. The value of CO_2 fugacity together with the temperature and Mg^{2+} and Si^{4+} concentrations, was used to calculate the actual pH value using EQ3/6.

2.3 Modelling

Following Hänchen et al. (2007), olivine dissolution was modelled by a 1-D population balance equation (PBE) model, assuming constant particle shape. This equation (Equation 2.3) together with a flow-through reactor model (Equation 2.4) allows the description of the temporal evolution of olivine particles.

$$\frac{\partial f}{\partial t} - D\frac{\partial f}{\partial L} = 0 \tag{2.3}$$

$$V\frac{dc}{dt} + Qc = -\frac{dm}{dt} \tag{2.4}$$

The parameters of these equations are: *f,* the unscaled particle size distribution number density (m^{-1}); *D,* the dissolution rate (m s^{-1}); *m,* the total mass of particles (moles of olivine); *V,* the volume of the suspension (m^3); *Q,* the flow rate through the reactor (m^3 s^{-1}); *c,* the concentration of olivine in solution (moles m^{-3}) and *L*, the characteristic length of a particle (m), which is related to a physical property of the particle.

The model, described by Equations 2.3 and 2.4, must be solved numerically for a given initial mass of olivine and a given initial particle size distribution, thus yielding the time evolution of the olivine concentration *c* in solution. To this aim, a combination of the method of characteristics and of the method of moments was used (Hänchen et al., 2007). Here below the main equations employed to formulate the model are reported.

The population balance equation (Equation 2.3) was solved in terms of the characteristic length *L* with the method of characteristics and the solution is reported in Equation 2.5, considering as an initial condition Equation 2.6, which expresses the assumption that during dissolution the solution in contact with the minerals is undersaturated and nucleation does not occurr, hence the particle size distribution coincides with the initial particle size distribution ($f_0(L)$).

$$f(L,t) = f_0(L + Dt) \tag{2.5}$$

$$f(L,0) = f_0(L) \tag{2.6}$$

In order to reformulate Equation 2.5 in terms of the total particle surface and volume of the distribution, these properties must be related to the characteristic length *L*. The following

Equations (2.7 and 2.8) were employed to express the surface area (*a*) and volume (*v*) of a single particle as a function of *L* respectively:

$$a = k_a L^2 \tag{2.7}$$

$$v = k_v L^3 \tag{2.8}$$

in which k_a and k_v are size-independent and time-invariant shape factors that depend on the geometry of the particles and on the choice of the characteristic length *L*.

Most experimental techniques provide a measurement of the particle size distribution as a volume distribution, $\phi(v, t)$, instead of as a function of the characteristic length, hence the solution of the population balance equation, *f(L,t)*, was rewritten in terms of the particle volume distribution, considering:

$$f(L,t)dL = \phi(v,t)dv \tag{2.9}$$

To calculate the total surface area (*A*) and volume (*V*) of the particles, the method of moments was used, defining the n^{th} moment of a particle as:

$$\mu_n(t) = \int_0^\infty L^n f(L,t)dL = \int_0^\infty (\frac{v}{k_v})^{n/3} \phi(v,t)dv \tag{2.10}$$

and relating the total surface and volume of the particle distribution to the second and the third moments of the distribution respectively:

$$A(t) = k_a \mu_2(t) \tag{2.11}$$

$$V(t) = k_v \mu_3(t) \tag{2.12}$$

Substituting Equation 2.5 in Equation 2.10 yields:

$$\mu_n(t) = \int_{Dt}^\infty f_0(L)(L - Dt)^n dL = \frac{1}{k_v^{n/3}} \int_{(k_v^{1/3}Dt)^3}^\infty \phi_0(v)(v^{1/3} - k_v^{1/3}Dt)^n dv \tag{2.13}$$

To obtain an equation that allowed the determination of the dissolution rate from measured particle volume distributions, the right hand side of Equation 2.4 was expressed using Equations 2.12 and 2.13, with ρ being the molar density of olivine (mol cm^{-3}), obtaining:

$$\frac{dm}{dt} = \rho k_v \frac{d\mu_3}{dt} = -3\rho k_v^{1/3} D \int_{(k_v^{1/3}Dt)^3}^\infty \phi_0(v)(v^{1/3} - k_v^{1/3}Dt)^2 \tag{2.14}$$

Grouping all constants into a new parameter γ and recalling Equation 2.4, Equation 2.14 was recast as:

$$-\frac{dm}{dt} = 3\rho\gamma r \int_{(\gamma rt)^3}^{\infty} \phi_0(v)(v^{1/3} - \gamma rt)^2 dv = V\frac{dc}{dt} + Qc \qquad (2.15)$$

with $\gamma r = k_v^{1/3} D$

in which r (mol cm^{-2} s^{-1}) is the specific dissolution rate and the parameter γ (m^3 mol^{-1}) is expressed as a function of measurable properties:

$$\gamma = \frac{a_{BET} M_{mol} m_0}{3\rho \int_0^{\infty} \phi_0(v) v^{2/3} dv} \qquad (2.16)$$

with: a_{BET} the BET specific surface area (cm^2 g^{-1}); M_{mol} the molar mass of olivine (g mol^{-1}) and m_0 the total initial mass of particle population (mol). By fitting Equation 2.15 to the experimental concentrations of Mg^{2+} (c_{Mg}) and Si^{4+} (c_{Si}), expressed as olivine equivalents (c) that in a perfect stoichiometric dissolution process, is given by:

$$c = c_{si} = \frac{c_{Mg}}{1.82} \qquad (2.17)$$

the product γr was calculated; dividing then γr by the value of γ obtained for the particle size fraction of olivine used in this work, (90-180 μm), the value of r was obtained.

For olivine with similar bulk properties (e.g. composition and crystal defects) the dissolution rate D can be assumed to be a function of the experimental conditions (pH, CO_2 fugacity and salinity) only and independent of particle size and shape, since by definition of γr, D can be expressed as:

$$D = \frac{\gamma r}{k_v^{1/3}} = \cos t \qquad (2.18)$$

2.4 Results and discussion

Specific data regarding olivine dissolution experiments carried out at 120 °C are reported in Table 2.1. In particular, for each experiment, the applied operating conditions, i.e.: CO_2 fugacity (f_{CO2}), LiOH (Li^+) and salt (either $NaCl$ or $NaNO_3$) concentrations, flow rate (Q), suspension volume (V), initial olivine mass (m_0), and duration of the experiment are listed, together with the resulting specific dissolution rate (r), and the calculated pH. Two sets of experiments are shown:

- Experiments 27 to 37 (reported also in Hänchen et al., 2006), carried out with neither CO_2 nor salt, in which the pH was set by adding HCl or LiOH;
- Experiments 54 to 135, performed under a CO_2 atmosphere with or without salt addition, all of which previously unpublished data, except for experiments 54 to 68 already reported by (Hänchen et al., 2006).

As an example, in Figure 2.2 Exp. No. 92 (carried out at pH = 3.44, corresponding to fast dissolution) is analyzed in more detail. In particular, the measured Mg^{2+} and Si^{4+} concentrations, expressed in olivine equivalents according to Equation 2.17, are plotted over time, together with their arithmetic average. These experimental data are compared with the simulation results, obtained by solving numerically Equations 2.3 and 2.4, as described in the previous section. The specific dissolution rate r, reported in the figure legend, was obtained by least-squared minimization of the residuals between the experimental data and the results of the model. In this case, the agreement is rather satisfactory, as in all the other experiments.

In Figure 2.2, the Mg^{2+} and Si^{4+} concentrations vary in time according to the dissolution dynamics, but remain always in their stoichiometric ratio. This was not always the case, as illustrated in Figure 2.3, where the time evolution of the ratio of the two concentrations is plotted in the case of the Exps. No. 36, 60, and 119. The behaviour observed in this figure is indeed general, thus indicating that after an initial transient phase, the Mg^{2+} to Si^{4+} concentration ratio stabilized to its stoichiometric value. For modelling and regression purposes and to reduce the variability, the arithmetic average of the two concentrations expressed in olivine equivalents was used (Equation 2.17).

Table 2.1 Olivine dissolution at 120 °C: operating conditions and experimental results.

pH	f_{CO2}	Li^+	Salt	Q	V	m_0	Duration	r	Exp.
	bar	mol/ kg	mol/ kg	ml/min	ml	mg	h	$(mol/cm^2/s)*10^{10}$	No.
2.01	-	0	0	10.37	160	55	10	10.3	28
2.02	-	0	0	10.37	160	59	9.5	11.2	27
2.02	-	0	0	10.37	160	68	7	15.0	34
4.24	-	0	0	10.3	180	149	3	0.95	37
5.13	-	0	0	4.95	168.4	203	5	0.41	36
6.31	-	0	0	10.34	163	401	4	0.12	29
6.49	-	0	0	10.37	163	401	4	0.13	30
8.33	-	0	0	5.05	160	1002	10	0.017	32
3.35	103.8	0	0	1.9	116.47	6.6	3	7.43	55
3.4	80.5	0	0	1.9	163.7	6.4	7	6.65	54
3.43	102.9	0	0	1.9	130.87	4.9	6	5.00	114
3.44	80.5	0	0	1.9	177.86	11.3	7	4.50	92
3.45	123.2	0	0	1.9	203.54	6.1	6	8.50	56
3.83	19.8	0	0	2	158.37	5.2	6	4.35	115
3.87	80.6	0	0	4.9	203.25	27.7	6	2.90	64
3.89	80.5	0	0	5.1	184.05	30.6	7	2.25	94
4.22	79.6	0.004	0	1.9	199.97	13.3	7	1.67	60
4.5	14.3	0.0013	0	5	168.92	13.9	6	1.00	116
4.75	14.3	0.0024	0	5	172.57	34.1	7	0.70	117
5.08	13.8	0.0053	0	5	175.05	68.8	7	0.60	66
5.08	13.5	0.0053	0	5.1	166.67	60.8	7	0.717	96
5.42	13.7	0.012	0	5.1	171.73	123.4	6	0.60	118
5.69	12.6	0.026	0	5.1	154.95	187	12	0.20	68
5.71	13.8	0.026	0	5.1	169.38	186.8	6	0.377	97
5.96	14.7	0.053	0	5.1	162.16	62	6	0.110	95
6.04	13.5	0.06	0	5.1	138.77	211.6	5	0.195	98
6.21	13.5	0.096	0	4.8	170.85	101	9	0.148	106
6.34	13.4	0.14	0	5.1	173.93	106.8	7	0.155	112
6.4	15.1	0.19	0	5.1	174.01	229.3	2	0.0695	99
6.45	13.5	0.19	0	5.1	180.10	302	7	0.101	100
6.59	5.6	0.096	0	5.1	192.57	103	9	0.058	109
6.68	4.5	0.096	0	5.1	174.84	101.5	4	0.115	107
6.82	4.5	0.14	0	5.1	184.05	108.9	8	0.118	108
6.84	4.3	0.14	0	5.1	180.56	109.1	9	0.071	113
7.1	1.8	0.096	0	5.1	191.98	104.8	4	0.051	110
7.81	0.4	0.14	0	5	201.02	105.6	5	0.020	111

Table 2.1 continued.

pH	f_{CO2}	Li^+	Salt	Q	V	m_0	Duration	r	Exp.
	bar	mol/ kg	mol/ kg	ml/min	ml	mg	h	$(mol/cm^2/s)*10^{10}$	No.
3.21	80.6	0	1*	5	181.03	12	6	8.64	63
3.45	79.6	0	2.5*	5	213.17	23	7	2.28	70
3.64	80.6	0	0.1*	4.4	198.81	100.2	3	3.67	62
4.08	13.7	0.0013	2*	5.4	165.25	13.4	6	5.37	122
4.1	13.7	0.0013	1**	5.3	171.15	13.2	7	1.67	120
4.14	13.7	0.0013	1*	5.2	169.18	13.1	6	3.42	119
4.31	13.7	0.0024	2*	5.4	208.17	51.3	7	0.743	131
4.64	13.7	0.0024	0.1*	5	180.37	47.5	5	0.878	130
4.73	13.7	0.0024	0.01*	5	173.34	54.9	5	0.90	129
4.8	4.1	0.0024	2*	5.3	185.85	47.3	7	0.878	125
4.85	4.8	0.0024	1*	5.3	179.65	43.8	7	0.830	121
4.9	4.1	0.0024	1**	5.3	177.36	52.8	6	0.634	127
5.4	14.3	0.026	1*	5.1	189.35	47.4	6	1.15	128
5.41	13.7	0.026	1*	5.3	175.33	49.2	5	0.107	123
5.65	14.3	0.06	2*	5.5	223.86	48.5	6	0.228	135
5.74	14.3	0.06	1*	5.2	173.4	51.9	5	0.319	133
5.76	13.7	0.06	1*	5.2	174.92	45.5	6	0.454	134
5.96	13.7	0.096	1*	5.9	176.73	47.4	4	0.092	124

Symbols indicate the type of salt: *NaCl, **$NaNO_3$.

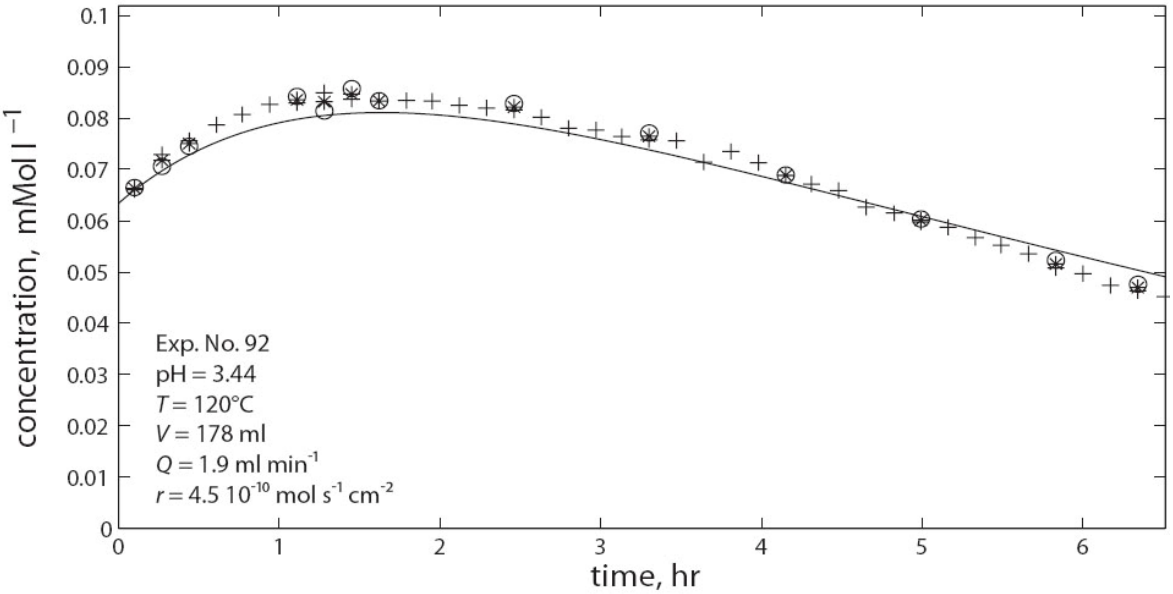

Figure 2.2 Ion concentration over time during a fast dissolution experiment (Exp. No. 92) with (+) Mg^{2+} concentration, (○) Si^{4+} concentration, (*) arithmetic average and (-) model.

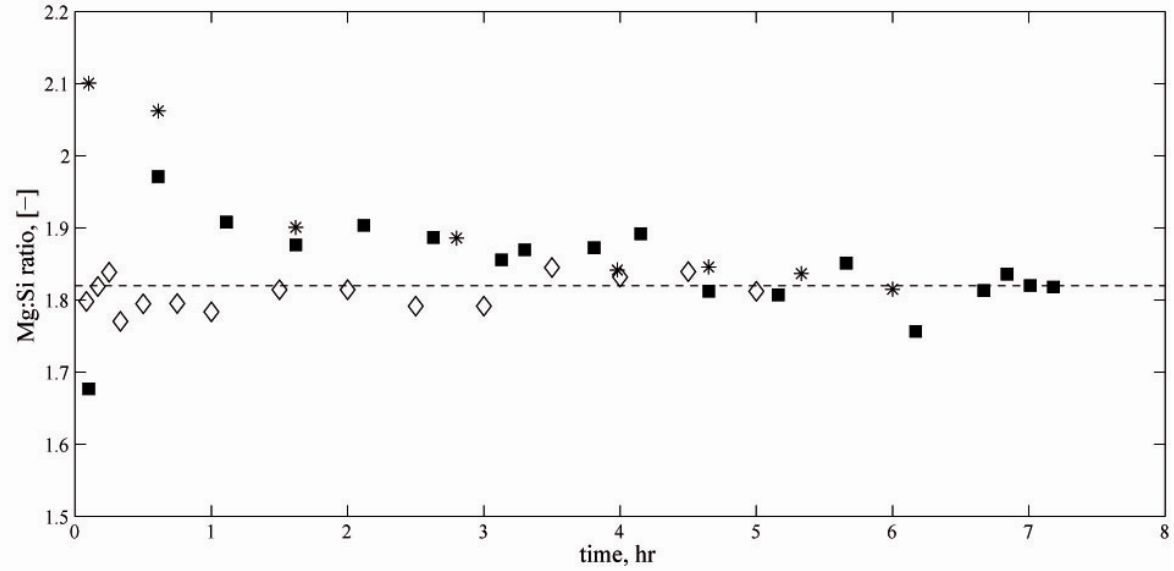

Figure 2.3 Mg/Si ratio over time for three different experiments. Symbols: (◊) experiment without CO_2 at pH 5.14 (Exp. No. 36 in Hänchen et al., 2006); (■) experiment with CO_2 without salts at pH 4.22 (Exp. No. 60 in Table 2.1); (*) experiment with CO_2 and 1 mol/kg NaCl at pH 4.14 (Exp. No. 119 in Table 2.1).

For all the experiments reported in Table 2.1, the logarithm of the value of *r*, estimated using the method described in Section 2.3, is plotted as a function of the calculated pH value in Figure 2.4. In this figure, also the values obtained in eight experiments without CO_2, in which HCl was used to acidify the solution, reported and analyzed in Hänchen et al., 2007 are reported. Experiments carried out with and without CO_2, with and without salt addition, can be distinguished by the different symbols.

The main conclusion that can be drawn by analyzing these results is that the change in the dissolution rate could be accounted for by the change in solution *pH* only. Varying the CO_2 fugacity, LiOH or HCl concentration, or the salinity, produced a change in the *pH* value, which in turn led to a change in *r*, but there was no evidence of a direct and independent effect of these parameters on the dissolution rate. Therefore, all experimental data in Figure 2.4 were regressed using a single equation, namely the following linearized form of Equation 2.2:

$$\log r = -npH + B \tag{2.19}$$

with *r* in mol cm^{-2} s^{-1}, $pH = -log(a_{H+})$, $n = 0.523 \pm 0.047$ and $B = -7.59 \pm 0.24$, defined as:

$$B = \log(Ae^{-\frac{E_a}{RT}}) \tag{2.20}$$

based on a 95% confidence interval (this corresponds to A = 0.264 mol cm^{-2} s^{-1} in Equation 2.2) with a regression coefficient R^2 = 0.91. The corresponding straight line is plotted as a solid line in the same figure, where it can be compared with the same regression determined earlier (dash-dotted line) and based on a much smaller set of CO_2-free dissolution experiments, where n = 0.46 ± 0.03, B = - 8.05 ±0.13 and R^2 = 0.98 (Hänchen et al., 2006; 2007). It is worth noting that although the regression coefficient was higher in the earlier work because the regression was based on a smaller number of more homogeneous data (neither CO_2 nor salt present) the value of the reaction order *n* obtained in this study was closer to the theoretical value of 0.5. The two regression lines were anyhow in good agreement, considering also the experimental variability. The only noticeable difference was a slight dissolution enhancement at low pH values in the new regression. As to the effect of CO_2, which was considered to be detrimental at pH values larger than 5 in the earlier work (Hänchen et al., 2006), the large amount of consistent experimental evidence reported in this work demonstrates that such an effect was an artefact. The inconsistency of the earlier measurements (Hänchen et al., 2006), was presumably due to the very small amount of dissolved olivine on which the estimated values of dissolution rate were based.

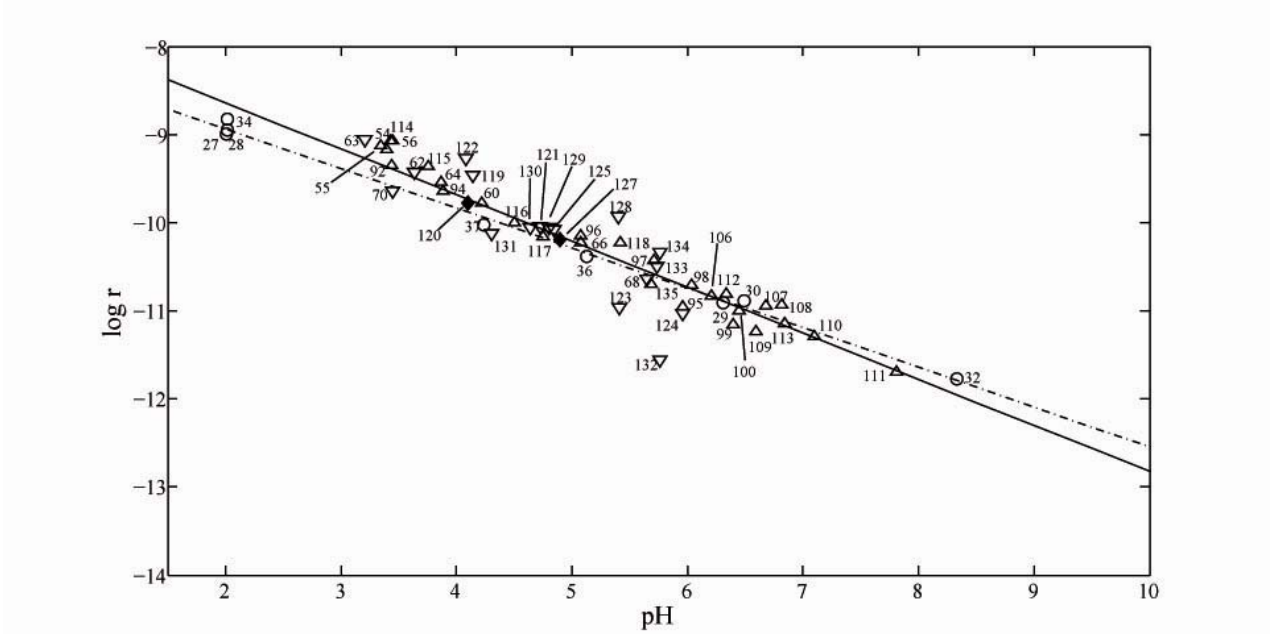

Figure 2.4 Logarithm of *r* values plotted over pH for each run at 120 °C and linear model described in Equation 2.2. Namely: (○) experiments without CO_2, (△) experiments with CO_2 with or without LiOH; (▽) experiments with CO_2 and NaCl; (◆) experiments with CO_2 and $NaNO_3$; (——) Equation 2.19 with n = 0.52 and B = -7.59 (this work); (– · -) Equation 2.19 with n = 0.46, B = - 8.05 (Hänchen et al., 2007).

2.5 Conclusions

The conclusion of this comprehensive experimental work is simple but rather significant. The specific dissolution rate of olivine at a given temperature in the pH range between 2 and 8 depends on pH only. The effects of CO_2 fugacity, LiOH, HCl, salt concentrations, and combinations thereof are important inasmuch as they affect the pH, but not directly and independently. There is no inhibition effect of the presence of CO_2 on olivine dissolution at pH higher than 5 as previously reported, which is important because these are the conditions where carbonate precipitation is favoured. This investigation was carried out at 120 °C, but it could be argued that these conclusions are general and can be applied to any temperature in the range between 25 °C and 150 °C, for which several studies have reported the dissolution mechanism to stay the same. This may constitute an interesting finding in view of the design and optimization of an effective mineral carbonation process.

Chapter 3: Carbonation of MSWI residues

On the basis of the main results of previous studies, which were overviewed in Chapter 1, it appears that accelerated carbonation can be applied to different types of MSWI residues with different purposes.

For APC residues, the high contents of readily reactive calcium hydroxides make carbonation potentially suitable for CO_2 sequestration objectives, with possible integrations of the carbonation process within waste combustion facilities in order to reduce the net CO_2 emissions from these industrial plants. However, due to the relatively low amounts of such residues as compared to the original waste, but also with respect to other alkaline industrial waste streams, a quite limited reduction in CO_2 emissions can be anticipated for carbonation processes using only MSWI APC ash as a feedstock.

In the case of MSWI bottom ash, due to its typically limited content in Ca and Mg reactive phases, accelerated carbonation has been chiefly applied with the aim of attaining a chemically stable structure with improved leaching behaviour. Yet, as shown by several studies, the composition and reactivity of BA varies greatly with particle size and hence some classes of this material may show significant CO_2 uptake potential.

Concerning the release of contaminants from carbonated MSWI residues, leaching mechanisms have been found to differ for APC residues as compared to bottom ash, depending on the different role played by major components towards the stabilization of trace contaminants. The higher Al and Si content in bottom ash, as compared to the other solid residues, accounts for the formation of larger amounts of mineral phases which likely possess sorption capacity towards trace contaminants, implying generally higher contaminant immobilization efficiencies. The higher organic matter contents in bottom ash as compared to APC residues can also account for a different effect of accelerated carbonation on the mobility of metals like Cu and Pb which can be complexed by dissolved organic carbon.

The experimental studies carried out on MSWI residues within this doctoral project have regarded in particular, the study of the effects of accelerated carbonation on humidified APC ash and specific particle size fractions of bottom ash at mild operating conditions, to assess the CO_2 uptake potential of the material and investigate the effects of the process on the mineralogy and leaching behaviour of the residues. In particular, for each material, the

effects of the main operational parameters (temperature, CO_2 partial pressure, particle size and liquid to solid ratio) on CO_2 uptake were studied, so to select the most effective conditions to enhance the Ca conversion yield and also to gain insight on the prevalent reaction mechanisms for both types of materials. For APC ash, the results of carbonation tests on humidified ash, in terms of the Ca conversion yield and carbonation kinetics, were compared to those obtained on the same material applying the gas-solid route (Prigiobbe et al., 2009), so to asses the feasibility of applying each process route to sequester part of the CO_2 contained in the flue gas emissions of waste incineration plants.

Regarding the leaching behaviour of the residues, both landfill compliance and characterization (pH-dependant) tests were conducted to investigate the effects of carbonation on the different types of residues. For APC residues in particular, for which a lack of specific studies on the effects of accelerated carbonation on the mechanisms of heavy metal leaching was noted, an extensive and detailed study on the leaching-controlling mechanisms of fresh and carbonated APC residues was performed by applying geochemical modelling to the results of pH-dependant leaching tests.

Regarding bottom ash carbonation experiments, RDF (refuse derived fuel) incineration residues were selected, due to the significant amounts of Ca detected in particular in the finest size fractions of the slag. The mineralogy of each particle size class was analyzed in detail before and after the carbonation treatment so to identify the reactive species with CO_2 and the reaction products. The leaching behaviour of heavy metal and oxyanion forming elements was assed for untreated, naturally weathered and carbonated slag by comparing the results of leaching compliance tests to Italian landfill acceptance regulations. Furthermore pH-dependence tests were also carried out on fresh and carbonated slag so to investigate the effects of the treatment on the release of some heavy metals and oxyanion forming elements.

3. 1 Accelerated carbonation of MSWI air pollution control residues

This section presents the results of the experimental study carried out on accelerated carbonation of incinerator air pollution control residues.

An extended characterization of the residues prior and after the treatment was performed to assess the amount of CO_2-reactive species in the ash and the effects of carbonation on ash mineralogy and microstructure. Batch carbonation experiments were carried out (in a stainless steel reactor with controlled gas humidity) on humidified ash using 100% CO_2 at different temperatures, pressures and liquid-to-solid ratios in order to assess the influence of these parameters on process kinetics, CO_2 uptake and the leaching behaviour of major and trace elements. A few experiments were also performed with a gas atmosphere of 9% CO_2, in order to assess the feasibility of applying this process directly to industrial flue gases, avoiding the CO_2 capture step.

The maximum Ca conversion to carbonate achieved was 70% and corresponded to a CO_2 uptake of 250 g/kg residues. The operational parameters that proved the most effective in enhancing reaction kinetics were the liquid to solid ratio of the samples (with an optimal value of 0.2 l/kg at 30°C) and reaction temperature (with an optimal value of 50°C for un-humidified ash).

The main effects of carbonation on trace metal leaching involved a significant decrease in mobility for Pb, Zn and Cu at high pH values, a slight change or mobilization for Cr and Sb, and no major effects on the release of As and soluble salts. Geochemical modelling of leachates indicated solubility control by different minerals after carbonation. In particular, in the stability pH range of carbonates, solubility control by a number of metal carbonates was clearly suggested by modelling results. Such findings indicate that accelerated carbonation of incinerator ashes has the potential to convert trace contaminants into sparingly soluble carbonate forms, with an overall positive effect on their leaching behaviour.

3.1.1 Introduction

[3]The correct management of the solid residues generated by waste incineration is an environmentally relevant issue that has been extensively and systematically investigated by numerous researchers (see e.g.: IAWG, 1997, Sabbas et al., 2003 and references therein). The progressively more stringent air emission criteria implemented over the last decades in most countries worldwide have forced and driven flue gas cleaning systems in waste incineration installations to improve significantly their treatment efficiency. This in turn causes inorganic contaminants contained in the original waste to be mainly transferred to the solid residues generated during the incineration process (Sabbas et al. 2003), where these are concentrated in a mass which is typically up to 20% of the feed waste (IAWG, 1997).

The main environmental concern with respect to the utilization or final landfill disposal of incinerator residues is associated to the release of inorganic contaminants including soluble salts and trace metals as a result of leaching processes (e.g.: Hjelmar, 1996). In recent years, researchers have addressed aspects related to investigating the leaching mechanisms and geochemical reactions involved (e.g.: Kirby and Rimstidt, 1994; Astrup et al. 2006a; Dijkstra et al., 2006; Cornelis et al., 2008) and assessed the effects of specific treatments for the improvement of the leaching behaviour of the material, in order to reduce the environmental impact of waste incineration residues and allow for their safe disposal and reuse in specific applications (e.g.: Arickx et al., 2006; Quina et al., 2008). Among these treatments, carbonation, both via natural weathering and/or accelerated carbonation, has been applied in several works, as described in Chapter 1, as a technique for the chemical stabilization of incineration residues characterized by high contents of alkaline phases which present high reactivity towards CO_2.

Notwithstanding the fair amount of studies recently conducted on accelerated carbonation of incinerator ashes, as reviewed in Section 1.4.2, the effects of the process on the mechanisms governing major elements and trace metals leaching from the material have not been adequately elucidated so far, so that conflicting results still exist in the literature and hence require further investigation. Furthermore, the works regarding the effects of accelerated carbonation on the mechanisms controlling the leaching behaviour of the ash, generally do not elaborate on the outcome of the treatment in terms of the CO_2 uptake, the achieved calcium conversion yield and the kinetics of the process.

[3]Most of this section is under publication as Baciocchi et al., 2009c.

The present work was aimed at investigating the effects of accelerated carbonation on humidified samples of APC residues to assess the CO_2 storage capacity of the ash and the influence of the main operational parameters on the kinetics of the reaction as well as the leaching-controlling mechanisms for carbonated APC residues, motivating the effects of carbonation on metal release by means of geochemical modelling.

3.1.2 Materials and methods

APC residues were sampled from the baghouse section of a hospital waste incinerator located near Rome, at the outlet of the flue gas dry treatment section where pulverized hydrated lime and activated carbon are added to remove acid gases and organic micropollutants.

Characterization of the APC ash included the determination of the water content and loss on ignition (LOI), element and major anion content, carbonate content, mineralogical and morphological composition, acid/base neutralization capacity (ANC/BNC) as well as leaching behaviour. Water content and LOI were determined following the ASTM D2216 and ASTM C25 standard procedures, respectively. The elemental composition was determined by alkaline digestion with $Li_2B_4O_7$ in platinum melting pots at 1050 °C, followed by dissolution of the molten material in a 10% HNO_3 solution and measurement of element concentrations using an atomic absorption spectrometer (AAS) equipped with an air-acetylene flame, a graphite furnace and a hydride generation system. Chloride and acid-soluble sulphates were measured using the Italian standard test procedure UNI 8520, which involves dissolution with hot deionised water and titration with $AgNO_3$ for chloride analysis, and dissolution with 3% HCl followed by spectrophotometric analysis for acid-soluble sulphates.

The carbonate content was evaluated both by calcimetry analysis of HCl-digested ash using a Dietrich-Frülingh calcimeter and by TG/DTA thermogravimetric analysis in an O_2 + N_2 (23 + 77% w/w) atmosphere in the temperature range 50–1210 °C at a heating rate of 10 °C/min.

The mineralogical composition was evaluated by TG/DTA and also by powder XRD analysis with Cu Kα radiation using a Philips Expert Pro diffractometer (equipped with a copper tube operated at 40 kV and 40 mA) with an angular step of 0.02° held for 2 seconds

with 2ϑ spanning from 5 to 85°. Morphological investigations were carried out by scanning electron microscope (SEM) analysis.

The ANC/BNC was evaluated by contacting several subsamples of the material with solutions (L/S = 6 l/kg) with increasing HNO_3 or NaOH concentrations to span a wide pH range (typically from 3 to 13 units). The concentrations of heavy metals, major elements and soluble salts in the eluates at different pH values were then analyzed by AAS. The EN 12457-2 leaching test was also conducted for comparison with regulatory limits. All chemical analyses were performed in duplicate except for the leaching experiments, which were run on a single replicate.

APC residues were carbonated in a 150 ml stainless steel reactor placed in a thermostatic bath to allow for temperature control at 30, 40 and 50 °C. Ash samples were oven dried at 105 °C, then mixed with distilled water at L/S ratios of 0.02 (the natural water content of the ash), 0.1, 0.2, 0.4 and 0.6 l/kg and placed in aluminium foil containers. Three samples of 1 g of dry ash were treated in each experiment with a continuous 100% CO_2 flow (except for a few experiments which were carried out under a 9% CO_2, 21% O_2 and 70% N_2 volume flow). Gas pressure was set at 1, 3, 5, 7 or 10 bar. Temperature was monitored with a thermocouple, while gas humidity was maintained at 75% using a saturated NaCl solution in the reactor. For each experiment, a control sample was prepared with the same procedure and stored in closed containers in contact with air at atmospheric pressure in the thermostatic bath for the whole length of the experiment. The reactor was flushed with CO_2 at the beginning of each run to ensure air expulsion. The experiments were conducted for reaction times from 10 min to 48 h to study the CO_2 uptake kinetics under different operating conditions.

The influence of gas humidity was also investigated using saturated solutions of K_2CO_3 and KNO_3 to obtain a relative humidity in the reactor of 43 and 92% respectively, but no significant changes in both CO_2 uptake and carbonation kinetics could be observed.

The degree of carbonation was estimated by the CO_2 uptake of treated samples as determined by calcimetry and TGA measurements.

To derive information on leaching-controlling mechanisms, metal concentrations as a function of pH as obtained from the ANC/BNC test for both the untreated and the carbonated ash were inputted into the Visual Minteq (ver. 2.3) geochemical speciation code, a Windows version of MINTEQA2 (Allison et al., 1991), which uses Debye-Huckel

and Davies equations to estimate the activity coefficients of the aqueous species. This allowed for estimation of the composition of the leachates in equilibrium with potential solubility-controlling minerals. The default database was integrated by adding the solubility constant ($\log K_{sp}$) of a number of minerals (see Table 3.1) based on data available from different literature sources. The application of the speciation code followed a three-step procedure:

(1) the program was run using the measured concentrations and pHs as input data and suppressing precipitation for all solid phases;

(2) potential solubility-controlling minerals where chosen among those displaying saturation indices (SI) in the range $-1.5 \leq SI \leq +1.5$ and on the basis of the likelihood of formation in APC ash leachates;

(3) the program was run a second time enabling precipitation of the selected minerals as "infinite solids", and the predicted concentrations of each element in equilibrium with the selected mineral phases were derived. In the calculations, the hypothesis of oxidizing conditions was always assumed.

Table 3.1 Values of the stability constants for different minerals used for Visual Minteq's thermodynamic database update

Mineral name	Chemical formula	log K_{sp}	Reference
---	$Ca(Sb(OH)_6)_2$	-12.55	Johnson et al., 2005
---	Ca_2SiO_4	39.04	Blanc et al., 2007
---	$Ca_3(AsO_4)_2 \cdot 4.25H_2O$	-21.0	Hyks et al., 2009
---	$Ca_3(AsO_4)_2 \cdot 3.66H_2O$	-21.0	Hyks et al., 2009
---	$Fe_2(MoO_4)_3$	38.82	Dijkstra et al., 2002
---	$PbSO_4 \cdot PbO$	-0.19	Dijkstra et al., 2002
---	$Pb_2V_2O_7$	-0.95	Astrup et al., 2006a
---	$Pb_3(VO_4)_2$	3.07	Astrup et al., 2006a
---	$ZnFe_2O_4$	9.85	Dijkstra et al., 2002
---	$ZnSiO_3$	2.93	Astrup et al., 2006a
Akermanite	$Ca_2MgSi_2O_7$	46.08	Blanc et al., 2007
Anorthite	$CaAl_2Si_2O_8$	25.31	Blanc et al., 2007
Calcium olivine	Ca_2SiO_4	37.65	Höglund, 2001
Calcium zincate	$CaZn_2(OH)_6 \cdot 2H_2O$	43.9	Astrup et al., 2006a
Cr-monosulphate	$Ca_4Al_2(CrO_4)(OH)_{12} \cdot 9H_2O$	71.62	Hyks et al., 2009
Forsterite	Mg_2SiO_4	28.60	Blanc et al., 2007
Friedel's salt	$Ca_4Al_2Cl_2O_6 \cdot 10H_2O$	-27.6	Hyks et al., 2009
Gehlenite	$Ca_2Al_2SiO_7$	55.23	Blanc et al., 2007
Leucite	$KAlSi_2O_6$	6.42	Astrup et al., 2006a
Merwinite	$Ca_3Mg(SiO_4)_2$	69.27	Blanc et al., 2007
Monosulphate	$Ca_4Al_2O_6(SO_4) \cdot 12H_2O$	72.57	Hyks et al., 2009
Stratlingite	$Ca_2Al_2Si(OH)_{16}$	49.44	Hyks et al., 2009
Wairakite	$CaAl_2Si_4O_{12} \cdot 2H_2O$	18.87	Astrup et al., 2006a
Wollastonite	$CaSiO_3$	12.99	Astrup et al., 2006a

3.1.3 Results and discussion

Ash characterization

The physical and chemical properties of the APC ash used in the present study are reported in Table 3.2. Due to the dry hydrated lime-based system used in the incinerator for acid gas removal, Ca and chloride were by far the major constituents, accounting for more than 50% of total ash mass. Significant heavy metal concentrations were also observed, namely with regard to Zn, Cu and Pb. These results are in good agreement with the average composition values reported in the literature for these types of residues (Quina et al., 2008).

Table 3.2 Main physical and chemical characterization of the APC ash.

Physical Property	Value (% w/w)
Water content	1.78
LOI	21.37

Anion	Concentration (g/kg)
Cl^-	179.7
SO_4^{-2}	33.6

Element	Concentration (mg/kg)	Element	Concentration (mg/kg)
Al	2140	Mg	8440
Ca*	350000	Mn	30.0
Cd	2.1	Na	38440
Cr	38.0	Ni	20.0
Cu	712.0	Pb	588.0
Fe	934.0	Si	10080
K	5620	Zn	4456

* indirect calculation based on Ca speciation

Figure 3.1a reports the results of the TG/DTA analysis of the untreated material, the total weight loss showing good accordance with the LOI value, reported in Table 3.2. Three major weight losses were observed on the TG curve, two between 400 and 450 °C and one between 650 and 800 °C, that can be associated to the decomposition of calcium hydroxides (endothermic peak on the DTA curve), organic carbon oxidation (exothermic peak) and decomposition of carbonates (endothermic peak), respectively.

The main crystalline phases detected in the untreated ash by XRD analysis (see Figure 3.2) were found to include $Ca(OH)_2$, CaClOH, $CaCO_3$, $CaSO_4$, NaCl and KCl, in accordance with previous mineralogical analyses of APC residues (Bodénan and Deniard, 2003; Li et al. 2007). Calcimetry results confirmed TGA data, indicating a quite high $CaCO_3$ content (18% w/w) in the untreated material, which was likely due to natural carbonation upon contact with CO_2, either during the flue gas treatment process or during the storage period. Calculation of Ca speciation among the above mentioned phases was made (see results in Table 3.3) in order to estimate the amount of Ca available for the carbonation process, i.e. in the form of $Ca(OH)_2$ and CaClOH. The $CaSO_4$ content was calculated assuming that all

acid-soluble sulphates were in the form of Ca species, as suggested by XRD results. For chloride species, it was assumed that the amounts of Na and K extracted during the EN 12457-2 leaching test derived entirely from the corresponding chloride salts (the presence of which was again indicated by XRD results). The remaining amount of chloride was assumed to be in the form of CaClOH. The $Ca(OH)_2$ content was then calculated as the difference between the total weight loss measured by TGA (see Figure 3.1) and that associated to $CaCO_3$ and CaClOH, considering for the latter the thermal decomposition reaction described by Equation 3.1, (Allal et al., 1998):

$$2CaClOH \rightarrow CaO \cdot CaCl_2 + H_2O \qquad (3.1)$$

The amount of Ca available for carbonation was estimated to be 38% as $Ca(OH)_2$ and 29% as CaClOH. Mg species were not considered since they could not be detected by XRD analysis and the Mg content of the ash (0.8%) was much lower than the Ca content.

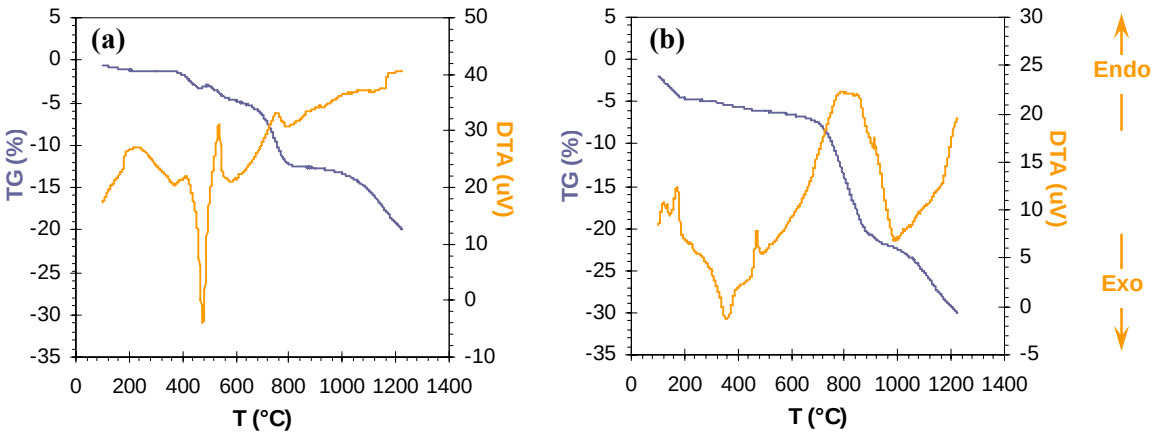

Figure 3.1 TG/DTA curves for (a) untreated and (b) carbonated (24 h, 30 °C, 3 bar, L/S 0.02 l/kg) APC ash.

Table 3.3 Calculated Ca speciation in the APC ash.

Species	Amount (% w/w)	Measurement/Assumption
$Ca(OH)_2$	37.8	Indirect calculation based on the difference between TG/DTA and calcimetry analysis and CaClOH content
CaClOH	28.9	Indirect calculation based on Na and K leaching, Cl^- content and XRD analysis
$CaCO_3$	18.0	Direct calculation from TG/DTA and calcimetry analyses
$CaSO_4$	4.8	Direct calculation based on SO_4^{-2} content and XRD analysis

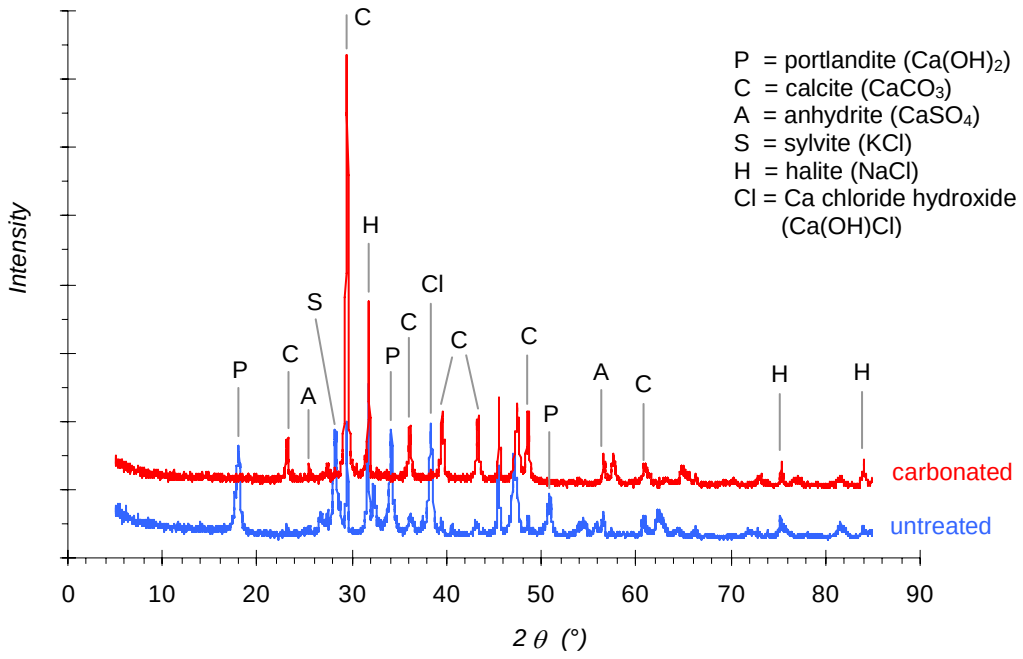

Figure 3.2 XRD patterns of untreated and carbonated (24 h, 30 °C, 3 bar, L/S 0.02 l/kg) APC ash.

Evidences of carbonation

Carbonated samples exhibited a markedly different mineralogy, morphology and acid neutralization capacity compared to the untreated ash.

TGA and XRD analysis on carbonated ash (see Figure 3.1b and Figure 3.2), as previously mentioned, showed a significant presence of $Ca(OH)_2$ and Ca(OH)Cl in the untreated material, but not in the carbonated samples, which instead were characterized by a strong predominance of $CaCO_3$, proving the two calcium hydroxides to be the reacting species with CO_2 and calcite to be the main product of this reaction.

The acid/base neutralization capacity (ANC/BNC) of the APC ash is shown in Figure 3.3. The curve for the untreated material exhibited a high buffering capacity at a pH value of around 12, typical of calcium hydroxide species, with a total acid neutralization capacity of approximately 13 meq/g, in good agreement with the estimated amount of calcium hydroxides (see Table 3.3) of (13.3 meq of $Ca(OH)_2$ + CaClOH). For the carbonated ash instead, upon addition of 1 meq/g HNO_3, the pH dropped to approximately 5.5, at which a plateau, typical of carbonate and bicarbonate species, was observed. The total amount of acid neutralized at this pH was of about 12 meq/g, corresponding to a $CaCO_3$ content of 60% wt., in good agreement with the values measured by calcimetry analysis for fully

carbonated samples. Conversely, NaOH additions resulted in very similar shapes of titration curves for untreated and carbonated ash.

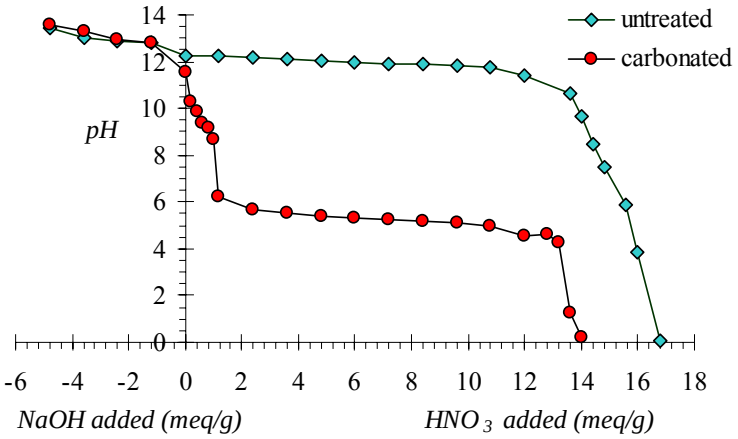

Figure 3.3 ANC/BNC curves for untreated and carbonated (1.5 h, 30°C, 3 bar, L/S 0.2 l/kg) APC ash.

The ash microstructure was also affected to some degree by carbonation. SEM images of untreated and carbonated APC residues (see Figure 3.4) indicated that carbonated ash had a larger grain size and a reduced pore space as compared to the untreated residues, exhibiting a more regular and rounded-out morphology, characteristic of calcium carbonate particles. This result is in agreement with previous observations, where an increase in particle size due to particle agglomeration and a decrease in porosity and tortuosity were observed for APC ash (Fernández-Bertos et al., 2004).

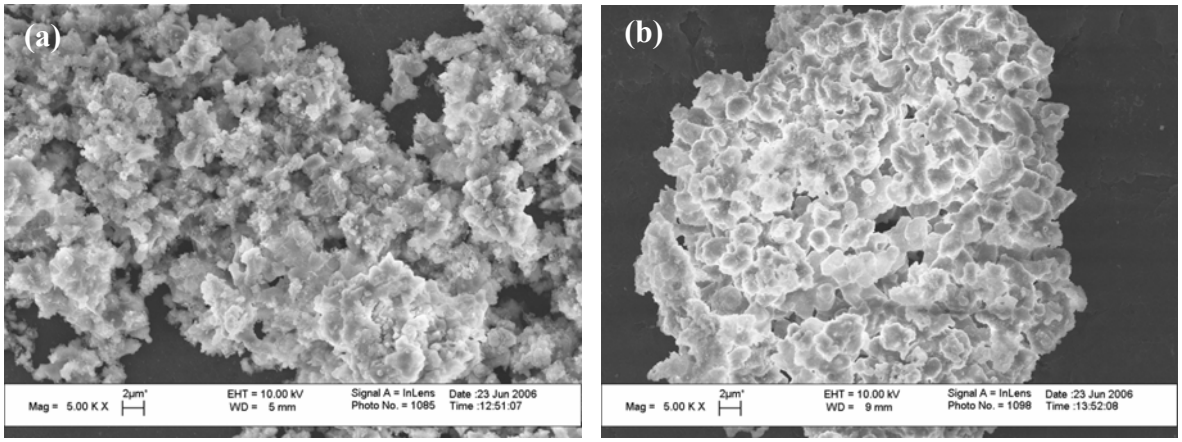

Figure 3.4 SEM images of (a) untreated and (b) carbonated (1.5 h, 30 °C, 3 bar, L/S 0.2) APC ash.

Calcium conversion and carbonation kinetics

The extent of carbonation was assessed by measuring the weight gain upon carbonation and the CO_2 uptake of the ash. This latter parameter was measured by calcimetry and TG analysis of both untreated and carbonated samples, subtracting the CO_2 content of treated samples ($CO_{2(final)}$) by the amount of CO_2 measured in the residues prior to carbonation ($CO_{2(initial)}$), accounting for the weight increase upon carbonation, as shown in Equation 3.2. Results from calcimetry and TG analyses were in good agreement and both indicated maximum CO_2 uptakes of 25%.

$$CO_{2\,uptake}[\%] = \frac{CO_{2\,(final)}[\%] - CO_{2\,(initial)}[\%]}{100 - CO_{2\,(final)}[\%]} \times 100 \qquad (3.2)$$

The differences with the results of previous studies (Ecke 2003; Li et al., 2007), which reported significantly lower CO_2 uptakes than those obtained in this work, could be due, other than to the operating conditions applied, which were quite similar to those used by Li and co workers (2007), to the amount of Ca reactive species in the APC samples analyzed in this study. The ash in fact, as previously shown, had a high content of unreacted hydrated lime due to the large excess of reagents used in the air pollution control units of hospital waste incineration plants.

The resulting Ca conversion yields, η, were estimated according to equation (3.3), in which $Ca_{reactive}$ is the sum of the initial contents of CaOHCl and $Ca(OH)_2$:

$$\eta[\%] = \frac{CO_{2\,uptake}[\%] \times 40/44}{Ca_{\,reactive}\,[\%]} \times 100 \qquad (3.3)$$

The maximum yield (70%), corresponding to a 25% CO_2 uptake, was found to be similar to the one achieved by Prigiobbe et al. (2009a) applying the direct gas solid route to the same APC residues.

The dependence of CO_2 uptake kinetics upon the operating variables: L/S ratio and treatment temperature are reported in Figure 3.5. The trend of CO_2 uptake with time was in fact, found to be largely affected by the process conditions with a major effect of L/S ratio and temperature, compared to other parameters.

The L/S ratio had a strong impact on CO_2 uptake (see Figure 3.5a) particularly at low (< 8 h) treatment durations, with an approximately five-fold increase in carbonation yield as the L/S ratio was increased from 0 to 0.2 l/kg. As an example, after 4 h the dry samples

showed only 8.6% CO_2 uptake (corresponding to 23.6% conversion of reactive Ca species to calcite), compared to 15.5% (42.6% Ca conversion), 22.9% (63.2% Ca conversion) and 24.0% (66.3% Ca conversion) at L/S ratios of 0.02, 0.1 and 0.2 l/kg, respectively. However at L/S ratios above 0.3 a decrease in CO_2 uptake was observed. This behaviour is explained considering that a certain amount of water, which in turn depends on the specific characteristics of the material, is required for hydration and solvation of CO_2 and Ca^{2+} ions. In previous works on APC incinerator ashes, carried out under similar operating conditions, optimal L/S ratios of 0.2-0.3 l/kg for reaction times of 2.5-3 h were reported (Fernández-Bertos et al., 2004; Li et al. 2007). The decrease in CO_2 uptake above the optimal L/S ratio was likely related to a higher resistance towards CO_2 diffusion through the intergranular water film as this increased in thickness.

An insight into the effect of temperature on CO_2 sequestration capacity of the APC residue (see Figure 3.5b) showed that an increase from 30 to 50 °C greatly affected carbonation kinetics at L/S 0.02 l/kg, enhancing CO_2 uptake after 1-h reaction from 8.0 to 24.0%, or from 22.1 to 66.3% Ca conversion, respectively. Conversely, temperature increase at L/S 0.2 l/kg did not affect the carbonation rate, indicating that this parameter has a similar effect to the L/S ratio in enhancing Ca dissolution, and is therefore significant only for water contents considerably below the optimal value.

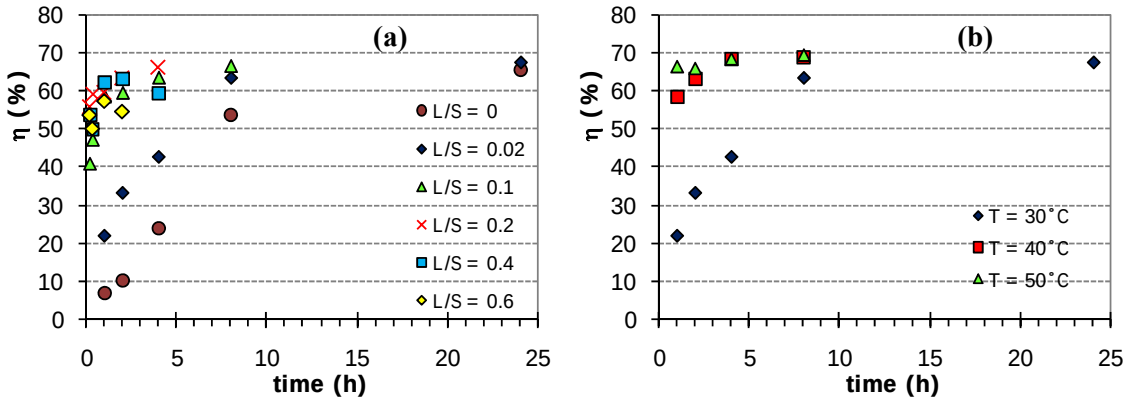

Figure 3.5 CO_2 uptake kinetics as a function of: (a) L/S ratio (at 30 °C and 3 bar), (b) temperature (at 3 bar and L/S 0.02 l/kg).

Pressure did not appear to largely influence carbonation kinetics for 100% CO_2 flows, (see Figure 3.6a), particularly for low reaction times; this was probably related to the fact that under the tested CO_2 partial pressures the carbonation process was kinetically controlled by Ca dissolution rather than by CO_2 diffusion. However when 9% CO_2 flows were applied,

very different results were obtained. As shown in Figure 3.6b at these operating conditions, an equivalent CO_2 uptake as the 100% CO_2 flow experiments was achieved only for a reaction time of 24 hours with a CO_2 partial pressure of 0.9 bar. Experiments carried out at a lower pressure showed limited CO_2 uptake and slower kinetics, which was due to the decrease in the kinetics of both Ca dissolution (higher pH in the water film) and CO_2 diffusion. However, also for similar CO_2 partial pressures, experiments performed with 9% CO_2 flows showed remarkably lower CO_2 uptake kinetics for reaction times up to 8 hours for L/S of 0.02 l/kg (comparing the results of the experiments at 1 bar in Figure 3.6a and 10 bar in Figure 3.6b) and up to 4 hours for L/S of 0.2 l/kg (see figure 3.6c). This result indicates hence, that probably under the experimental conditions applied in this work (static batch experiments with down-flow gas supply) physical inhibition due to N_2 and O_2 presence in the gas feed occurred. Therefore, for gas compositions similar to combustion flue gas, it appears that this experimental configuration was not ideal, and instead fluidized-bed configurations may provide better results in terms of kinetics enhancement.

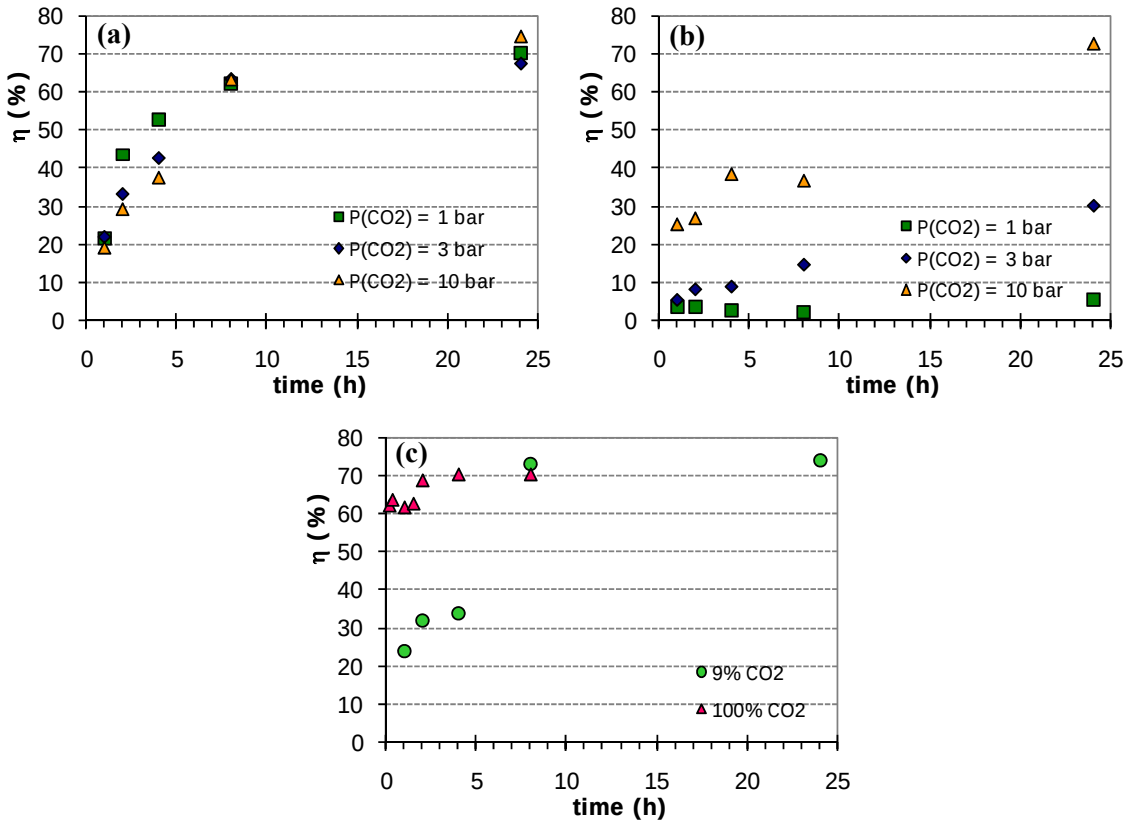

Figure 3.6 CO_2 uptake kinetics (at 30 °C and L/S 0.02 l/kg) as a function of pressure with: (a) 100% CO_2, (b) 9% CO_2; (c) CO_2 uptake kinetics (at 30 °C and L/S 0.2 l/kg) with 9% CO_2 at 10 bar and 100% CO_2 at 1 bar.

[4]The resulting maximum CO_2 uptakes measured in this study were very similar to those achieved by Prigiobbe et al. (2009) applying the gas-solid route to the same batch of APC residues, hence proving that CO_2 uptake depended primarily on the amount of reactive species in the residues and not on the chosen process route. Reaction kinetics instead, depended strongly on the process, proving much faster for the gas-solid route. The other interesting aspect of dry carbonation was that fast kinetics could be achieved also with 10% CO_2 gas flows, indicating that CO_2 capture and storage processes could be carried out in a single step by directly contacting the flue gases with these residues. Dry route carbonation though required temperatures above 400°C for kinetics optimization and hence should be carried out in sections of the incineration plant where flue gas is at an appropriate temperature, or where part of the steam used for energy production could be used to re-heat the gas. Wet carbonation experiments instead showed fast kinetics at 30°C with a liquid to solid ratio of 0.2 or at 50°C with un-humidified ashes. However as shown in Figure 3.6 this process, proved to be fast only for 100% CO_2 gas flows, implying that a CO_2 capture unit would be required before the actual carbonation reactor.

Leaching behaviour

Table 3.4 reports the results of the EN 12457-2 leaching test on untreated and carbonated (1.5 h, 30 °C, 3 bar, L/S 0.2 l/kg) ash along with a comparison with the Italian regulatory limits for landfill disposal of waste.

For the untreated material the main critical species were Pb, Zn, Cu, Cr, Sb and soluble salts (chloride and sulphate), similarly to what generally reported in the literature for this type of incineration residues (e.g.: Hjelmar, 1996). In particular, the leaching of Pb and chloride was above the limits for disposal in hazardous waste landfills, Zn release exceeded the limits for disposal in non-hazardous waste landfills, while for the other species mentioned the leachate concentrations were higher than those prescribed for inert waste landfills. Carbonation strongly reduced leaching to below the limits for non-hazardous (Pb) and inert waste landfills (Cu and Zn). Oxyanion-forming elements showed a different behaviour, with Cr being only slightly affected by the treatment, and Sb leaching increasing upon carbonation to values corresponding to disposal in hazardous waste landfills. As for soluble salts, chloride was not largely affected by carbonation, so that the leachate concentration still considerably exceeded the limit for hazardous waste landfills; sulphate leaching was reduced by a factor of 2, which is believed to be related to

[4]For more on the comparison between the dry and wet carbonation routes for APC carbonation see Baciocchi et al., 2009a.

a reduction in the solubility of the leaching-controlling mineral(s) as a result of chemical changes occurring upon carbonation (see discussion below on geochemical modelling for additional details). The leaching of major elements such as Ca, Na and K was only slightly affected by carbonation. These results are in good agreement with previous studies investigating the effects of carbonation on the leaching behaviour of major and trace elements in APC ash at the material's natural pH (Bone et al., 2003; Ecke et al., 2003; Fernández-Bertos et al., 2004; Li et al., 2007; Li, 2008; Baciocchi et al., 2006a,c).

Table 3.4 Leaching test (EN 12457-2) results for untreated and carbonated APC ash and comparison with Italian landfill acceptance criteria.

Element/ Species	Untreated	Carbonated	Limit concentrations		
			HW landfills	n-HW landfills	IW landfills
	(mg/kg)	(mg/kg)	(mg/kg)	(mg/kg)	(mg/kg)
As	0.013	0.006	25	2	0.5
Cd	0.004	0.001	2	0.2	0.04
Cu	*10.1*	0.052	100	50	2
Cr	*1.73*	*1.2*	70	10	0.5
Mo	*< 10*	*< 10*	30	10	0.5
Ni	< 0.01	< 0.01	40	10	0.4
Pb	**392**	*2.3*	50	10	0.5
Sb	*0.1*	2.24	5	0.7	0.06
Zn	122	3.6	200	50	4
Cl^-	**237 690**	**198 080**	25 000	15 000	800
SO_4^{2-}	*15 075*	*7650*	50 000	20 000	1000
Al	< 20	< 20	---	---	---
Ca	91 000	77 000	---	---	---
Fe	0.4	< 0.1	---	---	---
K	4150	4880	---	---	---
Mg	12.5	6.9	---	---	---
Mn	< 0.01	< 0.01	---	---	---
Na	42 600	34 500	---	---	---
Si	< 100	< 100	---	---	---
V	< 1	< 2	---	---	---

Legend: **bold values**: > limit for hazardous waste (HW) landfills
underlined values: > limit for non-hazardous waste (n-HW) landfills
italic values: > limit for inert waste (IW) landfills

The release of major elements and trace metals measured in the eluates of the ANC/BNC batch tests, for which the obtained pH trends for untreated and carbonated APC ash were previously discussed (see Figure 3.3), are reported in Figure 3.7 and Figure 3.8 as a function of pH for the untreated and carbonated (1.5 h, 30 °C, 3 bar, L/S 0.2 l/kg) APC residues respectively. The theoretical solubility curves of different potential solubility-controlling mineral phases, when identified by geochemical modelling calculations, are also plotted in the same graphs.

Among the major elements, **Ca leaching** from the untreated ash was fairly constant at ~65-75 g/l in the pH range 1-12, then decreased steeply with pH down to ~0.5 g/l. According to geochemical modelling results, anhydrite largely dictated Ca solubility even at highly alkaline pHs; solubility control by anhydrite was also confirmed by the good match between the solubility curve for this phase and the experimental results of SO_4 leaching. Although other authors (Astrup et al., 2006a; Hyks et al., 2007) suggested solubility control of Ca by gypsum, in this case anhydrite appeared to more closely describe the measured Ca concentrations within a large pH range; possible control of solution concentrations of both Ca and SO_4 by anhydrite alternatively to gypsum has also been suggested by previous studies (Kirby and Rimstidt, 1994). For pHs > 12, even though the shape of the predicted solubility curve for portlandite (whose presence in the ash was yet detected by XRD analysis; see Figure 3.2) was very similar to that of the experimental Ca leaching curve, the SI values for this phase ($0.35 \leq SI \leq 1.38$) were higher than those for anhydrite ($-0.80 \leq SI \leq 0.30$). Thus, in this case solubility control by portlandite in the highly alkaline pH region indicated by other studies (Astrup et al., 2006a; Hyks et al., 2007; Li, 2008) might be excluded. This may be supported by the fact that in such studies the match between the theoretical portlandite solubility curve and the measured leachate concentrations was not so good as to univocally infer on leaching control by this phase, and also considering that other results on the leaching of elements and soluble salts from combined waste incinerator APC residue/bottom ash (Kirby and Rimstidt, 1994) indicated portlandite as capable of dictating the release of Ca in some instances only.

For the carbonated material, the Ca levels in the leachates were similar to those of the untreated ash up to pH ≅ 4, then decreased by about one order of magnitude in the pH range 4-6, where the pH plateau in the acid titration curve was detected. Within such a pH interval, the hydrated Ca carbonate form, $CaCO_3 \cdot H_2O$, was clearly identified as the solubility-controlling phase, describing the experimental leaching data much better than calcite, which was oversaturated by a factor of 2.5-100 depending on pH. This finding represents a major difference from other studies on carbonated APC residues available in the literature, where solubility control by Ca carbonate could hardly be detected (Astrup et al., 2006a, b). The different Ca leaching observed could be motivated by the higher degree of ash carbonation achieved in the present research as compared to other experimental studies, which were mainly conducted on ash samples which had been naturally carbonated

upon contact with atmospheric air under much milder conditions than those used in the present study (pure CO_2 at a pressure up to 10 bar, controlled temperature (30 to 50 °C) and L/S ratio of 0.2 l/kg).

In the pH range 6-12, Ca leaching from the carbonated ash appeared to be well described again by anhydrite, and also by Ca-zincate ($CaZn_2(OH)_6 \cdot 2H_2O$), which had quite similar solubility curves. Ca-zincate is a solid solution of zinc hydroxide and portlandite which has been documented for cementitious systems (Kersten et al., 1997; Ziegler and Johnson, 2001). In our study, Ca-zincate also appeared to be a good candidate for leaching control of Zn for the carbonated material at pHs above 10, as tentatively proposed by other authors (Astrup et al., 2006a).

In the strongly alkaline pH range (pH > 12.5), as noted already for the untreated ash, leachates were again found to be oversaturated with respect to portlandite by a factor of approximately 10 ($1.0 \leq SI \leq 1.3$). Nevertheless, on the basis of the results from TGA measurements (see Figure 3.1), the presence of portlandite in the carbonated material was not detectable; as a consequence, any solubility control by portlandite for the carbonated material appeared not to be reasonable in this study and was thus excluded.

The amount of **Mg leached** from the untreated and the carbonated ash was very similar in the whole pH range investigated. For the fresh material solubility appeared to be controlled by forsterite (Mg_2SiO_4) in the pH range 8-11, and by $Mg(OH)_2$ at higher pHs; a number of outliers at pH > 12 were found to be described by sepiolite A ($Mg_4Si_6O_{15}(OH)_2 \cdot 6H_2O$). For the carbonated residue, the controlling phases were brucite in the pH range 10-12, and again $Mg(OH)_2$ at higher pHs. The absence of any significant solubility control by Mg-carbonate phases may be taken as an indication of the low reactivity of Mg species towards CO_2 under the carbonation conditions tested in this investigation; the fact that $Mg(OH)_2$ controlled Mg leaching for both the untreated and carbonated residue may support this hypothesis.

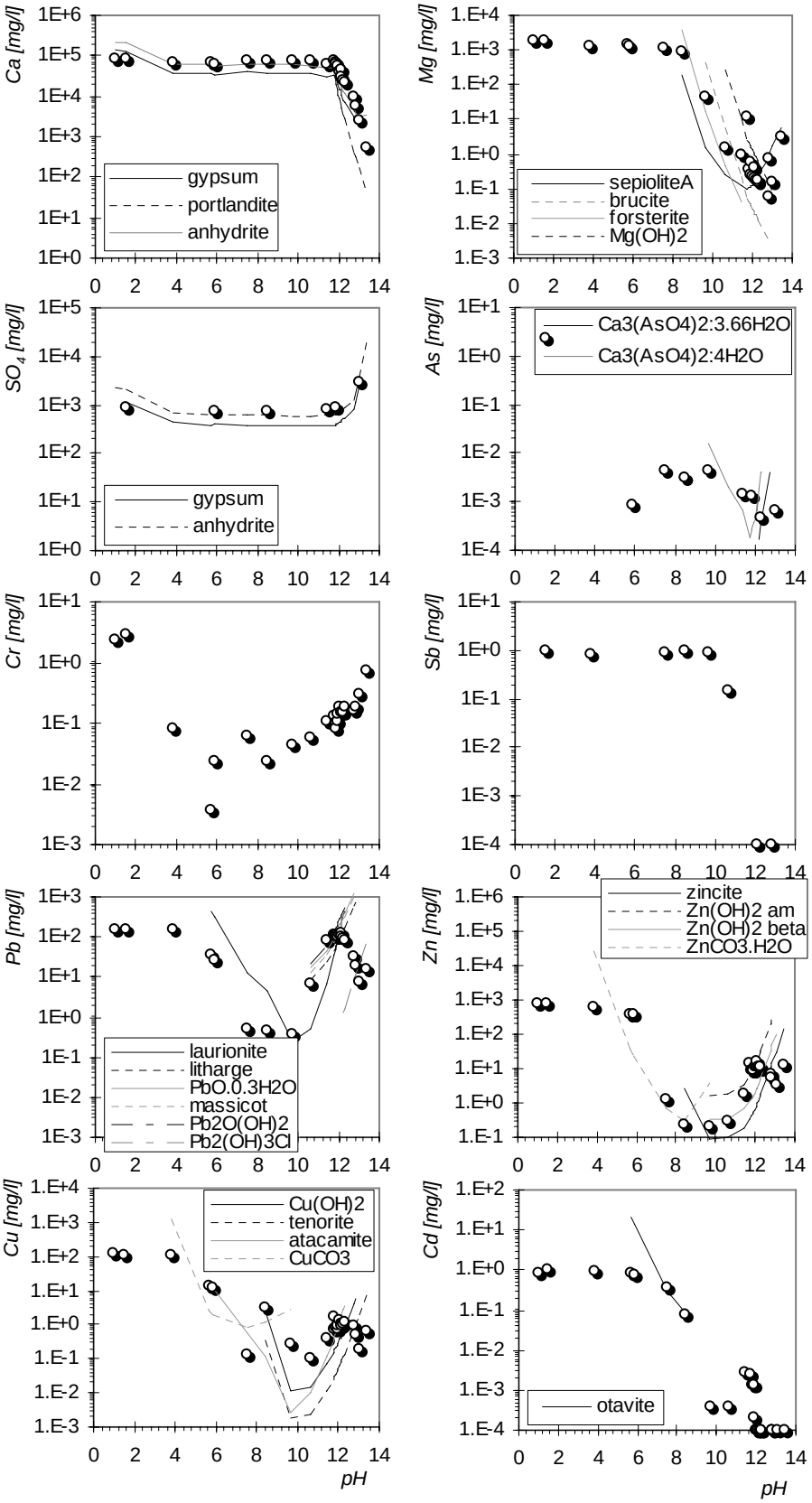

Figure 3.7 Metal release as a function of pH for untreated APC residues.

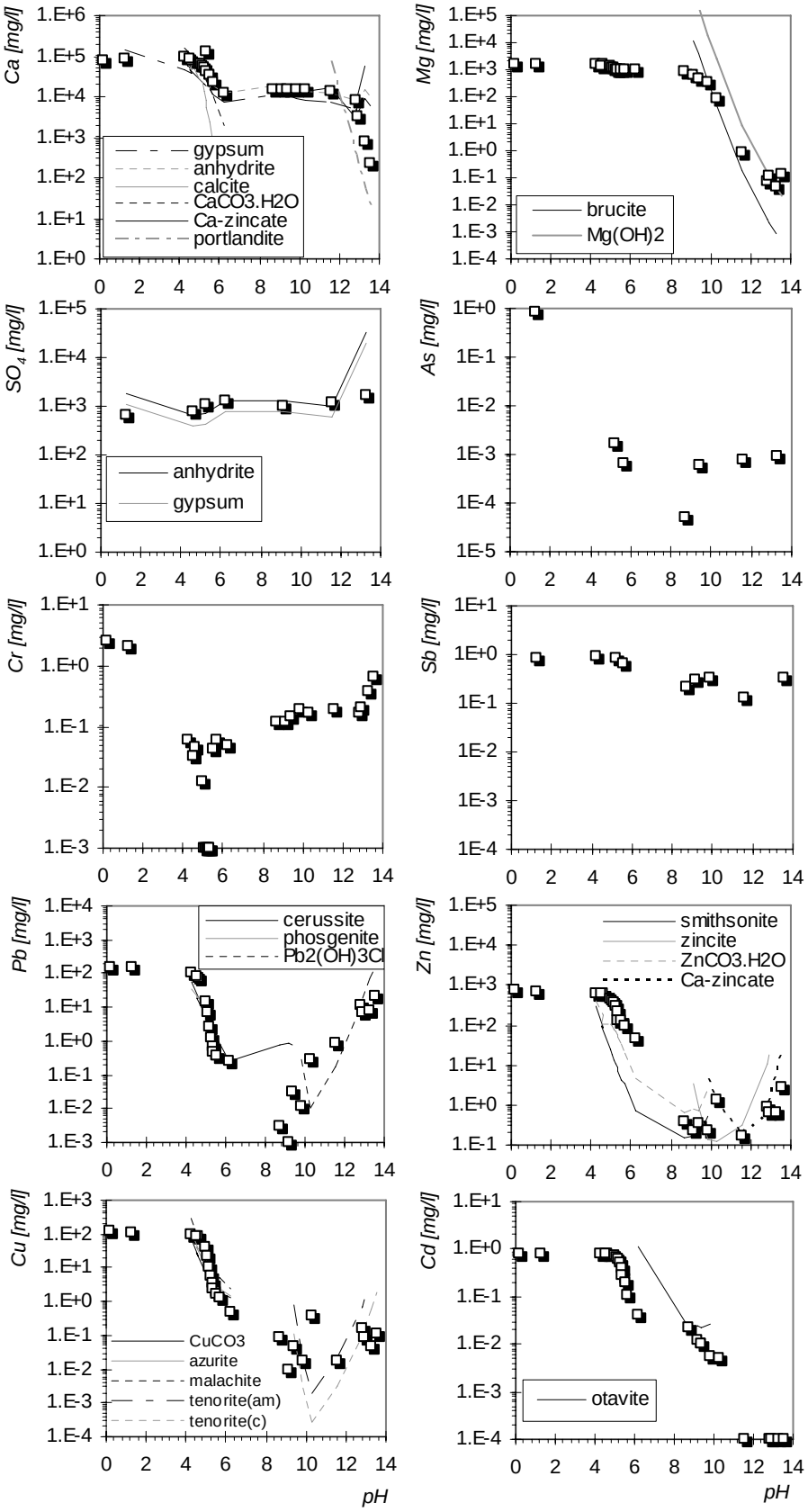

Figure 3.8 Metal release as a function of pH for carbonated APC residues.

In the present study, differently from what indicated by other investigators (Astrup et al., 2006a), the **release of Si** (results not shown here) appeared to be slightly enhanced by carbonation (from levels in the range <10-20 mg/l up to 12-65 mg/l) for all the pH values tested except for the very acidic conditions, where the Si levels in the leachates were comparable for the two ash samples. For the untreated ash none of the minerals contained in the Visual Minteq thermodynamic database was capable of describing the measured leachate concentrations; for the carbonated material Si leaching was adequately described by amorphous silica in the pH range 4-6 and also by wairakite ($CaAl_2Si_4O_{12}\cdot 2H_2O$) in the pH range 5.5-9. Under alkaline conditions the predicted solubility curves did not adequately match the measured data; quartz may have been responsible for Si solubility control in a limited pH range, although the shape of the curve was qualitatively different from the measured concentrations, as also observed by other authors (Astrup et al., 2006a). Both akermanite and wollastonite, identified by a number of investigators as possible solubility-controlling phases for Si (Astrup et al., 2006a; Hyks et al., 2007), showed poor fitting of the experimental data.

Among the trace elements investigated, **Pb leaching** was considerably reduced as a result of carbonation, with concentration levels in the leachates from the untreated and carbonated material differing by ≥ 1.5-2 orders of magnitude in the pH range 5-12. Although the reduction in the leaching of trace metals (including Pb) upon carbonation has been postulated by some authors to be merely due to the change occurring to the material's pH as CO_2 uptake proceeds and not to the formation of carbonate phases (Astrup et al., 2006a; Zhang et al., 2008), the results obtained from these experiments clearly showed that the whole Pb leaching curve was affected by carbonation, with an immobilization effect in a wide pH interval. A similar result has also been suggested by Ecke (2003) using a different analytical approach based on statistical analysis of carbonation runs. Control of Pb leaching for the untreated ash in the pH range 10-12.3 could be ascribed to a number of possible (hydr)oxide minerals including litharge and massicot (both PbO forms), that gave the best fitting to measured data points, or $PbO\cdot 0.3H_2O$ and $Pb_2O(OH)_2$, which had SI values still relatively close to 0 ($-1.5 \leq SI \leq 0.3$, and $-0.6 \leq SI \leq 0.3$, respectively). The mineral laurionite (PbClOH) also displayed a reasonably good match with measured concentrations down to pH ~9. Under strongly alkaline conditions (pH > 12) another chloride hydroxide mineral, $Pb_2(OH)_3Cl$, appeared to be a good candidate for solubility

control. For the carbonated material, the release of Pb appeared to be controlled by the carbonates cerussite ($PbCO_3$) and phosgenite ($Pb_2CO_3Cl_2$) in the pH range 4-6, again corresponding to the presence of the pH plateau in the acid neutralization curve. As observed for the untreated ash, under alkaline conditions Pb leaching was found to be governed by the chloride form $Pb_2(OH)_3Cl$.

Solubility control by carbonate minerals was also clearly observed for the other trace metal cations **Zn, Cu and Cd**, indicating a strong effect of the carbonation process on the leaching mechanisms. For such metals the best fit in the pH range 4-6 was given by the hydrated carbonate $ZnCO_3$·H2O for Zn (smithsonite, $ZnCO_3$, instead, generally displayed much higher SI values), by $CuCO_3$, azurite ($Cu_3(CO_3)_2(OH)_2$) or malachite ($Cu_2CO_3(OH)_2$) for Cu, and otavite ($CdCO_3$) for Cd, although in this case the fitting was worse.

For the untreated ash, Zn leaching in the pH interval 9-12.3 appeared to be controlled by different Zn hydroxide phases including $Zn(OH)_{2am}$ and $Zn(OH)_{2\beta}$ (confirming the results obtained by Hyks et al., 2007), while at higher pH values such phases became too soluble to describe the measured concentrations and Zn release appeared to be better controlled by zincite (ZnO), as also indicated by other researchers (van der Bruggen et al., 1998). As previously observed for Ca, for the carbonated ash Zn leaching appeared to be adequately described by Ca-zincate at high pH levels.

Even in the case of Cu, the release from the carbonated ash was appreciably reduced in a wide pH range (pH = 5.5-13.5), since the measured concentrations differed approximately by one order of magnitude at each pH value. Cu leaching from the untreated ash was controlled by $Cu(OH)_2$ at pH values from 8 to 12 units, while at higher pHs tenorite (CuO) appeared to match the experimental data more closely. Atacamite ($Cu(OH)_3Cl$) was also identified as a possible solubility-controlling mineral in the two pH ranges 6-8 and 10.5-12; the formation of Cl-containing minerals in APC residues is judged to be highly probable, given the high chloride concentrations in the material due to the acid gas neutralization treatment applied.

Comparison of the experimental leaching curves of Cd for the untreated and carbonated APC residues confirmed the reduction in Cd mobility from the ash as a result of carbonation, even though for this metal the observed immobilization effect could not be univocally stated outside the pH range of carbonate stability (pH = 4-6).

The leaching curves for the **oxyanion-forming species** showed quite a different behaviour as compared to those of the amphoteric elements. The leaching of oxyanionic species is generally recognized to be indirectly affected by carbonation due to the influence of the process on the solubility of ettringite. It has been documented that the precipitation of Ca in the form of carbonate minerals leads to the dissolution of other Ca-containing phases including ettringite (Meima and Comans, 1997; Bodénan et al., 2000; Sabbas et al., 2003; Polettini and Pomi, 2004); since this phase is known to act as a host mineral for a number of oxyanions which can substitute for sulphate and therefore be immobilized in its mineral structure (see Cornelis et al., 2006 and 2008 and references therein), the dissolution of ettringite may be responsible of an increased oxyanion release. However, in this study no evidence of any significant presence of ettringite in the fresh ash was gained from the experimental campaign (see results of modelling of Ca leaching discussed above), likely due to the low total Al/Ca molar ratio. As a consequence, any changes in oxyanion leaching observed after the carbonation treatment are to be related to a different effect than that caused by ettringite dissolution.

The **release of Cr** was found to vary considerably as a consequence of carbonation at intermediate pH levels (4-10 units), while no significant changes were observed outside this range. Specifically, two opposite trends could be identified: a decrease in leaching at pH 4-6 (as also noted by Astrup et al., 2006a) and an increase of roughly one order of magnitude at pH 8-10. No Ca-, Fe- or Pb-containing minerals, including $CaCrO_4$, Cr-ettringite, Cr-monosulphate, Cr-jarosite or crocoite ($PbCrO_4$), were found to control Cr leaching.

Sb leaching showed a slight reduction for carbonated samples at pH 8-11; but at higher pH values, while Sb concentrations dropped in the eluates of untreated samples from ~1 mg/l to < 0.1 μg/l, carbonated samples showed quite stable values in the range 0.1-1 mg/l. No solubility-controlling phases were detected for Sb by geochemical modelling; in particular, leachates of both untreated and carbonated ash were found to be strongly undersaturated in Ca antimonate ($Ca(Sb(OH)_6)_2$), which has been proposed for leaching control of Sb from carbonated MSWI in the neutral and acidic pH values (Cornelis et al., 2008). However, it should be noted that the stability constant for Ca antimonate used in this study ($\log K_{sp} = -12.55$, see Table 3.1) was determined at neutral pH, while the precipitation of this phase at high pHs is still under investigation (Cornelis et al., 2008).

The solubility curves of **As** showed solution concentrations of ~1-2 mg/l for very low pH values to ~0.05-4 μg/l in the alkaline region. Apart from a decrease by roughly one order of magnitude in the pH range 7-10, As leaching from the carbonated ash occurred almost at the same level of the untreated residue. For the untreated material geochemical modelling indicated possible solubility control by variously hydrated Ca arsenate forms ($Ca_3(AsO_4)_2 \cdot 3.66H_2O$, $Ca_3(AsO_4)_2 \cdot 4H_2O$, $Ca_3(AsO_4)_2 \cdot 4.25H_2O$) at pH values in the range 10-12.5; for the carbonated ash it was not possible to infer about solubility control by one of such phases due to the limited number of experimental points in this pH range.

3.1.4 Conclusions

The APC residues examined in this study showed a particularly high reactivity towards CO_2 due to the large content of calcium hydroxides of the ash. Under the most favourable reaction conditions (L/S of 0.2 l/kg or temperature of 50 °C), high CO_2 uptake capacities of over 250 g/kg of residue were achieved in less than 1 h using 100% CO_2 at 1 bar, with a maximum calcium conversion yield of about 70%. Under the experimental conditions applied in this work however, capture of CO_2 from stack gases appeared to be necessary in order to enhance carbonation kinetics, unlike experiments performed on the same ash applying the gas-solid route.

Waste incinerator APC residues could hence provide effective CO_2 storage, although due to the meagre amount of APC ash generated in waste incineration plants compared to CO_2 emissions (i.e. ~50 g ash/kg waste compared to 1320 g CO_2/kg waste) accelerated carbonation of only APC ash would be able to sequester around 1% of the total CO_2 emissions of the incineration plant.

Regarding the effects of accelerated carbonation on the environmental properties of the ash, the leaching behaviour of carbonated APC residues was investigated by means of the compliance EN 12457-2 extraction procedure and the ANC/BNC leaching test. The release of the critical species: Pb, Zn, Cu, Cr, Sb and soluble salts (chloride and sulphate) at the natural pH of the material appeared to be variously affected by carbonation, with a strong immobilization effect for Pb above all, as well as Cu, Zn, an only slight influence on major elements, Cr, Cl^- and SO_4^{2-} release, and finally a mobilization effect for Sb. Since the mobility of soluble salts was not significantly affected by carbonation, these compounds thus remained the critical compounds for the disposal of this type of incineration residues.

The analysis of the leaching behaviour of major elements and trace contaminants as a function of pH coupled with chemical speciation modelling indicated a change in the solubility-controlling minerals from the untreated to the carbonated ash. For the latter, metal release was found to be clearly controlled by a number of carbonate minerals, indicating the potential of the carbonation process to convert the initial metal-containing minerals into the generally less soluble carbonate forms, with positive implications on the environmental behaviour of the ash.

3. 2 Accelerated carbonation of RDF incineration bottom ash

This section investigates the effects of accelerated carbonation on the characteristics of bottom ash (BA) from Refuse Derived Fuel (RDF) incineration, in terms of CO_2 uptake, mineralogy and heavy metal leaching of different particle size fractions of the residues.

Due to the variable and heterogeneous composition of BA, which depends on the composition of the feed waste as well as the combustion technologies applied in the incineration plant, an important part of the study consisted in the physical, chemical and mineralogical characterization of the selected fresh BA aimed at identifying the potential Ca-reacting phases with CO_2 and the leaching behaviour of the slag. As reported in Section 1.4.1, BA composition and leaching behaviour were found to depend greatly also on the particle size of the slag, hence the freshly-sampled BA was divided by sieving into 5 particle size classes which were separately analyzed and subjected to carbonation tests. Accelerated carbonation batch experiments were then carried out with 100% CO_2 gas flows on humidified BA to assess the CO_2 uptake of each fraction and the influence of some of the main operating parameters (temperature, CO_2 pressure, L/S ratio and original particle size of the slag) on reaction kinetics.

The material showed a significant Ca content that ranged from 26 to 35% weight of the samples, increasing in the smaller size fractions of the BA. Also the mineralogy of the slag changed significantly with particle size, the finer fractions exhibiting significant contents of Ca-hydroxide phases such as portlandite and hydrocalumite, but also calcite, whereas the coarser classes were characterized by noticeably higher amounts of Ca-(Al)-silicate phases, such as gehlenite in particular, but also dicalcium silicate and anorthite.

The operating pressure was found to be the most relevant parameter affecting the carbonation yield. Temperature showed to exert a significant effect on the CO_2 uptake particularly for the coarse fractions, owing to its effect in enhancing the dissolution of Ca-silicate phases. CO_2 uptakes ranging from ~40 g CO_2/kg residues for the coarse fractions to ~140 g CO_2/kg residues for the finest one were achieved.

Carbonation showed to affect the mineralogical characteristics of the BA analyzed in this study, with a noteworthy increase of calcite in all samples and a decrease of the reacting phases (portlandite and hydrocalumite in particular, but also dicalcium silicate) proportionally to the degree of carbonation attained for each particle size fraction.

The leaching behaviour of both main elements and trace metals was analyzed by performing leaching compliance tests and pH-dependence tests. The untreated material was found to release significant amounts of Pb (above the limits prescribed for hazardous waste landfilling), Cu and Zn (above the acceptance criteria of unhazardous landfills). Both accelerated carbonation and long term (over 1 year) natural weathering were found to significantly decrease Pb, Cu and Zn leaching (by over 3 orders of magnitude for Pb and by 1-2 orders of magnitude for Cu and Zn); an evident enhancing effect and a slight increase were instead observed for Cr and Mo, respectively. Accelerated carbonation appeared to generally cause a higher pH reduction compared to natural weathering, although the effects on heavy metal leaching were quite similar, the main differences being a stronger decrease in Pb leaching and an evident effect on Mg mobilization of accelerated carbonation as opposed to natural weathering. To investigate the leaching controlling mechanisms for both fresh and carbonated material, pH-dependence tests were conducted on the fine fraction (class D) and on a mixture of the coarser ones (classes A, B and C). The ANC curves for both types of carbonated BA showed a buffering plateau at pH values between 6 and 7 which was associated to calcite formation, the one for class D being roughly double that of the mixture. The pH dependent leaching curves for most compounds showed not to vary considerably between fresh and carbonated samples, indicating that the changes in the leaching behaviour at the natural pH of the BA upon carbonation were mainly related to the decrease in the pH of the ash caused by carbonation to the values corresponding to the minimum solubility of amphoteric metals such as: Pb, Zn and Cu and the release of others as: Mg and Cr.

3.2.1 Introduction

[5]With the final objective of optimizing municipal solid waste management, thermal treatment of the combustible fraction of the waste coupled with energy recovery may be considered as one of the best strategies to reduce the waste volume and to exploit part of its energy content (Vehlow et al., 2007). To increase the environmental soundness of this process, the identification of suitable measures to mitigate the potential environmental impacts of thermal waste treatment have become one of the crucial aspects of this technology. Thus, appropriate approaches for gaseous emissions control and solid residues management have been extensively studied in the last decades (see e.g. IAWG, 1997;

[5]Most of this section was published as Baciocchi et al., 2008.

Sabbas et al., 2003; Vehlow et al., 2007). As described in Section 1.4.1, among the solid residues generated by waste combustion, BA accounts for ~20-30% in mass of the original waste. Promoting its use in civil engineering applications and improving its technical properties prior to final disposal are recognized as two complementary approaches to reduce the amount of landfilled waste, at the same time simplifying the management and emission control operations in sanitary landfills (Sabbas et al., 2003).

Due its origin, bottom ash is mainly characterized by an amorphous mineralogical structure, with reactive phases including (hydr)oxides, aluminosilicates and amorphous silica. Such minerals are metastable under atmospheric conditions, so that weathering of BA is commonly observed with time, leading to changes in the chemical and physical properties, as well as the leaching behaviour of the material, as previously described in Section 1.4.1. Carbonation is one of the BA weathering reactions that occur over long-term scenarios, and results in a decreased BA reactivity due to $Ca(OH)_2$ depletion (Piantone et al., 2004). Accelerated carbonation was shown to cause the transformation of Si-, Al- and Ca-containing minerals in fresh BA, including ettringite, anhydrite and corundum, with formation of new phases including calcite, gypsum, quartz and gehlenite (Meima et al., 2004; Fernándes Bertos et al., 2004b; Polettini and Pomi, 2004). As described in detail in Section 1.4.1, modifications in BA leaching are expected to occur as well. The reactivity of the ash depends chiefly on its composition and content of calcium hydroxide species, which, along with heavy metal leaching, have been shown to vary significantly with particle size (Chimenos et al., 1999; 2003; Izquierdo et al., 2002). Hence, in this study accelerated carbonation tests were performed on different size fractions of BA in order to assess the capability of this treatment technique of increasing the chemical stability of the ash and also to evaluate the maximum CO_2 uptakes achievable for each size fraction at mild operating conditions.

3.2.2 Materials and methods

The BA used in the present study was sampled from a grate-type RDF incinerator located in central Italy, characterized by a nominal size of 220,000 t/y and a BA production of approximately 24,000 t/y.

The sampled material was homogenized by quartering and screened to remove the 5 cm oversize fraction, which accounted for 6% by weight of the raw sample. After

homogenization and drying at 60 °C, BA was sieved to produce the following size fractions: > 12 mm; 12-5.6 mm (class A); 5.6-2 mm (class B); 2-0.425 mm (class C); 0.425-0.150 mm (class D); and < 0.150 mm (class E), which was mainly made up of grate siftings). The 12 mm oversize fraction was primarily composed of ceramic, glass and metal scraps fragments, therefore it was judged unsuitable for carbonation and discarded. Classes A, B and C were then milled to < 425 μm, so that the differences in reactivity between classes could be related solely to the chemical composition of each fraction and not to the specific surface.

Each fraction was thoroughly characterized in terms of elemental composition, anion content, mineralogy and leaching behaviour. The mineralogy of the material was determined by X-ray diffraction (XRD) and micro Raman spectroscopy analyses. The elemental composition of the untreated BA was determined by atomic absorption spectrometry (AAS) after lithium tetraborate digestion at 1050 °C. Chloride and acid-soluble sulphates were measured using the Italian standard test procedure UNI 8520, which involves dissolution with hot deionised water and titration with $AgNO_3$ for chloride analysis, whereas dissolution with 3% HCl followed by spectrophotometric analysis for sulphates. The carbonate content of untreated and carbonated BA was measured with a Dietrich-Frühling calcimeter. The loss on ignition (LOI) and water content of the BA were determined according to the ASTM C25 and ASTM D2216 procedures.

The leaching behaviour was investigated, prior and after carbonation, using the EN 12457-2 batch compliance test and the CEN/TS 14429 pH-dependence leaching test for evaluation of the acid neutralization capacity (ANC). Leaching compliance tests were also carried out as a comparison on the same particle size fractions of BA after a 1 year period of natural weathering in the laboratory under controlled conditions.

Batch accelerated carbonation tests were performed in a pressurized stainless steel reactor equipped with a 150 ml internal Teflon jacket, under wet conditions with a 100% CO_2 flow. Initial wet carbonation tests were carried out on class D to evaluate the influence of the operating parameters on CO_2 uptake and identify the optimal conditions to be adopted for the other classes. The ranges of variation for the operating parameters were: liquid-to-solid (L/S) ratio = 0-0.6 l/kg, temperature = 30-50 °C, pressure = 1-10 bar.

Carbonation kinetics was studied by carrying out carbonation tests under the same operating conditions for different durations, from 0.5 up to 48 h. For the purpose of

comparison, a mixture of the coarse classes A, B and C was also subjected to carbonation tests. In this case, a process temperature of 50 °C was adopted. After carbonation, the samples were oven dried at 60°C and sample weight gain, which provides a first qualitative indication of carbonate formation, was recorded. Subsequently, the mineralogy and leaching behaviour of the treated samples was investigated with the same procedure used for the fresh material.

3.2.3 Results and discussion

BA characterization

The particle size distribution of the BA was as follows: class A = 27.6% wt., class B = 34.6% wt., class C = 27.0% wt., class D = 4.9% wt. and class E = 0.9% wt. The 12 mm oversize fraction was ~4.7% wt. of the original BA and, for the reasons explained above, was discarded from the subsequent analyses. Overall, the coarse fractions (A, B and C) accounted for about 89% wt., and the fine fractions (D and E) ~ 6% wt. of the mass original BA sample.

The LOI values of classes A, B and C (2-5% wt.) were different from those measured for classes D and E (> 10% wt.). While the LOI values determined for the first three classes were in good agreement with the results from other studies (e.g.: Izquierdo et al., 2004; Giampaolo et al., 2002), the relatively high values measured for the fine fractions could be interpreted considering their higher amount of chemically bound water in hydroxide species, organic matter, SO_2 and volatile compounds, taking also into account the fact that most of this material does not undergo full combustion, passing through the grate mesh.

The elemental composition and anion content of the five size classes are reported in Table 3.5. The calcium content was equal to 262, 271 and 333 g/kg for classes A, B and C respectively, while the maximum concentration (352 g/kg) was measured for class E. The concentrations of Al, Na, K, Fe and Mn were shown to increase in the coarse fractions, while Mg appeared to be evenly distributed in all classes. Among the trace metals, Pb, Cr, and Sb were found to be enriched in classes D and E, As in classes A and B, while Cu, Zn, Ni and V appeared to be approximately evenly distributed among the different size fractions. Cl^- and SO_4^{2-} whose levels were in the ranges 0.36-1.14% and 0.93-2.59% wt., respectively, were more abundant in the fine fractions. A similar distribution was also found for calcite, whose presence in all fractions of BA was significantly higher than that

reported in previous studies and may have been due to the type of feed waste (RDF is made up by a significant fraction of paper, which contains Ca-based compounds).

The results of the EN 12457-2 compliance test indicated that all size fractions were alkaline in nature, with a pH between 11.8 for class A and 12.75 for class E, as shown in table 3.6. For all fractions Pb was highly mobile, with leachate concentrations above the limit for hazardous waste landfills (except for class A). The release of Pb, Zn and Cu, although higher than that prescribed for inert waste landfills, was less critical for all the investigated size fractions.

Table 3.5 Elemental composition (mg/kg dry wt.) and anion content (% dry wt.) of the different particle size fractions of BA.

Element	Class A 12-5.6 mm	Class B 5.6-2 mm	Class C 2-0.425 mm	Class D 0.425-0.150 mm	Class E < 0.150 mm
Al	66070	61680	64670	55490	37010
As	50.83	49.28	4.48	2.53	2.90
Ca	262000	270670	333330	32013	352000
Cd	12.13	40.20	7.13	9.40	21.07
Cr	426.67	565.33	530.67	624.00	738.67
Cu	6220	6090	6130	6200	4510
Fe	30773	32560	31520	22670	15520
K	5487	5160	5427	4487	3447
Mg	20493	25787	20160	20480	19840
Mn	2440.0	429.33	481.33	430.67	500.00
Mo	10.91	12.37	14.39	14.00	33.76
Na	27733	25867	21933	12000	8333
Ni	116.00	162.67	182.67	174.67	128.00
Pb	1328.0	1712.0	2313.3	3566.7	3206.7
Sb	65.92	60.59	69.92	125.28	159.31
V	25.83	26.05	20.35	21.00	20.95
Zn	2234.7	3505.3	3492.0	4032.0	3622.7
Anion					
Cl^-	0.36	0.49	0.65	0.75	1.14
SO_4^{2-}	1.12	1.01	0.93	1.51	2.59
CO_3^{-2}	6.7	8.3	10.2	9.5	19.3

Also the mineralogy between coarse and fine fractions differed considerably, as indicated by both XRD and micro Raman spectroscopy results. The former (Figure 3.8) confirmed the findings of other literature studies (Chimenos et al.,1999; Eusden et al., 1999; Freyssinet et al., 2002; Piantone et al., 2004), showing a prevalence of silicatic phases in the coarser fractions, as opposed to a higher content of hydroxide phases in the finer classes. In particular, gehlenite ($Ca_2Al_2SiO_7$), a mineral of the melilite group, exhibited the most intense diffraction peak for classes A, B and C. Conversely, hydrocalumite ($Ca_2Al(OH)_6[Cl_{1-x}O_x]\cdot 3H_2O$), $Ca(OH)_2$ and calcite ($CaCO_3$), which typically form as a

result of hydration and carbonation reactions during quenching and storage, were enriched in the finest fractions. Other important phases detected by XRD analysis included forsterite (Mg_2SiO_4), dicalcium silicate (Ca_2SiO_4) and hematite (Fe_2O_3) and were more abundant in the coarse fractions. Ettringite was not detected in none of the particle size fractions, probably owing to the lower content of SO_4^{2-} phases in the analyzed slag as compared to other types of BA; furthermore it has also been shown that in the presence of high Ca contents, hydrocalumite formation instead of ettringite is favoured (Zhang, 2000).

Raman spectroscopy (Figure 3.9) confirmed the results of elemental and XRD analyses, revealing the presence of Si and Al minerals including alumina (Al_2O_3, with a double peak at ~1410 and 1380 cm^{-1}, calcite (peaks at ~155, 280, 710 and 1090 cm^{-1}) and amorphous carbon (peak at ~1500 cm^{-1}; Figure 3.9a), amorphous silica (broad band at ~540 cm^{-1}; Figure 3.9a, inset 1) and olivine ($(Mg,Fe)_2SiO_4$, broad band at ~860 cm^{-1}; Figure 3.9a, inset 2) in the coarse fractions. For classes D and E, Raman spectroscopy indicated the presence of calcite (peaks at ~155, 280 and 710 cm^{-1}, Figure 3.9b, inset 1), gehlenite (peaks at ~620, 655 and 690 cm^{-1}, Figure 3.9b, inset 2), olivine (Figure 3.9b, inset 3), amorphous carbon and alumina.

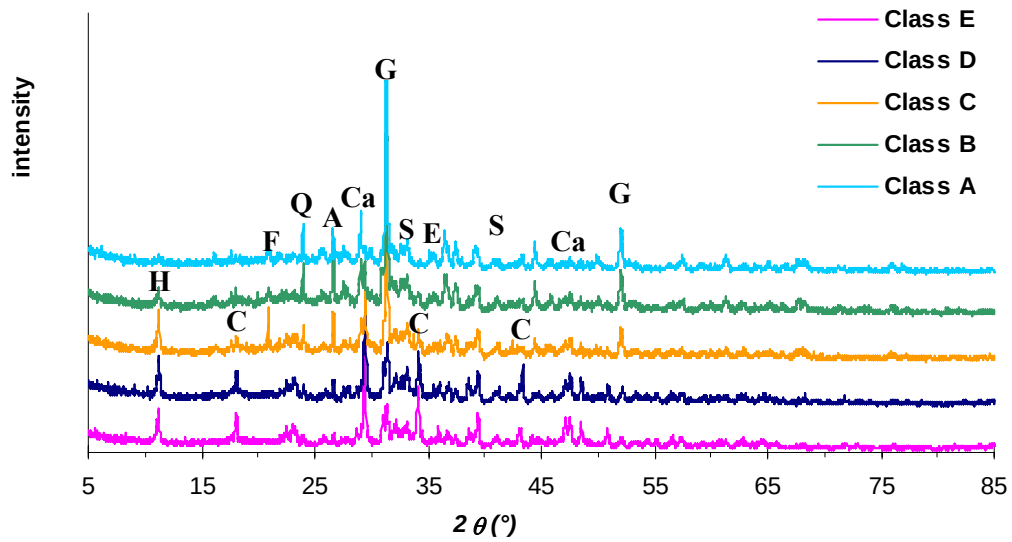

Figure 3.8 XRD pattern for untreated BA (A: anorthite; C: calcium hydroxide; Ca: calcite; E: hematite; F: forsterite; G: gehlenite; H: hydrocalumite; S: dicalcium silicate; Q: quartz).

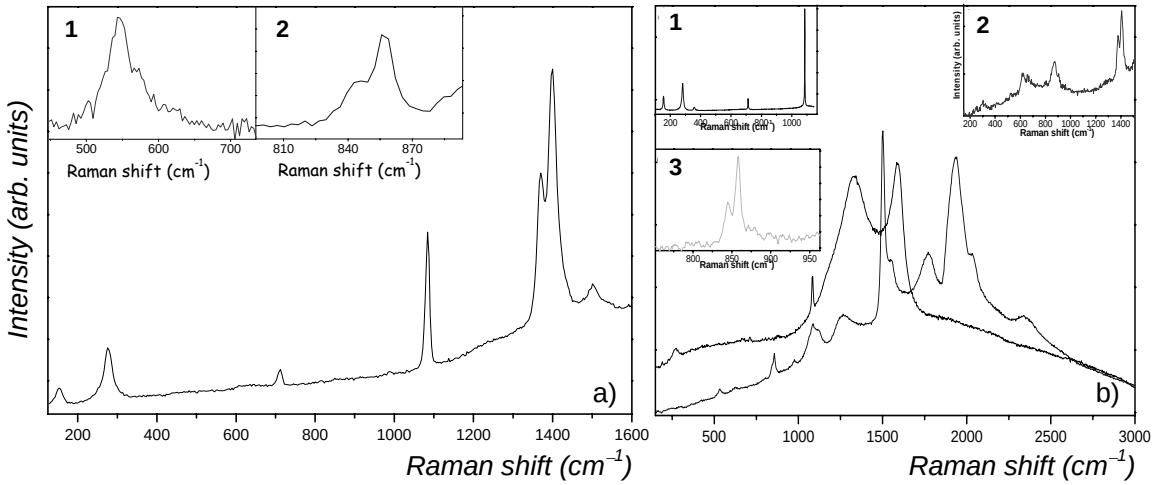

Figure 3.9 Examples of Raman spectra for (a) untreated class B and (b) untreated class D.

Evidences of carbonation

Mineralogical transformations induced by carbonation reactions were evidenced by XRD analysis (see Figure 3.10 comparing the differences in mineralogy between fresh and carbonated class D BA). The diffraction patterns showed the disappearance of peaks associated to such minerals as hydrocalumite and $Ca(OH)_2$, accompanied by the increase in the peak intensity for calcite and partly also for hematite. The increase in the amount of calcite in carbonated samples was also clearly assessed through Raman spectroscopy, as discussed in the next paragraph. Dicalcium silicate also showed to decrease upon carbonation in all particle size fractions, as opposed to Ca-Si-Al phases such as gehlenite and anorthite which appeared not to be affected by the CO_2 treatment. Quartz formation, which occurred for all the investigated BA fractions, was more evident for the coarse fractions. It may be argued that quartz formation was caused by re-precipitation of silica released upon calcium silicate dissolution occurring during carbonation (Meima et al., 2004). Forsterite (or olivine, as detected from the Raman measurements) did not appear to be significantly affected by the treatment with CO_2 and Mg-containing carbonate phases were not detected neither by Raman nor by XRD analysis, in agreement with prior studies on BA carbonation (e.g.: Fernándes Bertos et al., 2004b).

Figure 3.11 reports the acid titration curves obtained from the ANC test for classes D and A+B+C, which were chosen as being representative of the behaviour of fine and coarse bottom ash fractions, respectively. A significant change in acid neutralization capacity was observed as a result of carbonation, with the appearance of a plateau in the titration curve

at a pH in the range 6-7 units, which was related to the presence of carbonate species. The extent of the plateau was larger (almost double) for class D carbonated samples, confirming the results of the calcimetry analysis.

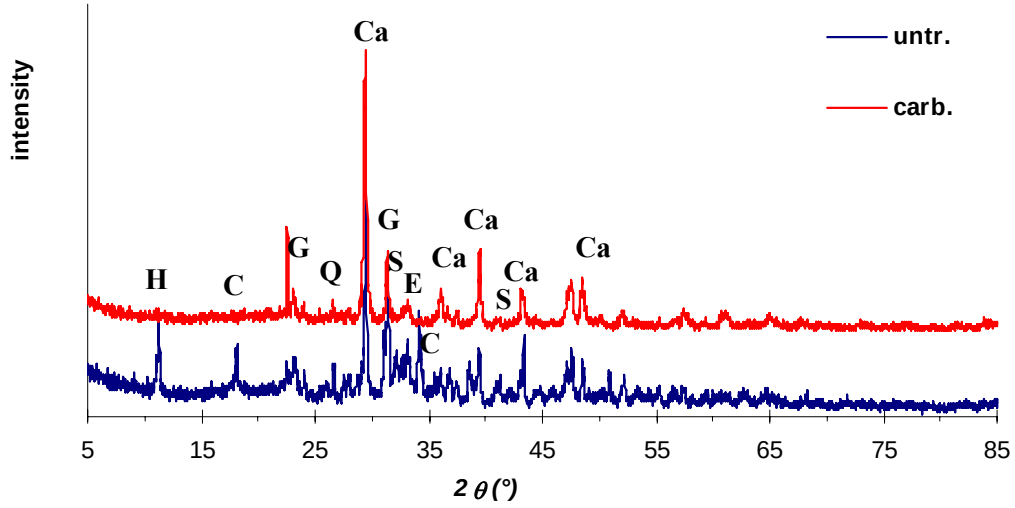

Figure 3.10 XRD pattern for untreated and carbonated (at 30°C, 10 bar with a L/S of 0.3 l/kg for 24 hours) class D BA (A: anorthite; C: calcium hydroxide; Ca: calcite; E: hematite; F: forsterite; G: gehlenite; H: hydrocalumite; S: dicalcium silicate; Q: quartz).

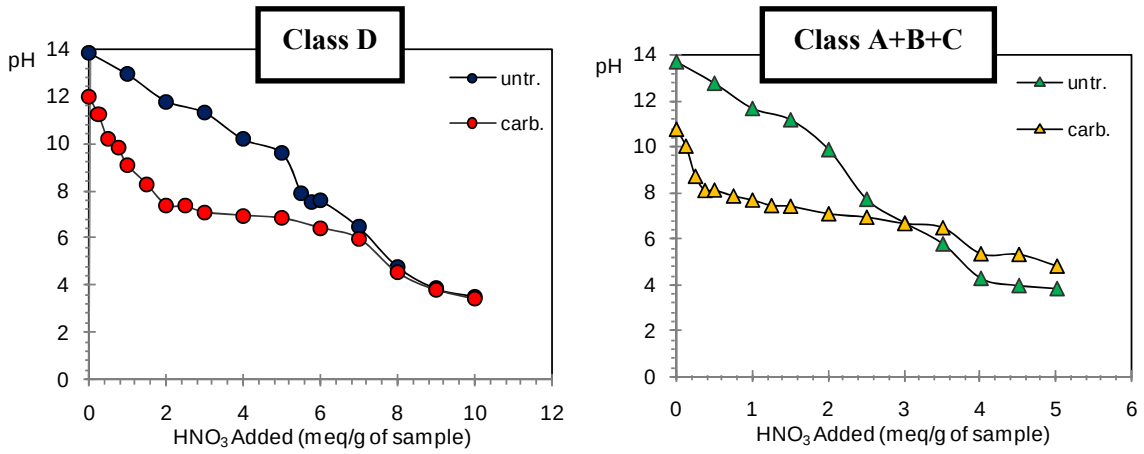

Figure 3.11 ANC curves for untreated and carbonated samples (classes D and A+B+C). (Carbonation of D samples was performed at 30°C, 10 bar with L/S = 0.3 l/kg for 2 hours; carbonation of A+B+C samples was performed at 50°C, 10 bar with L/S = 0.3 l/kg for 2 hours).

CO_2 uptake and carbonation kinetics

The influence of the operating conditions on the CO_2 uptake, calculated applying Equation 3.2, of class D samples is shown in Figure 3.12. This particle size fraction was chosen due to its considerable content in Ca-reactive phases, detected by XRD analysis (see Figure 3.8) and also its higher significance in weight % of the bulk BA compared to class E.

Carbonation kinetics was slower if compared to other types of incinerator residues, such as air pollution control ash, under similar operating conditions (see the results reported in the previous section), due to its appreciably lower content of reactive Ca species; however CO_2 uptake reached a plateau within 8 h for all the tested pressures, with a maximum CO_2 uptake of almost 100 g/kg residue for pressures of 3 or 10 bar (Figure 3.12 a). The results of micro Raman analysis on class D BA samples carbonated for different times are shown in Figure 3.12b, in which the main peak for calcite (280 cm^{-1}) measured for experiments carried out at 0.5, 4 and 24 hours is compared; the ratio between the areas of these three peeks, fitted with Lorentzian functions, showed to be in good agreement with the results of calcimetry tests.

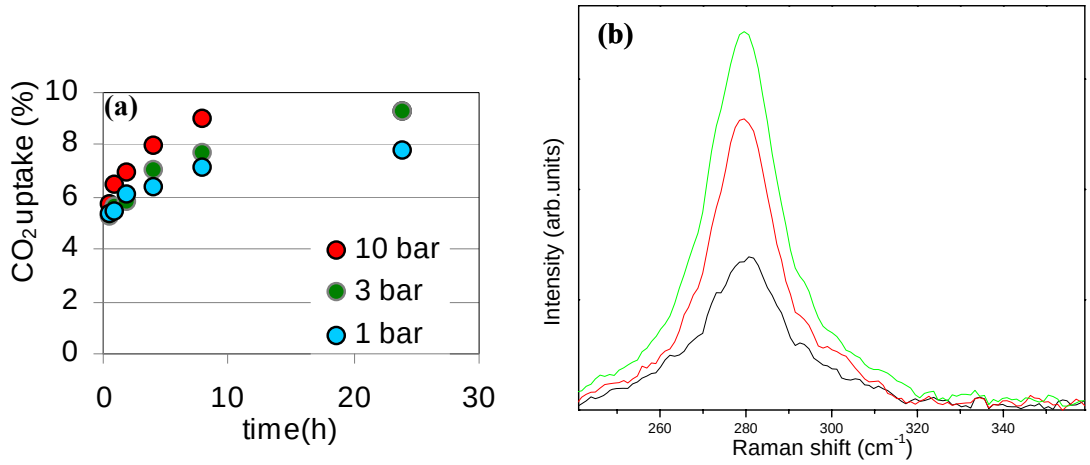

Figure 3.12 CO_2 uptake kinetics for class D BA, carbonated at 30 °C with a L/S = 0.3 l/kg (a) as a function of pressure, (b) results of Raman analyses, comparison of the main calcite peek for samples carbonated at 10 bar for 0.5 (black line), 4 (red line) and 24 (green line) h.

Regarding the influence of operating conditions on process kinetics, CO_2 pressure was found to play the most significant role, with the highest pressure yielding the best CO_2 uptake results. At P = 10 bar, T = 30 °C and reaction time = 2 h, an optimal L/S ratio of 0.3 l/kg was observed (Figure 3.13a), confirming that a certain amount of water promotes

carbonation as it enhances hydration and solvation of CO_2 and Ca^{2+} ions in the liquid phase, while water contents above the optimum may hinder CO_2 diffusion into the liquid film (Fernández-Bertos et al., 2004b). An increase in treatment temperature appeared to slightly affect carbonation at 50 °C only, likely due to a more pronounced effect on silicate dissolution, while no appreciable difference was detected between 30 and 40 °C (Figure 3.13b).

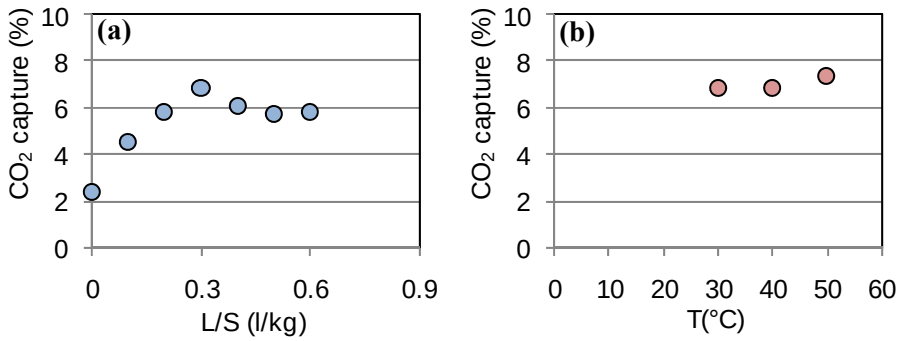

Figure 3.13 CO_2 uptake after 2 hours carbonation of class D BA (a) effect of the L/S (at 30 °C and 10 bar); (b) effect of temperature (at 10 bar with a L/S = 0.3 l/kg).

On the basis of the findings indicated above, the experimental campaign was continued for the other BA fractions using the following operating conditions: P = 10 bar, T = 30 °C and L/S = 0.3 l/kg. It was found (Figure 3.14a) that the extent of CO_2 uptake varied largely depending on the individual BA size fraction investigated: the coarse fractions behaved very similarly to each other and displayed the lowest CO_2 uptake potential (42, 41 and 40 g/kg residue after 8 h for classes A, B and C, respectively), while the fine fractions showed higher carbonation yields (90 and 140 g CO_2/kg residue after 8 h for classes D and E, respectively).

However, it should be considered that the coarse fractions are by far quantitatively more abundant in BA and may thus give a larger contribution to CO_2 sequestration when this is evaluated in absolute terms. For this reason, additional carbonation runs were performed on a mixture of classes A, B and C in the same proportions as in the original BA sample, increasing the operating temperature to 50 °C with the purpose of enhancing the dissolution of silicate minerals. As shown in Figure 3.14b, the CO_2 uptake after 4 h was increased to ~5%, suggesting the possibility for further improvement of the carbon sequestration potential of BA if more severe operating conditions were adopted.

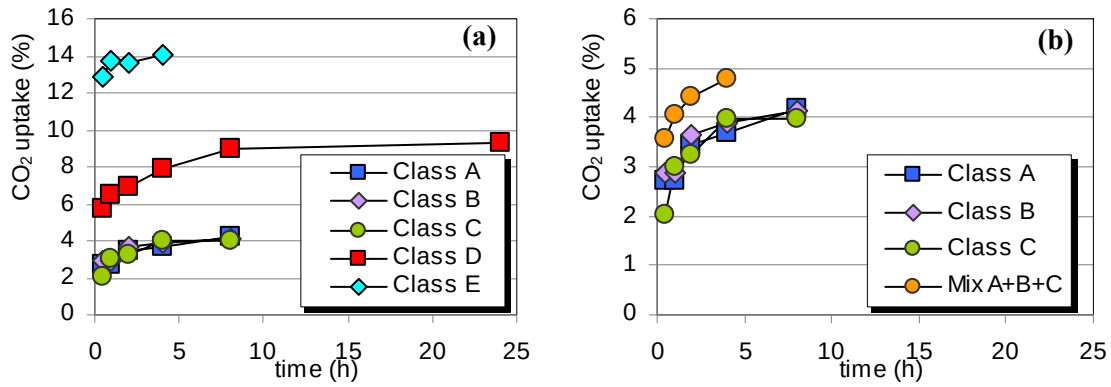

Figure 3.14 CO_2 uptake kinetics (at 30 °C and 10 bar with a L/S = 0.3 l/kg) (a) for the different particle size classes; (b) for class A+B+C at 50 °C compared to the individual classes A, B and C at 30 °C.

These results are in quite good agreement with the results of prior investigations on BA carbonation reported in the literature (see Section 1.4.1). In particular, the optimal L/S ratios were very similar to those reported by Fernández-Bertos et al. (2004b) and by Rendek et al. (2006a), and pressure showed to exert a similar effect as that described by Rendek et al. (2006a). CO_2 uptakes were slightly higher than those up to now reported in the literature (30-65 g/kg residue), probably owing to the higher Ca content of the slag analyzed in this work (BA from RDF incineration) and the separate optimization of the carbonation treatment for the different size fractions of the BA.

However, the conversion yields, calculated with Equation 3.4 were quite lower than the value reported in the previous section for APC carbonation. Mg phases were not considered also in this case, even though the content of Mg in BA (2-2.5 % weight) is significant, owing to the fact that Mg-silicate phases did not show to be affected by the treatment with CO_2, nor Mg-carbonates were detected in the slag upon carbonation.

The following Ca to carbonate maximum conversion yields were estimated for the different particle size fractions analyzed in this study: ~16% for classes A and B, ~12% for class C, ~ 18% for the mixture of classes A, B and C (carbonated at 50 °C), ~31% for class D and ~47% for class E.

$$\eta\,[\%] = \frac{CO_{2uptake}[\%] \times 40/44}{Ca^{2+}[\%]\text{-}CaCO_{3(initial)}[\%] \times 40/100} \times 100 \qquad (3.4)$$

Leaching behaviour

As for the effects of accelerated carbonation on different particle size fractions of BA, the results of the EN 12457-2 compliance leaching test (see Table 3.6 and Figure 3.15) revealed a decrease in the natural pH for all the carbonated samples, along with a significant leaching reduction for most contaminants. In particular, Pb release was reduced by two to three orders of magnitude, with leachate concentrations for the carbonated materials below the limit for inert waste landfills. Cu and Zn showed a similar behaviour, while Cr was generally mobilized by carbonation, confirming the results of previous studies (Bone et al., 2003; Polettini et al., 2005; Van Gerven et al., 2005b) and indicating Cr as the most critical contaminant with regard to carbonation. A slight mobilization effect was also observed for Mo, another oxyanion forming element.

Comparing the results of the accelerated carbonation tests with the results of leaching tests conducted on the same material after a 1-year weathering period, (Figure 3.15) it may be observed that generally the accelerated treatment allowed to obtain lower pH values, in particular for class A. For the macro constituents of the slag, while for Ca and Fe leaching the two processes appeared to exert a very similar effect, Mg showed to be significantly mobilized (around 1 order of magnitude increase) only for the carbonated samples. This result may indicate hence that as a result of accelerated carbonation Mg may have partially reacted (although evidences were not detected by XRD or Raman analysis) forming more soluble phases than the original Mg-silicate mineral constituents of the fresh slag.

Table 3.6 Comparison of the EN 12457-2 leaching test results for untreated and carbonated BA (values in mg/l) (Carbonation of A, B, C, D and E samples was performed at 30°C, 10 bar with L/S = 0.3 l/kg for 2 hours; carbonation of A+B+C samples was performed at 50°C, 10 bar with L/S = 0.3 l/kg for 2 hours.)

	Class E		Class D		Class C		Class B		Class A		Mix A+B+C	
	untr.	carb.	untr.	carb.	untr.	carb.	untr.	carb.	untr.	carb.	untr.	carb.
pH	12.75	9.76	12.64	11.28	12.72	10.85	12.53	10.58	11.87	9.73	12.48	9.88
Cr	0.15	3.82	0.10	1.15	0.04	0.20	0.02	0.09	0.04	0.04	0.01	0.11
Cu	0.20	0.00	0.22	0.05	0.55	0.24	0.63	0.02	0.41	0.00	0.36	0.02
Mo	0.03	0.05	0.02	0.04	0.01	0.05	0.01	0.05	0.03	0.03	0.01	0.02
Pb	5.76	0.00	8.90	0.00	7.59	0.00	4.74	0.00	0.24	0.00	2.64	0.00
Zn	0.47	0.02	0.53	0.03	0.73	0.08	0.48	0.01	0.31	0.02	0.34	0.02
Ca	1085	460	995	278	945	272	710	144	725	144	740	152
Mg	0.08	12.90	0.07	0.51	0.31	0.86	0.17	4.92	0.07	21.20	0.88	54.60
Na	123	46	63.4	47	36.7	13.1	32.8	35.4	38.3	38	43	46
K	86.0	8.2	38.2	7.5	27.1	6.4	24.1	6.0	20.7	5.4	13.3	7.1
Al	<2.0	19.3	<2.0	60.4	<2.0	64.1	3.05	16.7	284	6.9	7.4	<2.0
Fe	0.07	0.03	0.06	0.11	0.05	0.11	0.07	0.05	0.94	0.06	0.04	0.07
Mn	<0.05	<0.05	<0.05	0.01	<0.05	0.02	<0.05	0.01	<0.05	0.06	0.04	0.03

For amphoteric elements, accelerated carbonation appeared to generally exert a stronger effect on reducing the release of these elements, in particular for Pb, from the eluates of most particle size fractions. Cr leaching was enhanced by carbonation only for the finest particle size fractions, while Mo release did not seem to be affected by the type of treatment, except for class D. It is important to note finally, that no significant variation between the $CaCO_3$ content of untreated and weathered slag was detected by calcimetry analysis, hence confirming that, as indicated also by previous studies, modifications of the leaching behaviour of BA do not depend directly on the amount of sequestered CO_2.

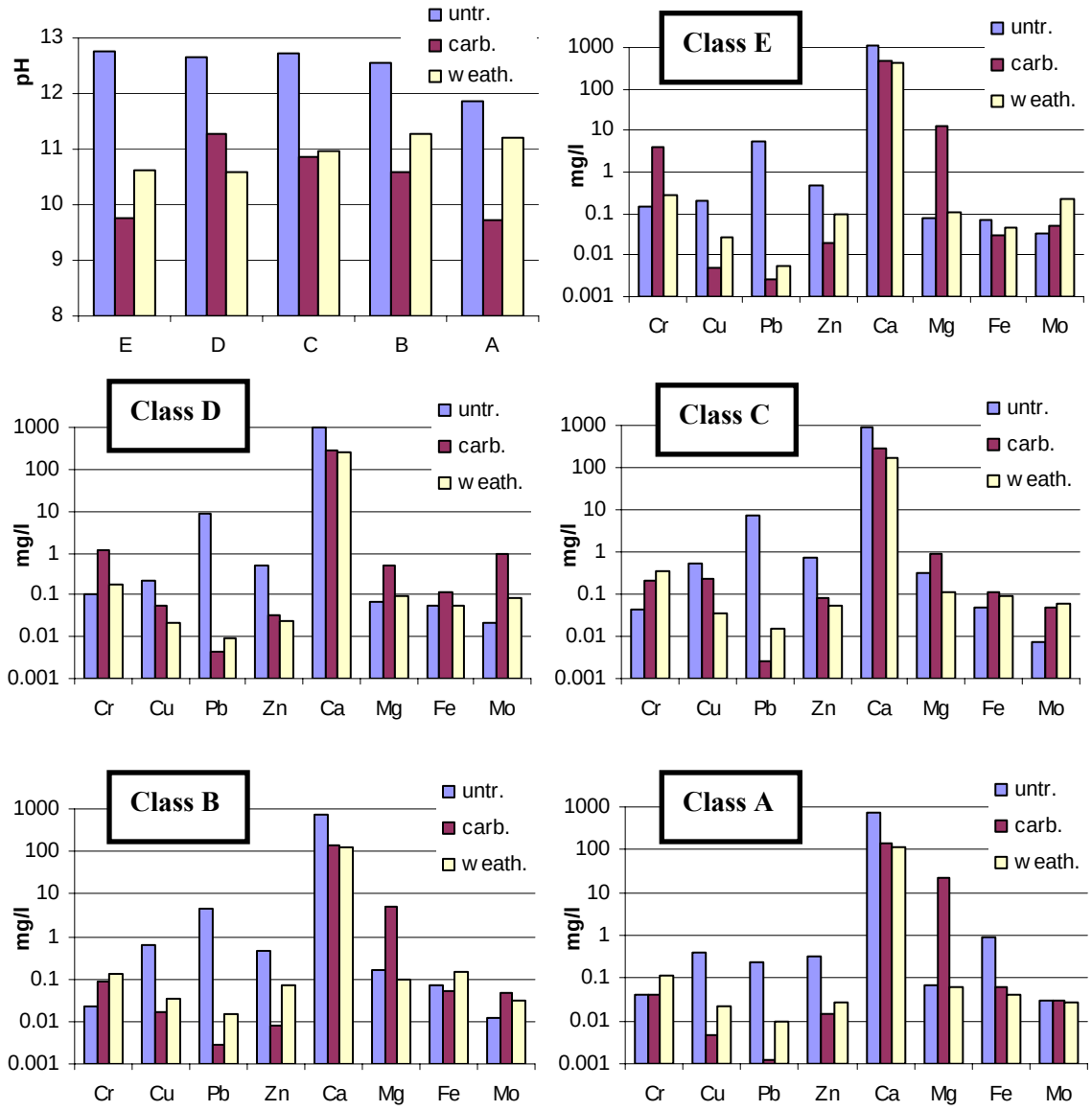

Figure 3.15 Comparison of the EN 12457-2 leaching test results for untreated, carbonated (as described in Figure 3.14) and naturally weathered BA.

The results of the pH-dependence tests carried out on both untreated and carbonated class D and A+B+C mixtures are reported as a function of pH in Figure 3.16.

As can be noted by comparing the results obtained separately on the two fractions of the slag, the leaching curves of the different elements were quite similar, except for Cr and Mo. Furthermore, the shapes of the leaching curves of most of the investigated elements were not appreciably modified by the carbonation process.

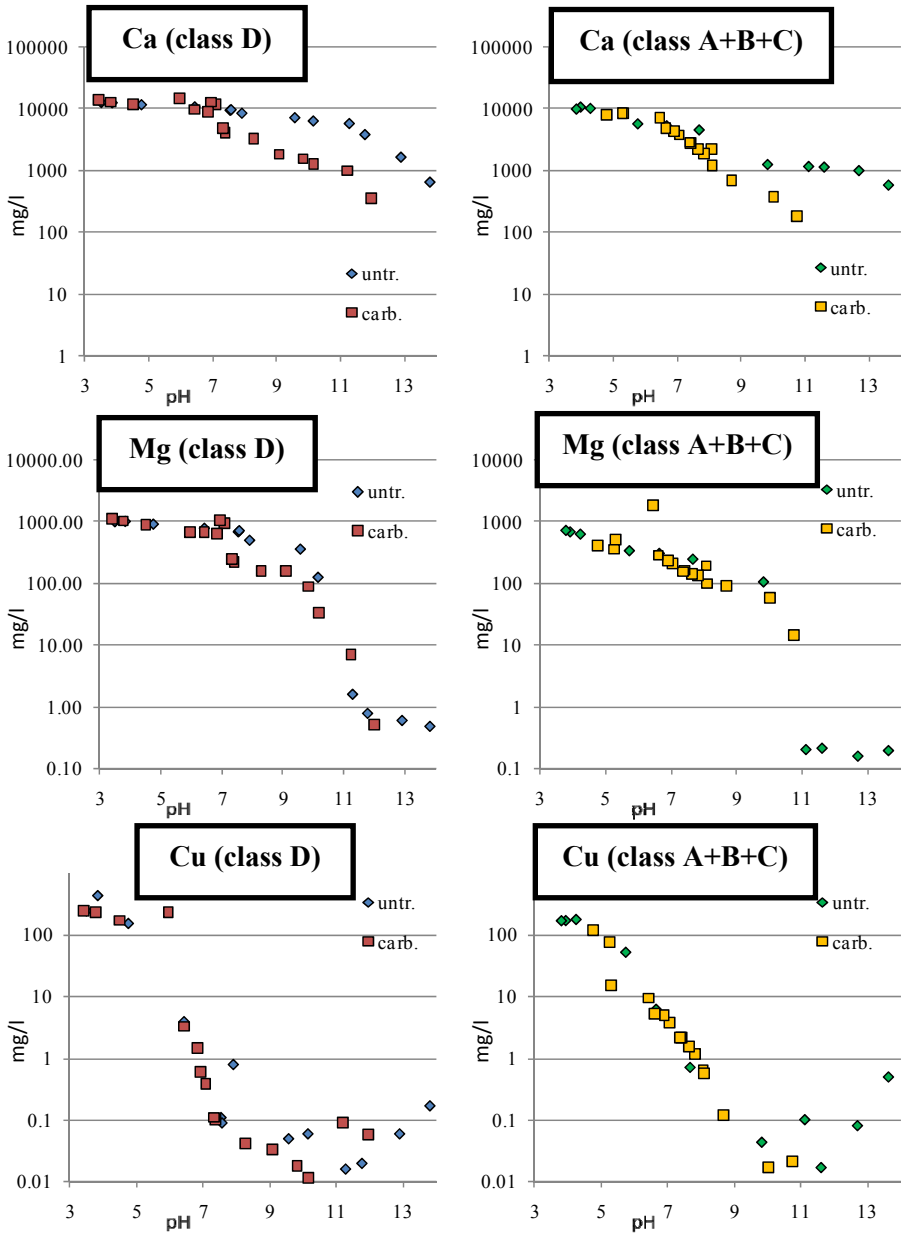

Figure 3.16 Leaching of main and trace elements from class D and A+B+C mixtures of untreated and carbonated (as described in Figure 3.14) BA.

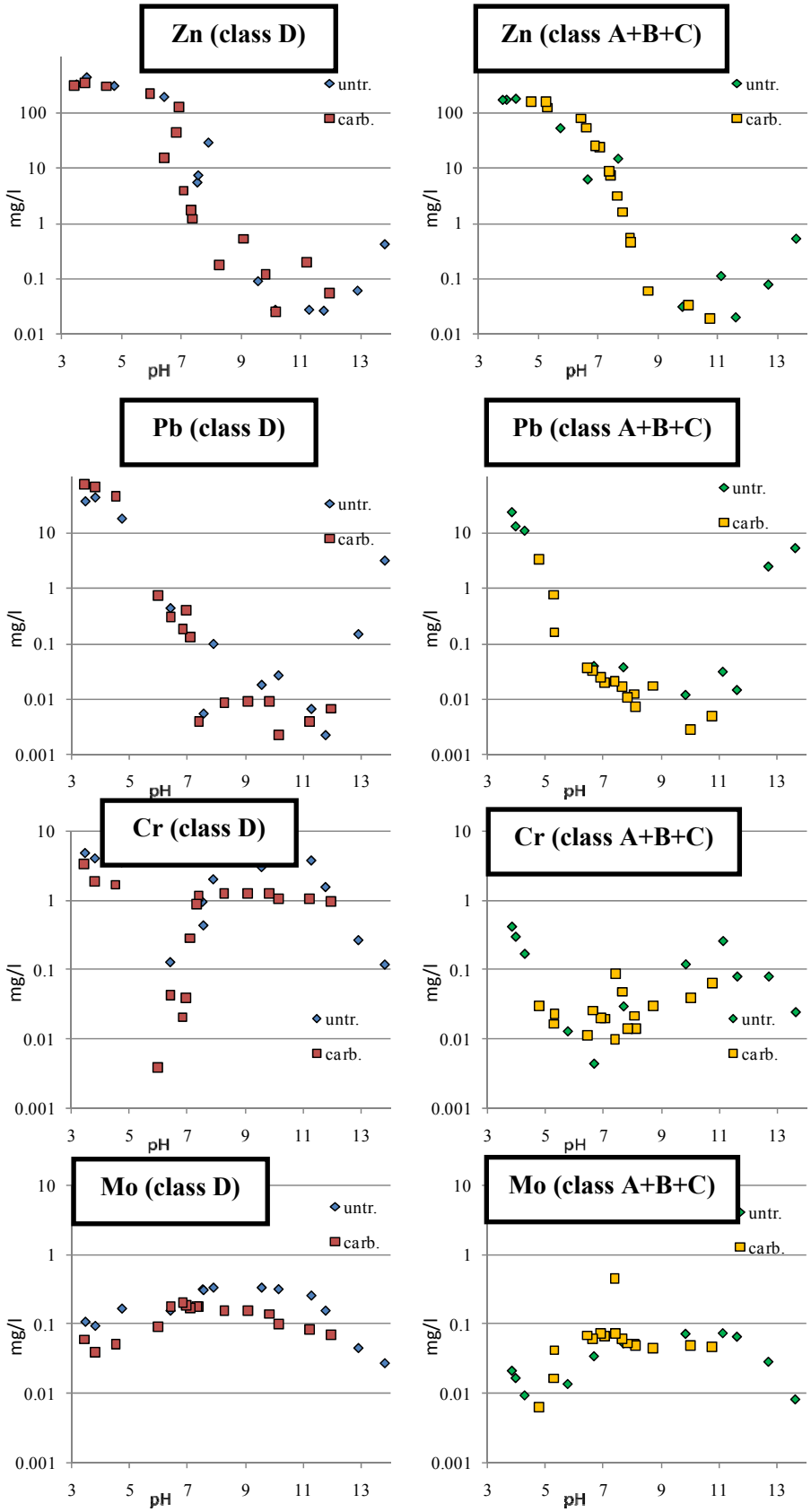

Figure 3.16 continued.

For Ca however, a reduction in mobility above pH 7 was observed for both D and A+B+C fractions, which, as showed in the previous section for APC residues carbonation, can be related to the formation of Ca carbonate phases which present a lower solubility than Ca-hydroxide or -silicate phases, as indicated also by previous studies on BA carbonation (e.g.: Zevenberger and Comans, 1994; Meima and Comans, 1997; Polettini and Pomi, 2004). It is also interesting to note that Ca leaching from fresh class A+B+C was quite lower (almost an order of magnitude) than class D, confirming the reduced content of Ca-hydroxide phases in the coarser fractions.

The similar trends of Cu, Zn and Pb leaching for both fresh and carbonated samples allowed to infer that the observed changes in the release of these metals as a result of carbonation, measured by the EN 12457-2 test, are to be ascribed to the reduction in the natural pH of the slag corresponding to the minimum solubility of these elements, similarly to the results reported by Arickx et al. (2006) for Cu. Analogously, also the increase in Mg leaching after carbonation measured by the EN 12457-2 test can be related to the variation in pH, however as described earlier, the differences found with natural weathering could indicate that carbonation exerted also an additional effect on Mg leaching.

In the case of Cr and Mo leaching, a significantly different behaviour between the two different fractions of BA was observed. Cr leaching from fraction D was about 1 order of magnitude higher than from fraction A+B+C in the whole pH interval, except for pH values between 5 and 7. For class D, Cr leaching from carbonated BA was lower than for fresh slag up to a pH value of 12; a reduction in pH-dependant leaching in the pH range 8-12 upon carbonation was also reported by Van Gerven et al. (2005b) and linked to the sorption of oxyanion forming species onto the surfaces of Al and Fe (hydr)oxides precipitates in BA, caused by the decrease in pH produced by carbonation. The higher abundance of Al and Fe in the coarser fractions of slag could also hence partly explain the lower leaching of Cr and Mo from class A+B+C. Due to the decrease in the natural pH of the slag caused by the carbonation treatment, a significant enhancement of Cr release (by ~1 order of magnitude) and Mo, in accordance with the results of the EN 12457 test, was observed. Oxyanion forming elements have in fact been indicated by several studies (e.g.: Zhang, 2000; Crysochoou and Dermatas, 2006) to be incorporated in hydration phases such as ettringite and hydrocalumite; the significant decrease in the hydrocalumite and portlandite content of the slag upon carbonation and corresponding decrease in pH, hence

may explain the mobilization effect observed for Cr and Mo from carbonated slag compared to untreated residues at the natural pH of the material.

3.2.4 Conclusions

The findings of the present work indicate that carbonation of RDF incineration BA is capable of affecting several properties of this material, including its acid neutralisation behaviour, mineralogical composition and trace metal leaching. Carbonation was able to modify the natural pH of the material, which shifted towards values corresponding to the minimum solubility for most metal cations (Pb, Zn and Cu). The reduction in Pb leaching was found to be the most relevant. For Cr, a typical oxyanionic forming metal, the decrease in natural pH led to a mobilization effect, which is a critical issue that needs to be addressed when BA carbonation is proposed as a stabilization technique. 1-year natural weathering in the laboratory showed to exert quite similar effects (although generally less pronounced) on the leaching behaviour of the ash, even if an increase in the CO_2 uptake of the weathered slag was not observed.

The experimental results indicated that the carbonation process was strongly affected by the chemical and mineralogical composition of the individual BA size fraction investigated, with an increase in the CO_2 uptake potential after 8 hours from ~4% for the coarse fractions to ~14% for the finest class. However, considering that the coarse classes were quantitatively predominant in the original BA sample, in order to improve the overall carbon sequestration capacity of the material further investigation is required on the application of more severe operating conditions to enhance the dissolution of complex Ca and Mg minerals (mainly silicates) contained in the coarse fractions.

Considering the CO_2 uptakes measured in this study for the different particle size fractions of BA, a total sequestration capacity of 0.4% of the total CO_2 emissions of the incineration plant can be estimated, similarly to values reported by other studies on BA carbonation (e.g.: Rendek et al., 2006a). It must be also pointed out that, taking into account the total amounts of BA produced from typical waste or RDF incineration facilities, even if the Ca conversion to carbonate yield were significantly improved (e.g. increased up to 90%) nevertheless a maximum sequestration potential of 2% of the CO_2 emitted from the plant could be achieved.

Chapter 4: Carbonation of steel slag

Accelerated carbonation of stainless steel slag is the focus of this Chapter. The experimental work herein presented was aimed at assessing the CO_2 storage capacity of various size fractions of a mixture of the main by-products of stainless steel manufacturing (EAF and AOD slag) under mild operating conditions. Furthermore, the influence on process kinetics of some of the main operating parameters (temperature, pressure and liquid to solid ratio) were studied, as well as the effects of carbonation on the mineralogy and leaching behaviour of the residues.

Alike the studies conducted on the other types of industrial residues, an important part of the experimental work consisted in the characterization of the material in terms of its physical, chemical and mineralogical characteristics. As explained in Section 1.4.3, the composition of steel slag may vary significantly depending on the manufacturing process and the additives used. The mineralogical composition of these types of industrial by-products is also generally more complex than that of other types of residues (e.g. APC ash) but its assessment is crucial to identify the possible reacting phases with CO_2, as well as the main reaction products of the carbonation process.

The studies carried out up to now on steel slag carbonation have concluded that the particle size of the slag grains, and secondly reaction temperature, are the main controlling factors influencing the Ca conversion yields achieved by the accelerated carbonation reaction. Hence in this work, after studying the particle size distribution of the slag, the material was subdivided into 4 different particle size fractions which were separately characterized and tested for carbonation, in order to evaluate if the different results obtained for each fraction of the slag were to be ascribed to the differences in the composition of each class, similarly to what observed for BA (see Section 3.2), or merely to the variations in the specific surface of the slag particles, as indicated by several literature studies (e.g. Huijgen et al., 2005; Lekakh et al., 2008a).

All classes of stainless steel slag presented a very high Ca content (40-50% wt.) which, similarly to the BA investigated in the previous chapter, showed a decreasing trend with particle size. The mineralogy of the slag did not appear to vary significantly with particle size with a predominance of silicate phases, including dicalcium silicate and akermanite, in

all fractions, although the finest class appeared to be enriched in periclase, Mg-Cr oxide and Ca-Fe-Al oxide.

The mineralogy of the ash was affected by the treatment, showing a significant reduction of Ca and Mg oxides, a slight decrease of silicate phases (Ca_2SiO_4), and a significant increase of calcite, as well as the possible formation of some dolomite.

Maximum CO_2 uptakes of 130 g CO_2/kg slag were achieved for the finest fraction of the residues. CO_2 uptake decreased with increasing particle size, owing partly also to a lower availability of reacting species, but especially to the lower specific surface.

Carbonation kinetics was relatively fast, reaching completion in around 1 hour with a CO_2 pressure of 3 bar and an optimal liquid to solid ratio of 0.4 l/kg; temperature, besides particle size, was the parameter that most influenced CO_2 uptake, due to the enhancement of silicates dissolution. The estimated calcium conversion yields were quite lower than those achieved by the slurry phase process at optimal operating conditions (Huijgen et al., 2005), owing to the lower Ca dissolution yield achieved at these milder conditions.

The leaching behaviour of the carbonated ash was also modified, exhibiting a pH reduction of 1-2 units depending on particle size, a decrease of Ca leaching and an increase of Si leaching. Cr, which was the only trace compound significantly leached, in particular from the finer grain size classes, was not appreciably affected by carbonation. pH-dependence tests performed on the finest fraction of carbonated slag showed, similarly to those performed on carbonated BA (see Section 3.2), at pH values above 8 a reduction in Ca mobility and conversely an enhancement in Mg leaching. The leaching behaviour of Si and Cr instead appeared not to be significantly affected by the carbonation treatment in the whole pH range investigated.

4.1 Introduction

[6]In developed countries various industrial processes including fossil fuel combustion, cement production, iron and steel manufacturing and others, are among the major point-source contributors to CO_2 anthropogenic emissions. The steel industry is globally the largest energy consuming manufacturing sector and accounts for 7-12% of anthropogenic greenhouse gas emissions (OECD, 2002). Several measures, such as scrap steel recycling, are hence being developed to improve energy efficiency and cut CO_2 emissions but more

[6]Most of this section was published as Baciocchi et al., 2009b.

drastic measures are needed if the reduction goals established by the Kyoto Protocol are to be met (Rynikiewicz, 2007).

Along with the emissions of GHGs from the mentioned industrial processes, considerable amounts of solid residues are also generated, which are either variously reused in different applications or finally landfilled; in either case, the predominantly inorganic constituents (heavy metals, metalloids and alkalies) associated to these residues may be released into the environment, with potential environmental impacts on terrestrial ecosystems and human health. For such reasons, careful control of atmospheric emissions and appropriate management of the solid residues generated are both claimed in view of attaining environmental sustainability. Within this framework, a combined approach aiming at reducing CO_2 emissions, at the same time improving the environmental behaviour of the solid waste streams generated by a given industrial process, appears to be highly desirable.

Accelerated carbonation of steel slag has hence been proposed and investigated by several research groups, as reviewed in Section 1.4.3, as a technology for both sequestering CO_2 in a stable solid form and for improving the environmental and mechanical properties of steelmaking slags. Steelmaking slag in fact is one of the most abundant (together with cement construction and demolition waste) industrial residues streams that present chemical characteristics potentially suitable for achieving significant CO_2 uptakes (Lekakh et al., 2008a). Ca and Mg bearing phases in steel slag are mainly made up by various types of oxides but prevalently silicates that may also contain elements such as Fe, Al or Cr, depending on the type of process that generated the slag, and hence may present different reactivity towards CO_2.

As described in Section 1.4.3, accelerated carbonation of SS consists of two sequential processes: the dissolution of alkaline elements (Ca and Mg) from the silicate minerals and the precipitation of the corresponding carbonates. As reported in Section 1.4.3, the two processes have been investigated up to now both in a single or double stage. In the latter case, dissolution and precipitation can be optimized separately by selecting the proper pH for each reaction, but specific additives must be used (Teir et al., 2007; Eloneva et al., 2008a,b,c; Kodama et al., 2008). 1-stage slurry phase carbonation of finely milled BOF slag showed to achieve significant Ca conversion yields in 30 minutes at 19 bar CO_2 pressure and 100 °C (Huijgen et al., 2005); the costs evaluated for this process route, although lower than those estimated for mineral ore carbonation, were however still quite

high (Huijgen et al., 2007), as well as the use of significant amounts of process water. Hence in this work milder operating conditions on humidified (L/S < 1 l/kg) stainless steel slag were tested. Similar operating conditions had been previously adopted in previous studies (Johnson, 2000; Johnson et al., 2003a,b; Chen et al., 2007) mainly to investigate the effects of accelerated carbonation on the mechanical and leaching properties of the slag; a detailed study on the feasibility of this process route in terms of the attained CO_2 uptakes and Ca conversion to carbonate yields, as well as the assessment of the effects of the operating conditions on carbonation kinetics, were not specifically investigated.

In this work accelerated carbonation tests were carried out on four particle size fractions of humidified stainless steel slag to assess the CO_2 uptake achievable by each fraction under mild operating conditions, to identify the reacting species and hence estimate the achieved Ca conversion to carbonate yield of the reaction, to investigate the influence of operating parameters on reaction kinetics and to analyze the effects of the treatment on the mineralogy and leaching behaviour of the slag.

4.2 Materials and methods

The stainless steel slag (SSS) analyzed in this study was a mixture of the main types of slag produced during stainless steel manufacturing, i.e. the residues generated from the Electric Arc Furnace (EAF) and from the Argon Oxygen Decarburization (AOD) converter units. A freshly produced 20 kg sample was collected from the slag deposit of the plant, homogenized and dried at 50 °C to constant weight.

After determining its particle size distribution curve according to the ASTM D422 standard procedure, the slag was divided by sieving into the following size fractions: 2-0.425 mm (class A); 0.425-0.177 mm (class B); 0.177-0.105 mm (class C); < 0.105 mm (class D). Class A was then milled to < 0.425 mm prior to chemical composition analysis and carbonation treatment. Each fraction was thoroughly characterized in terms of elemental composition, anion content, mineralogy and leaching behaviour.

The water content and loss on ignition (LOI) of the slag samples were determined according to the ASTM C25 and ASTM D2216 procedures, respectively. The elemental composition of the SSS fractions was analyzed by atomic absorption spectrometry (AAS) after digestion of slag samples with $Li_2B_4O_7$ at 1050 °C and dissolution of the molten material in a 10% HNO_3 solution. Chloride and acid-soluble sulphates were measured

using the Italian UNI 8520 test procedure, which involves dissolution with hot deionised water and titration with $AgNO_3$ for Cl^- analysis and dissolution with 3% HCl followed by spectrophotometric analysis for acid-soluble SO_4^{2-}. The carbonate content of untreated and carbonated SSS fractions was measured with a Dietrich-Frühling calcimeter. All chemical analyses were performed in triplicate.

The mineralogy of both untreated and carbonated SSS samples was determined by X-ray diffraction (XRD) and micro Raman spectroscopy analyses. Changes in the leaching behaviour of the slag were investigated by means of the EN 12457-2 standard compliance test and the CEN/TS 14429 pH-dependence test on both untreated and carbonated SSS samples; these leaching tests were run on a single replicate.

Batch accelerated carbonation tests were performed in a pressurized stainless steel reactor equipped with a 150 ml internal Teflon jacket and placed in a thermostatic bath for temperature control. Gas humidity was maintained at 75% using a saturated NaCl solution in the reactor. In each run, three 1 g slag samples were mixed with distilled water at specific liquid to solid (L/S) ratios, from 0 to 0.6 l/kg, placed in tin foil containers and exposed to a 100% CO_2 flow for set times, ranging from 0.5 up to 24 h. For each experiment a control sample was prepared with the same procedure and stored in closed containers in contact with air at atmospheric pressure in the thermostatic bath for the whole length of the experiment.

Initial wet carbonation tests were carried out on class D to evaluate the influence of temperature (varied from 30 to 50 °C), pressure (1-10 bar), and the L/S ratio (0 to 0.6 l/kg) on the CO_2 uptake kinetics of the slag. Accelerated carbonation tests were then performed, under the optimal conditions determined for class D, on the other slag fractions and also on un-grinded class A to evaluate the influence of composition and specific surface area on the carbonation yield. After treatment with CO_2, the samples were oven-dried at 50 °C, and sample weight gain, which provides a first qualitative indication of carbonate formation, was recorded. The three samples treated in each run were grinded, since after treatment the slag exhibited a compact hardened structure, mixed together and analyzed by calcimetry testing, to estimate the CO_2 uptake achieved by the treatment.

4.3 Results and discussion

SSS characterization

The analysis of the particle size distribution of the slag (see Figure 4.1) indicated that the residue could be classified as a sandy granular material with a significant (> 15% wt.) amount of fines (d < 100 μm), notably higher than values typically reported for steel slag (Proctor et al., 2000). Discarding the 2 mm oversize fraction (< 10% wt.), the slag was divided into the above mentioned 4 classes with the following weight distribution: class A = 45.9% wt., class B = 25.9% wt., class C = 12.8% wt., class D = 16.4% wt, as shown in Figure 4.2.

The LOI values decreased consistently with particle size from 3.3% wt. for class D to 0.6% wt. for class A, but were anyhow quite low, indicating a reduced content of hydroxide and carbonate species, the only compounds expected to decompose in this type of residues at T < 1000 °C. Comparing these results to the initial calcite content of the slag (see Table 4.1), it was inferred that only class D contained a small amount of hydroxide species (being the LOI higher than the CO_2 uptake of the material), whereas for classes A, B and C the LOI values were ascribed entirely to the partial initial weathering of the slag.

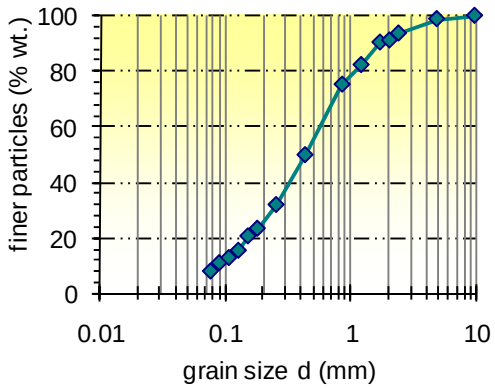

Figure 4.1 Particle size distribution curve of the stainless steel slag.

The elemental composition and anion content of the four size fractions of the SSS are reported in Table 4.1. The calcium content was very significant (from 40 to 50% wt.), in agreement with prior investigations on SSS (Johnson et al., 2004; Shen and Forssberg, 2003; Teir et al, 2008), (see also Table 1.4) and showed to decrease with particle size. The same trend, although with considerably lower concentrations, was observed for Mg (from 2.2 to 4.5% wt.). Significant concentrations of Fe (4.3-6% wt.), Cr (3-4.2% wt.), Al (1.7-

2.6% wt.), Mn (0.76-1% wt.) and V (0.09-0.15% wt.) were also measured and showed an increasing trend with particle size. Ni concentrations were quite lower than those found in other studies on SSS (0.04-0.075% wt. as opposed to 0.2-0.45% wt.; Shen and Forssberg, 2003), probably due to differences in the process used for stainless steel manufacturing. The concentrations of other heavy metals and soluble salts, as expected, were very low.

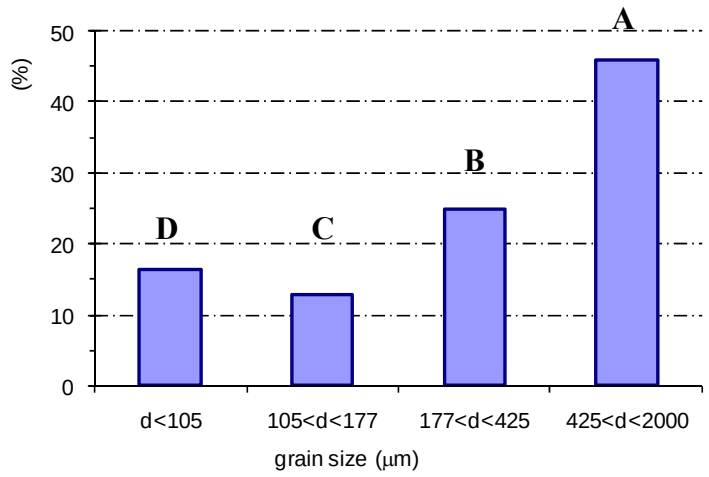

Figure 4.2 Weight distribution of the 4 particle size classes of SSS analyzed in this study.

Table 4.1 Elemental composition (mg/kg dry wt.) and anion content (% dry wt.) of SSS.

Element	Class A 2-0.425 mm	Class B 0.425-0.177 mm	Class C 0.177-0.105 mm	Class D < 0.105 mm
Al	26040	22080	17986.7	16840
As	3.5	3.1	4.1	6.2
Ca	432333.3	402000	445333.3	500333.3
Cd	51.7	1.8	14.3	3.5
Cr	42466.7	34066.7	29933.3	30466.7
Cu	228	234.7	145.3	166.7
Fe	59733.3	53000	43600	43266.7
K	310.7	334.7	313.3	356
Mg	22166.7	26466.7	29900	44600
Mn	10453.3	8773.3	7866.7	7600
Mo	230.7	186.7	168	225.3
Na	1960	1893.3	1738.7	1541.3
Ni	376	750.7	458.7	461.3
Pb	76	77.3	58	120
Sb	1.5	1.5	1.2	1.3
V	1520	1133.3	813.3	920
Zn	112.1	100.8	126.4	144.1
Anion				
Cl^-	0.035	0.044	0.056	0.05
SO_4^{2-}	0.19	0.18	0.25	0.25
CO_3^{2-}	2.33	2.96	3.5	5.25

The results of the EN 12457-2 compliance leaching test on untreated slag (see Table 4.2) indicated that the pH of the eluates was high, above 12, and very similar for the size fractions B, C and D, decreasing slightly for class A; a similar declining trend with particle size was also observed for Ca, Mg and Cr leaching. Cr, in particular, was the only trace compound that exhibited a higher eluate release than the limit prescribed for inert waste landfilling (0.5 mg/l), but was nonetheless lower than values reported for AOD SSS (Shen and Forssberg, 2003).

XRD analysis allowed to identify several oxides and silicate mineral phases in the different size fractions of the slag (see Figure 4.3). The mineralogy of the SSS did not appear to vary significantly with particle size: in all fractions a predominance of silicate phases including dicalcium silicate, merwinite, akermanite, anorthite, gehlenite and forsterite were found, confirming the results of other studies on SSS (Johnson et al., 2004; Shen and Forssberg, 2003). Cuspidine, a typical species formed during SSS hydration after addition of fluorine, along with silica and magnetite, were also detected in all particle size classes. Even though CaO or $Ca(OH)_2$ were not identified by XRD analysis, Ca-Al-Fe oxide, Mg-Cr oxide, periclase (detected also in the above mentioned studies) as well as calcite, showed higher peak intensities in class D.

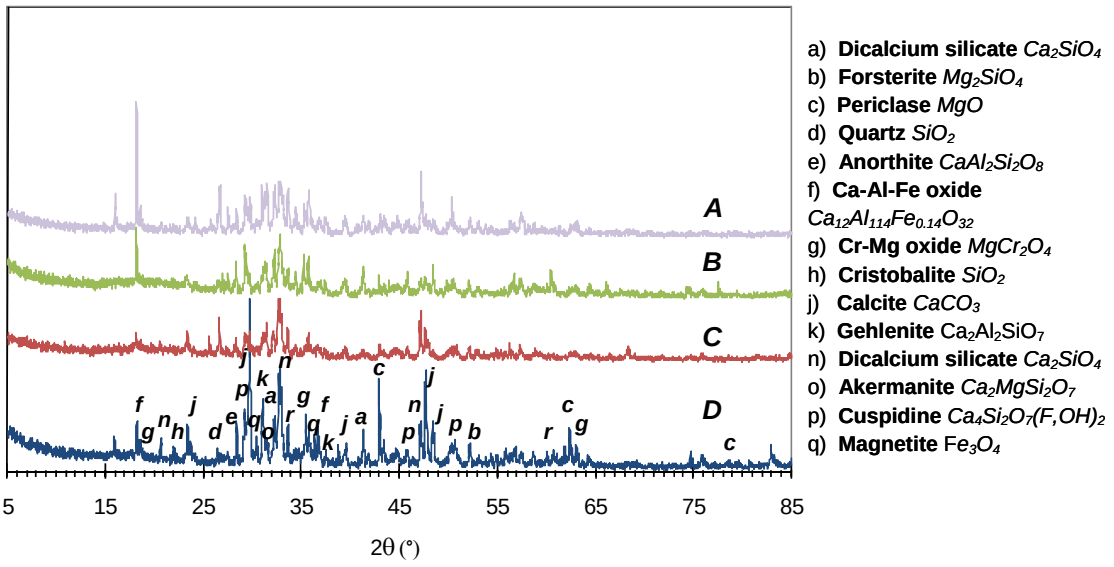

Figure 4.3 XRD patterns of the different particle size fractions of the slag.

Raman spectroscopy (results not shown here) confirmed some of the results of elemental and XRD analyses, revealing the presence of Si, Fe and Al minerals including alumina (Al_2O_3), magnetite, olivine $(Mg,Fe)_2SiO_4$ and also indicated calcite presence in all fractions, but was not able to detect calcium silicate or oxide phases.

Evidences of carbonation

Mineralogical transformations induced by carbonation reactions on class D samples are shown in Figure 4.4. Similar results were obtained also for the other particle size fractions, although due to the lower extent of carbonation achieved for these classes, the difference between the diffraction patterns of each class before and after treatment appeared to be less evident and hence to better highlight the differences, as an example, the XRD for untreated and carbonated class D sample was chosen. The diffraction patterns of carbonated samples indicated the disappearance of periclase, a significant reduction in the peak intensities for Mg-Cr and Ca-Al-Fe oxides, as well as a reduction of silicate phases such as dicalcium silicate, anorthite and cuspidine, accompanied by a significant increase in peak intensities for calcite and evidence of possible dolomite formation; only Mg-containing carbonates were not identified. Quartz and cristobalite peaks did not appear to change after the carbonation treatment. These results are in good agreement with findings by Johnson et al. (2003b), that evidenced the increase of calcite, the decrease of periclase, portlandite and partly also of dicalcium silicate, while an unmodified pattern for merwinite, akermanite and silica.

Figure 4.5 reports the acid titration curves of the ANC test performed on untreated and carbonated class D samples. Both slag samples showed a significant (around 10 meq/g) acid buffering capacity in the pH range 8-10. The buffering capacity of the treated slag at pH > 10 was reduced, owing to the decrease in free oxides, whereas no significant increase in the pH range 7-8, typical of calcite control, could be observed for carbonated slag compared to untreated samples; this was probably due to the fact that partially reacted silicates buffer in similar pH ranges. Similar results had been previously reported also by Johnson et al. (2003b). The acid titration curves obtained for the other particle size classes showed similar trends to class D, although the extent of the acid buffering capacity of each fraction in the pH range 8-10 decreased progressively with increasing particle size (from 7.5 meq/g for class C to around 4 for classes B and A).

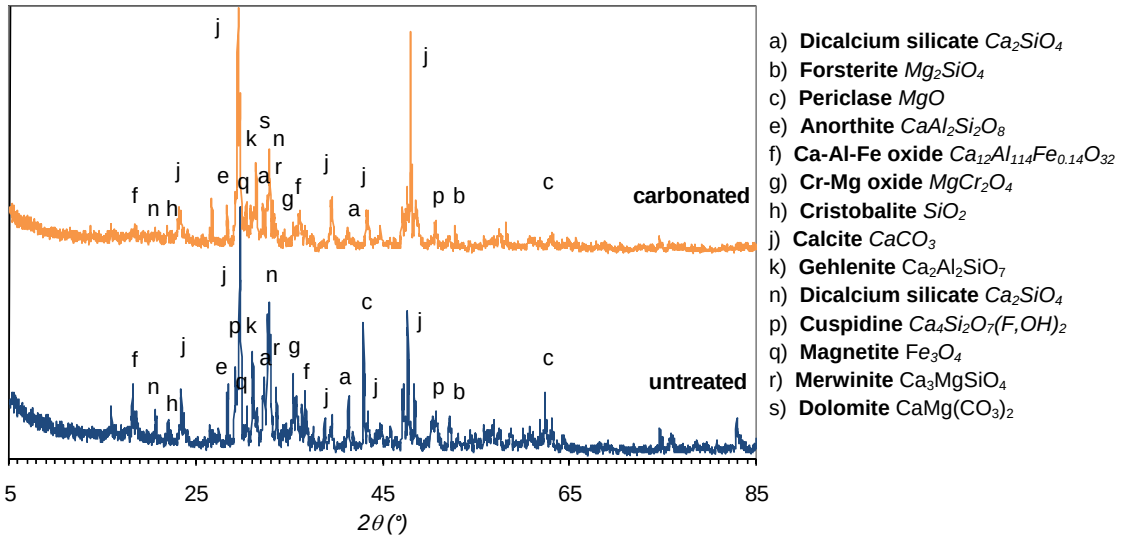

Figure 4.4 XRD pattern for the untreated and carbonated (2 h, 0.4 l/kg, 50 °C and 3 bar) class D fraction.

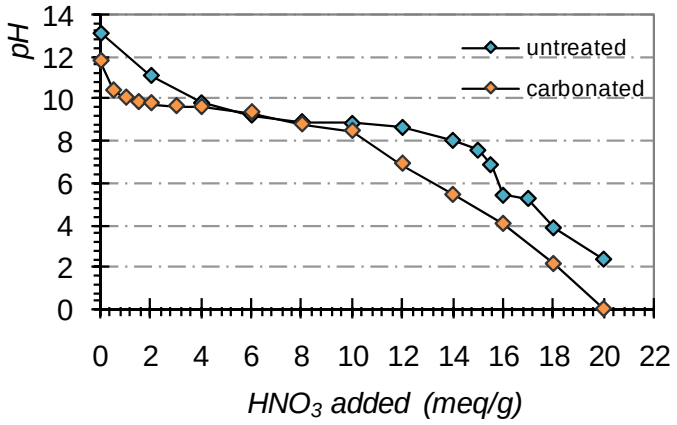

Figure 4.5 ANC curves for untreated and carbonated (2 h, 0.4 l/kg, 50 °C and 3 bar) class D fraction.

Calcium conversion and carbonation kinetics

The main results of the accelerated carbonation tests are schematically represented in Figure 4.6. Carbonation kinetics proved to be quite fast, reaching completion in 2 to 4 hours depending on operational conditions. A maximum CO_2 uptake, calculated applying Equation 3.2, of 130 g CO_2/kg slag was achieved for class D after a reaction time of 4 hours at 50 °C, 3 bar CO_2 pressure and a L/S of 0.4 l/kg.

In Figures 4.6a and 4.6b the influence of CO_2 pressure and temperature on the carbonation kinetics for class D are shown respectively; similar trends were also found for the other particle size fractions, although the values of the achieved CO_2 uptakes were significantly lower (see Figure 4.6d). Pressure did not appear to affect neither the CO_2 uptake, nor the kinetics of the reaction, in agreement with results of carbonation tests performed under similar operating conditions and 100% CO_2 on other types of combustion residues (e.g. see the results found for MSWI APC residues, reported in Section 3.1).

Temperature, other than grain size, was the parameter that seemed to most affect slag reactivity towards CO_2, leading to CO_2 uptakes of just below 13% wt. in 2 hours. This effect was ascribed to the enhancement of silicate dissolution, indicated as an important factor in slurry phase steel slag carbonation, for which an optimal temperature value of 200 °C was reported (Huijgen et al., 2005). The L/S ratio is also an important parameter for aqueous phase carbonation: while for slurry phase experiments an optimal value of 2 l/kg was indicated (Huijgen et al., 2005), for partially humidified SSS, an optimal value of 0.125 l/kg was reported (Johnson, 2000). In this study, the highest CO_2 uptakes were achieved with L/S ratios ranging from 0.3 to 0.4 l/kg, as shown in Figure 4.6c. This dissimilarity could be due to differences in slag composition, since in Johnson's study portlandite was identified in the slag, whereas in this study no hydrated compounds were detected, indicating that part of the water added to the slag was employed for hydration of the oxide and silicate phases, other than for solvation of CO_2 and Ca^{2+} ions.

Similarly to results reported in other studies (Huijgen et al., 2005), CO_2 uptakes varied considerably with particle size (see Figure 4.6d); since no remarkable differences in elemental and mineralogical composition were detected, except for a slight increase of Ca and Mg oxides content in class D, the reduced surface area of the slag with increasing particle size was considered as the main mechanism behind the decrease in slag reactivity towards CO_2. This hypothesis was confirmed by results of accelerated carbonation tests on milled ($d < 0.425$ mm) class A slag, which displayed CO_2 uptakes similar to class C ($0.105 < d < 0.177$ mm), indicating that, as reported by Huijgen et al. (2005), even under the operating conditions investigated in this study, intensive milling could contribute to enhancing the carbonation yield considerably.

The conversion yields, calculated applying Equation 3.4, as expected, were quite lower than the values reported by Huijgen et al. (2005), due to the inferior degree of Ca

dissolution obtained from the silicate phases at 50 °C. Although for carbonated SSS samples a decrease in Mg phases, periclase in particular, was detected by XRD analysis especially for class D slag, and the possible presence of dolomite was also suggested, as a first approximation only Ca phases were considered. The Mg content of the ash was in fact an order of magnitude lower than the Ca content and secondly none of the other studies carried out at mild or enhanced operating conditions indicated significant CO_2 uptake by Mg oxide or silicate phases (e.g.: Johnson et al., 2003a,b; Huijgen et al., 2005; Chen et al., 2007). The following Ca to carbonate maximum conversion yields were estimated for the different particle size fractions analyzed in this study: ~25% for class D, ~15% for class C, ~ 8% for class B, ~3% or 13% for un-grinded or grinded class A respectively.

In addition, the carbonated slag, particularly for L/S > 0.2 l/kg and T = 50 °C, exhibited a compact, hardened cement-like structure, suggesting that through accelerated carbonation, aggregates of SSS with specific mechanical properties could be manufactured.

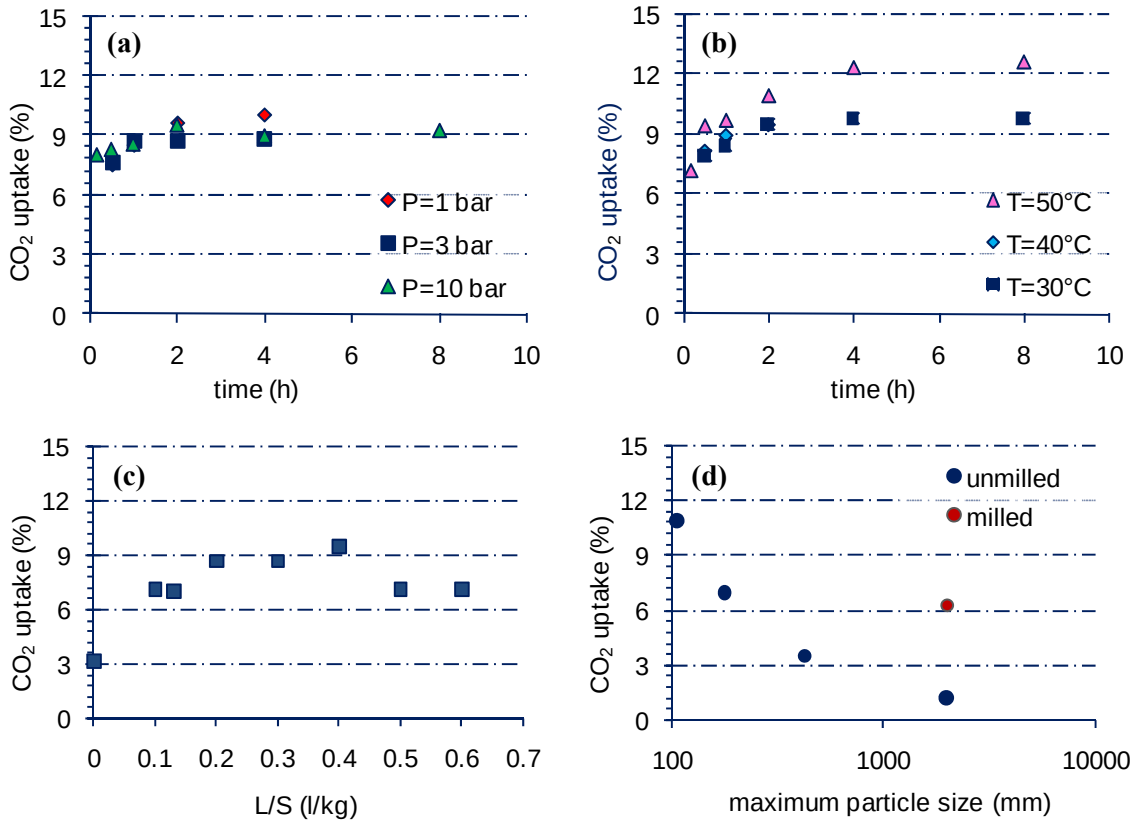

Figure 4.6 CO_2 uptake as a function of (a) pressure (class D, at 30 °C and 0.3 l/kg); (b) temperature (class D, 3 bar and 0.4 l/kg); (c) L/S ratio (class D, 2 h, 30 °C and 3 bar CO_2); (d) particle size (2 h, 50 °C, 3 bar and a 0.4 l/kg).

Leaching behaviour

The results of the EN 12457-2 leaching compliance test after carbonation (see Table 4.2) revealed a decrease in the natural pH for all the carbonated samples, which was more pronounced (by almost 2 units) for class D, the fraction that showed the highest reactivity towards CO_2. The only compounds whose leaching appeared to be significantly modified by the treatment were Ca and Si. Ca concentrations in the eluates were considerably reduced, by up to one order of magnitude, for all size fractions, indicating the formation of less soluble phases, such as calcite, than those making up the original slag. Contrarily, Si concentrations significantly increased in the eluates of all carbonated samples, except for class D, indicating that indeed part of the silicates reacted during the carbonation treatment, releasing more soluble silica phases. These results are in good agreement with findings by Chen et al. (2007) on steel slag carbonated under similar operating conditions. Cr release appeared to be slightly reduced only for class B and C samples, although remaining higher than the regulatory limit of 0.5 mg/l for inert waste disposal.

Table 4.2 EN 12457-2 leaching test results for SSS before and after the carbonation treatment (2 h, 0.4 l/kg, 50 °C, 3 bar).

	Class A		**Class B**		**Class C**		**Class D**	
	untr.	**carb.**	**untr.**	**carb.**	**untr.**	**carb.**	**untr.**	**carb.**
pH	12.43	11.38	12.82	11.18	12.81	11.29	12.87	10.59
Ca (mg/l)	399	67	882.5	105	1025	84	1050	23.1
Cr (mg/l)	0.04	0.06	0.15	0.06	0.16	0.08	0.18	0.17
Fe (mg/l)	0.07	0.03	0.06	0.01	0.06	0.09	0.13	0.03
Mg (mg/l)	0.08	0.08	0.2	0.17	0.19	0.23	0.43	0.24
Si (mg/l)	1.6	67.5	0.9	63.8	1.2	51.3	1.6	7.3

The pH-dependant leaching of Ca, Mg, Si and Cr for class D, as derived from the ANC test, is reported in Figure 4.7. The leaching curve for Ca confirmed the results of the EN 12457-2 test, showing a decrease in leachate concentration for pH > 8 due to calcite formation, whereas for Mg a mobilization effect in the same pH range was observed, which could be due to the formation of hydrated soluble species, indicating that no significant precipitation of Mg carbonates occurred, as observed also by Huijgen and Comans (2006). Si leaching as a function of pH did not show significant variations after carbonation, probably owing to the low degree of reactivity of silicate minerals under mild

carbonation conditions. The shape of the leaching curve for Cr was not appreciably modified by the carbonation process; this could be due to Cr^{3+} solubility, as previously reported by Huijgen and Comans (2006).

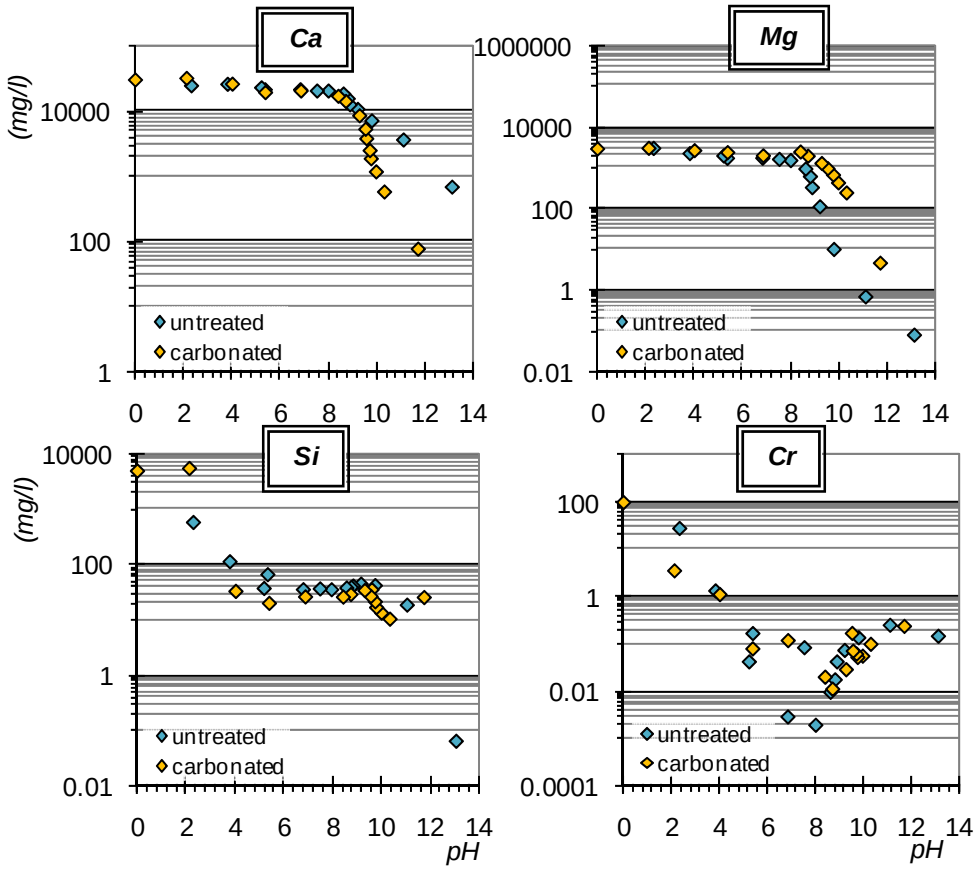

Figure 4.7 Leaching of Ca, Mg, Si and Cr as a function of pH for untreated and carbonated (2 h, 0.4 l/kg, 50 °C and 3 bar) class D fraction.

4.4 Conclusions

The results of the present study indicate that the carbonation tests performed under mild operating conditions on different particle size fractions of SSS were able to affect several properties of this industrial by-product. Chemical and mineralogical characterization indicated that all size fractions had a high potential for reacting with CO_2, owing to the particularly significant Ca and also Mg content of the slag, mainly in the form of silicates and secondly of oxides.

The experimental results indicated that the parameter that most affected the CO_2 uptake of the slag was grain size, and in particular the specific surface area of the particles. An

increase in temperature had also a positive effect on enhancing the CO_2 uptake of the slag, although it appeared to decrease the kinetics of the overall reaction.

The maximum CO_2 uptake found in this study (13% wt.) was not significantly lower than those reported for slurry steel slag carbonation at enhanced processing conditions (Huijgen et al., 2005); however, the Ca conversion to calcite yield measured in the present study was rather low (around 25% for class D), compared to that reported for the above mentioned study (75%). Hence it appears that the investigated stainless steel slag exhibits a high potential for CO_2 binding which could be fully exploited by optimizing the controlling operating parameters: temperature and particle size. Given the unsubstantial differences between the composition and mineralogy of the different particle size classes investigated in this study, it may be concluded that, by mixing and milling all classes down to a particle size <0.105 mm, similar results as those found for class D could be achieved. Assuming that the total amount of EAF and AOD generated annually by the plant (~180,000 t SSS/y) were to present the same CO_2 uptake obtained for class D, a sequestration capacity of ~ 6% of the total CO_2 emitted by the plant (400,000 t CO_2/y) may be anticipated. By enhancing the Ca conversion yield, for example increasing the operating temperature, a maximum CO_2 uptake of ~22% (assuming a conversion yield of 90%) could potentially be pursued, which may be considered as a noteworthy improvement, considering also the mild operating conditions applied (1-3 bar CO_2) and the absence of processing water consumption and treatment, respect to slurry phase treatment.

Furthermore, it appears that the environmental properties of the slag were not negatively affected by the carbonation treatment; on the contrary a reduction in the pH of the slag, which entails an improvement in the reuse potential of the SSS, was achieved. An aspect that needs to be further examined is the ability of accelerated carbonation to enhance the mechanical and structural properties of the slag, which may be an interesting effect in view of utilization of the treated material in engineering applications.

Chapter 5: Conclusions and perspectives

The results of the accelerated carbonation tests performed on minerals and different types of materials indeed confirmed one of the main findings derived from the literature review reported in Chapter 1, i.e. that this process exerts quite different effects depending on the chemical, physical and mineralogical composition of the treated materials.

Concerning the findings of the experimental study carried out on the dissolution kinetics of olivine in presence of CO_2 and salts, reported in Chapter 2, it was concluded that under all the examined operating conditions, the only factor governing the specific dissolution rate was the pH of the solution, with a linear dependence of the logarithm of the specific dissolution rate upon pH. Hence CO_2 pressure and salinity appeared to influence olivine dissolution kinetics only indirectly, by affecting the final pH of the solution. This is a significant finding, since it implies that carbonate precipitation, which occurs in presence of high pressure CO_2 at pH values above 6, and olivine dissolution could theoretically be carried out in the same reactor without inhibition effects on Mg dissolution kinetics. However, to confirm this finding, microstructural analysis on the remaining solids after direct aqueous carbonation processes should be performed in order to assess if during the magnesite ($MgCO_3$) precipitation partial inhibition of olivine dissolution could be obtained as a result of reaction product coating of the silicate mineral.

In conclusion, the results of this study may prove interesting in view of the design and optimization of an effective mineral carbonation process performed applying any type of process route (direct or indirect).

The results of accelerated carbonation experiments performed on alkaline industrial residues showed quite different CO_2 uptakes, Ca conversion yields and effects on heavy metal leaching, in dependence of the type of analyzed residue. The effects of operating conditions also proved to differ as a function of the treated material.

The air pollution control residues investigated in this study were essentially made up by Ca-hydroxide species, calcite and salts (halite and sylvite) and presented a fine particle size. The analyzed bottom ash and stainless steel slag instead, although also characterized by a significant Ca content, presented a more complex mineralogy. BA composition was significantly affected by particle size, with the finer classes exhibiting a significant content of Ca hydroxide species (hydrocalumite and portlandite) and calcite, compared to coarser

fractions, which instead presented higher contents of Ca and Al silicates. Steel slag mineralogy showed to vary less with particle size, exhibiting a prevalence of Ca silicate phases (such as dicalcium silicate, cuspidine and akermanite) but also oxide phases (such as periclase, Mg-Cr oxide and Ca-Al-Fe oxide).

The highest CO_2 uptakes and Ca conversion yields were achieved for accelerated carbonation of APC ash (250 g CO_2/kg residue corresponding to a maximum conversion of 70%). Temperature showed to exert an enhancing effect on process kinetics only for relatively dry ash. Under the experimental conditions applied in this work however, capture of CO_2 from stack gases appeared to be necessary in order to enhance carbonation kinetics, unlike experiments performed on the same ash applying the gas-solid route. The effective storage potential of this waste stream, in terms of the reduction of CO_2 emissions that could be achieved applying this process to an industrial facility such as a waste incineration plant, is anyhow definitely too low to be considered feasible, owing to the meagre amounts of APC ash generated in the plant compared to CO_2 emissions.

Similar conclusions may be extended also to the results of accelerated carbonation of RDF incineration bottom ash. In this case CO_2 uptake potentials from 40 g CO_2/kg residue for the coarse fractions to ~140 g CO_2/kg residue for the finest class were achieved. A slight enhancement effect of temperature on CO_2 uptake was measured only for the coarser fractions and associated to their higher content of silicate phases. CO_2 pressure was the only parameter that showed to significantly affect the reaction kinetics of the fine fractions.

The results obtained from stainless steel slag carbonation experiments indicated that the parameter that most affected the CO_2 uptake of the slag was grain size, and in particular the specific surface area of the particles. An increase in temperature had also a positive effect on enhancing the CO_2 uptake of the slag, although it appeared to decrease the kinetics of the overall reaction. The maximum CO_2 uptake determined for SSS (130 g CO_2/kg residue), although lower than that obtained from APC residues carbonation, proved to be more interesting in view of an industrial application of this process for CO_2 sequestration. The calcium conversion yield achieved in fact, was not high at the mild operating conditions tested, (around 25%), suggesting that increasing the process temperature in particular, or using specific extracting chemicals (such as chelating agents for example), and also finely milling the slag to a particle size < 100 μm may contribute in enhancing the yield significantly, which could contribute to a maximum uptake of ~22% of

the total CO_2 emissions generated by the stainless steel manufacturing plant, which may be considered as a noteworthy improvement.

Regarding carbonation kinetics, it may be concluded that, irrespective of the type of residue tested, the extent of carbonation with time showed similar trends to those reported by several studies conducted on different types of alkaline residues applying various process routes which were described applying the unreacted particle core model theory. In particular, optimizing operating conditions (such as increasing temperature or the L/S ratio for APC ash) showed to enhance the chemical reaction, reducing the first order kinetics trend of the curve, causing the extent of carbonation to tend to its maximum value determined by diffusion control, in only a few minutes.

As for the effects of accelerated carbonation on the leaching behaviour of the studied residues, it may be concluded that significant results were obtained in particular for the MSWI residues. For both types of these residues in fact, accelerated carbonation showed to exert a strong immobilization effect on Pb, Zn and Cu, which were among the critical elements in terms of heavy metal leaching for both types of untreated residues.

For APC ash, chemical speciation modelling indicated a change in the solubility-controlling minerals from the untreated to the carbonated ash. For the latter, metal release was found to be clearly controlled by a number of carbonate minerals, indicating the potential of the carbonation process to convert the initial metal-containing minerals into generally less soluble carbonate forms, with positive implications on the environmental behaviour of the ash. However, soluble salts, which were not significantly affected by carbonation, along with Sb, which showed instead to be considerably mobilized upon carbonation, proved to be the critical compounds for the disposal of the treated residues.

Accelerated carbonation proved instead to potentially be an interesting chemical stabilization technique to apply to RDF bottom ash treatment. The effects of the process on the leaching behaviour of oxyanion forming elements like Cr however, still need to be further investigated, as well as the differences in the mechanisms exerted by accelerated carbonation and natural weathering on the leaching of main and trace elements from BA.

The environmental properties of stainless steel slag did not show to be significantly affected by the carbonation treatment, Cr leaching remaining the most critical element with respect to the environmental behaviour of the material; however also in this case the effects of carbonation on oxyanion forming elements mobilization should be further investigated.

In conclusion, this study provided new insight on some of the main effects of accelerated carbonation on alkaline residues both in terms of achievable CO_2 uptake and Ca conversion yields and also of the effects of the treatment on the leaching behaviour of the material. In particular, the application of this treatment on MSWI APC does not appear to be a feasible process neither for CO_2 storage (owing to the scarcity of this material compared to CO_2 emissions) nor as a stabilization technique, since soluble salts (chlorides and sulphates) leaching would remain a critical issue for the safe disposal of these residues. The carbonation experiments performed on APC residues however, owing to the composition of this material, provided interesting information on the main mechanisms influencing both CO_2 uptake kinetics and the leaching behaviour of the ash. Accelerated carbonation of RDF bottom ash appears instead to exert potential benefits regarding the chemical stabilization of this type of material; in this case a direct carbonation treatment at the incineration plant of the produced BA using part of the combustion flue gas may be envisioned as a low cost process for speeding up the natural weathering of the slag. Finally, accelerated carbonation of stainless steel slag appears to be one of the most interesting techniques, in terms of attainable CO_2 uptakes, for carrying out mineral storage of carbon dioxide in industrial facilities using part of the waste streams generated in the same plant.

References

Alexander G., Maroto-Valer M.M. and Gafarova-Aksoy P. (2007). Evaluation of reaction variables in the dissolution of serpentine for mineral carbonation. *Fuel*, 86, 273-281.

Allal K.M., Doligner J.C. and Martin G. (1998). Reaction mechanism of calcium hydroxide with gaseous hydrogen chloride. *Revue de l'Institut Français du Petrole*, 53, 871-880.

Allison J.D., Brown D.S. and Novo-Gradac K.J. (1991). *MINTEQA2/PRODEFA2. A Geochemical Assessment Model for Environmental Systems. Version 3.0 User's Manual*. US Environmental Protection Agency, Athens, GA (U.S.A).

Antemir A., Gunning P.J., Hills C.D. and Carey P.J. (2008). Accelerated carbonation for the treatment of landfilled cement kiln dust. *Proceedings of the 2nd International Conference on Accelerated carbonation for Environmental and Materials Engineering ACEME08*, 1-3 October 2008, Rome, (Italy).

Anthony E.J., Bulewicz E.M., Dudek K. and Kozak A. (2002). The long term behaviour of CFBC ash-water systems. *Waste Management*, 22, 99-111.

Arickx S., Van Gerven T. and Vandecasteele C. (2006). Accelerated carbonation for treatment of MSWI bottom ash. *Journal of Hazardous Materials*, B 137, 235-243.

Astrup T., Rosenblad C., Trapp S. and Christensen T.H. (2005). Chromium release from waste incineration air-pollution-control residues. *Environmental Science and Technology*, 39, 3321-3329.

Astrup T., Dijkstra J.J., Comans R.N.J., van der Sloot H.A. and Christensen T.H. (2006a). Geochemical modeling of leaching from MSWI air-pollution-control residues. *Environmental Science and Technology*, 40, 3551-3557.

Astrup T., Mosbæk H. and Christensen T.H. (2006b). Assessment of long-term leaching from waste incineration air-pollution-control residues. *Waste Management*, 26, 803-814.

Astrup T., Cappai G., Lechner P., Muntoni A., Polettini A., Pomi R., Van Gerven T. and Van Zomeren A. (2007). State-of-the-art and outlook on management of waste-to-energy bottom ashes, part 1- utilization, *Proc. Sardinia 2007, Eleventh International Waste Management and Landfill Symposium*, S. Margherita di Pula (CA), October 1-5 2007, Cossu, R., Stegmann, R. (Eds.) (on CD ROM).

Baciocchi R., Polettini A., Pomi R., Prigiobbe, V., Von Zedwitz, V.N., Steinfeld, A. (2006a). CO_2 sequestration by direct gas-solid carbonation of APC residues. *Energy and Fuels*, 20, 1933-1940.

Baciocchi R., Polettini A., Pomi R., Prigiobbe, V., Von Zedwitz, V.N., Steinfeld, A. (2006b). *Performance and kinetics of CO_2 sequestration by direct gas-solid carbonation of APC residues*. Proceedings of the 8th International Conference on Green House Gas Technology, 19-22th June 2006, Trondheim (Norway).

Baciocchi R., Polettini A., Pomi R., Prigiobbe, V., Von Zedwitz, V.N., Steinfeld, A. (2006c). Accelerated gas/solid carbonation of incinerator residues: kinetics and effects on metal mobility. *Extended abstracts of the First International Conference on Accelerated Carbonation for Environmental and Materials Engineering*, June 12-14, London UK, Cement and Concrete Science (Ed.).

Baciocchi R., Costa G., Marini C., Polettini A., Pomi R., Postorino P. and Rocca S. (2008) Accelerated carbonation of RDF incineration bottom ash: CO_2 storage potential and environmental behaviour. Proceedings of the *2nd Int. Conf. on Accelerated carbonation for Environmental and Materials Eng. ACEME08*, Rome, Italy, 1-3/10/2008.

Baciocchi R., Costa G., Polettini A., Pomi R. and Prigiobbe V. (2009a). Comparison of different reaction routes for carbonation of APC residues, *Energy Procedia*, 1, 4851–4858.

Baciocchi R., Costa G., Polettini A. and Pomi R. (2009b). Influence of particle size on the carbonation of stainless steel slag for CO_2 storage, *Energy Procedia*, 1, 4859–4866.

Baciocchi R., Costa G., Di Bartolomeo E., Polettini A. and Pomi R. (2009c). The effects of accelerated carbonation on CO_2 uptake and metal release from incineration APC residues, submitted to *Waste Management.*

Back M., Kuehn M., Stanjeck H. and S. Peiffer (2008). Reactivity of alkaline lignite fly ashes towards CO_2 in water. *Environmental Science and Technology,* 42, 4520-4526.

Bearat H., McKelvy M.J., Chizmeshya A.V.G., Gormley D., Nunez R., Carpenter R.W., Squires K. and Wolf, G.H. (2006). Carbon sequestration via aqueous olivine mineral carbonation: Role of passivating layer formation. *Environmental Science and Technology*, 40, 4802-4808.

Belevi H., Stämpfli D.M. and Baccini P. (1992). Chemical behaviour of municipal solid waste incinerator bottom ash in monofills. *Waste Management & Research*, 10, 153-167.

Bhatia S.K. and Perlmutter D.D. (1983). Effect of the product layer on the kinetics of the CO_2-lime reaction. *AIChE Journal*, 29, 79-86.

Bin-Shafique M.S., Walton J.C., Gutierrez N., Smith R.W. and Tarquin A.J. (1998). Influence of carbonation on leaching of cementitious waste forms. *Journal of Environmental Engineering*, 124, 463-467.

Birat J.-P. (2009). Steel and CO_2 –the ULCOS program, CCS and mineral carbonation using steelmaking slag. *Proceedings of the 1st International Slag Valorization Symposium*, 6-7 April 2009, Leuven, (Belgium).

Blanc P., Lassin A., Nowak C., Burnol A., Piantone P. and Chateau L. (2007). *THERMODDEM: a thermodynamic database for waste materials*. Available on-line at http://thermoddem.brgm.fr/fichiers/Phreeqc_thermoddem_lvl1_no-org.txt.

Blencoe J.G., Anovitz L.M., Beard J.S. and Palmer D.A. (2003). *Carbonation of Serpentine for Long-Term CO_2 Sequestration*. In: FY 2003 ORNL Laboratory Directed Research and Development Annual Report, Oak Ridge National Laboratory.

Blencoe J.G., Palmer D.A., Anovitz L.M. and Beard J.S. (2004). *Carbonation of metal silicates for long-term CO_2 sequestration*, Patent application WO 2004/094043.

Bodénan F., Azaroual M. and Piantone P. (2000). Forecasting the long-term behaviour of municipal solid waste incineration bottom ash: rapid combined tests. In: Woolley, G.R., Goumans, J.J.J.M., Wainwright, P. (Eds.), *Waste Materials in Construction*, Studies in Environmental Sciences 71. Elsevier Sci, Amsterdam, pp. 475-482.

Bodénan F. and Deniard Ph. (2003). Characterization of flue gas cleaning residues from European solid waste incinerators: assessment of various Ca-based sorbent processes. *Chemosphere*, 51, 335-347.

Bone B.D., Knox K., Picken A. and Robinson H.D. (2003).The effect of carbonation on leachate quality from landfilled municipal solid waste (MSW) incinerator residues. *Proc. Sardinia 2003, Ninth International Waste Management and Landfill Symposium* S. Margherita di Pula (Cagliari, Italy), 6-10 October 2003, Christensen, T.H., Cossu, R., Stegmann, R. (Eds.) (on CD ROM).

Bonenfant D., Kharoune L., Sauvé S., Hausler R., Niquette P., Mimeault M. and Kharoune M. (2008a). CO_2 sequestration potential of steel slags at ambient pressure and temperature. *Industrial & Engineering Chemistry Research*, 47, 7610-7616.

Bonenfant D., Kharoune L., Sauvé S., Hausler R., Niquette P., Mimeault M. and Kharoune M. (2008b). CO_2 sequestration by aqueous red mud carbonation at ambient pressure and temperature. *Industrial & Engineering Chemistry Research*, 47, 7617-7622.

Brownlow A.H., 1996. *Geochemistry*, 2nd Edition. Prentice-Hall, U.S.A.

Butt D.P., Lackner K.S., Wendt C.H., Conzone S.D., Kung H., LU Y.C. and Bremser J.K. (1996). Kinetics of Thermal Dehydroxylation and Carbonation of Magnesium Hydroxide. *Journal of the American Ceramics Society*, 79, 1892–1898.

Chen Z.Y., O'Connor W.K. and Gerdemann S.J. (2006). Chemistry of aqueous mineral carbonation for carbon sequestration and explanation of experimental results, *Environmental Progres*s, 25, 161-166.

Chen Q., Johnson D.C., Zhu L., Yuan M., C.D. Hills (2007). Accelerated carbonation and leaching behaviour of the slag from iron and steel making industry, *Journal of University of Science and Technology Beijing*, 14, 297-301.

Chen Q., Ke Y., Zhang L., Tyrer M., Hills C.D. and Xue G. (2009). Application of accelerated carbonation with a combination of Na_2CO_3 and CO_2 in cement-based solidification/stabilization of heavy metal-bearing sediment. *Journal of Hazardous Materials*, 166, 421-427.

Chimenos J.M., Sagarra M., Fernandez M.A. and Espiell F. (1999). Characterization of the bottom ash in municipal solid waste incinerator. *Journal of Hazardous Materials*, 64, 211-222.

Chimenos J.M., Fernández A.I., Miralles L., Segarra M and Espiell F. (2003). Short-term natural weathering of MSWI bottom ash as a function of particle size. *Waste Management*, 23, 887-895.

Cizer O., Van Balen K., Elsen J., Van Gemert D. (2008a). Carbonation reaction kinetics of lime binders measured using XRD. *Proceedings of the 2nd International Conference on Accelerated carbonation for Environmental and Materials Engineering ACEME08*, 1-3 October 2008, Rome, (Italy).

Cizer O., Van Balen K., Elsen J., Van Gemert D. (2008b). Crystal morphology of precipitated calcite crystals from accelerated carbonation of lime binders. *Proceedings of the 2nd International Conference on Accelerated carbonation for Environmental and Materials Engineering ACEME08*, 1-3 October 2008, Rome, (Italy).

Cornelis G., Van Gerven T. and Vandecasteele C. (2006). Antimony leaching from uncarbonated and carbonated MSWI bottom ash. *Journal of Hazardous Materials*, B137, 1284-1292.

Cornelis G., Johnson C.A., Van Gerven T. and Vandecasteele C. (2008). Leaching mechanisms of oxyanionic metalloid and metal species in alkaline solid wastes: A review. *Applied Geochemistry* 23, 955-976.

Costa G., Baciocchi R., Polettini A., Pomi R., Hills C.D., Carey P.J. (2007). Current status and perspectives of accelerated carbonation processes on municipal waste combustion residues. Environmental Monitoring and Assessment 135, 55-75.

Crysochoou M. and Dermatas D. (2006). Evaluation of ettringite and hydrocalumite formation for heavy metal immobilization: literature review and experimental study. *Journal of Hazardous Materials*, 136, 20-33.

Dijkstra J.J., van der Sloot H.A., and Comans R.N.J. (2002). Process identification and model development of contaminant transport in MSWI bottom ash. *Waste Management* 22, 531-541.

Dijkstra J.J., van Zomeren A., Meeussen J.C.L. and Comans R.N.J. (2006). Effect of accelerated aging of MSWI bottom ash on the leaching mechanisms of copper and molybdenum. *Environmental Science & Technology*, 40, 4481-4487.

Ecke H. (2003). Sequestration of metals in carbonated municipal solid waste incineration (MSWI) fly ash. *Waste Management,* 23, 631-640.

Ecke H., Menad N. and Lagerkvist A. (2003). Carbonation of municipal solid waste incineration fly ash and the impact on metal mobility. *Journal of Environmental Engineering ASCE,* 129, 435-440.

Eloneva S., Teir S., Salminen J., Fogelholm C.J. and Zevenhoven R. (2008a). Fixation of CO_2 by carbonationg calcium derived from blast furnace slag. *Energy*, 33, 1461-1467.

Eloneva S., Teir S., Salminen J., Fogelholm C.J. and Zevenhoven R. (2008b). Steel converter slag as raw material for precipitation of pure calcium carbonate. *Energy*, 33, 1461-1467. *Industrial & Engineering Chemistry Research*, 47, 7104-7111.

Eloneva S., Teir S., Salminen J., Revitzer H., Kontu K., Forsman A.M., Zevenhoven R and Fogelholm C.J. (2008c). Pure calcium carbonate product from the carbonation of a steelmaking slag. *Energy*, 33, 1461-1467. *Proceedings of the 2nd International Conference on Accelerated carbonation for Environmental and Materials Engineering ACEME08*, 1-3 October 2008, Rome, (Italy).

Eusden J.D., Eighmy T.T., Hockert K., Holland E. and Marsella K. (1999). Petrogenesis of municipal solid waste combustion bottom ash. *Applied Geochemistry*, 14, 1073-1091.

Fernández-Bertos M., Simons S.J.R., Hills C.D. and Carey P.J. (2004a). A review of accelerated carbonation technology in the treatment of cement-based materials and sequestration of CO_2. *Journal of Hazardous Materials* B112, 193-205.

Fernández-Bertos M., Li X., Simons S.J.R., Hills C.D. and Carey P.J. (2004b). Investigation of accelerated carbonation for the stabilization of MSW incinerator ashes and the sequestration of CO_2. *Green Chemistry* 6 (8), 428-436.

Fernández-Bertos M., Simons S.J.R., Hills C.D., and Carey P.J. (2006). Kinetic studies of carbonation of MSWI ashes. Extended abstracts of the *First international conference on accelerated carbonation for environmental and materials engineering*, June 12-14, London UK, Cement and Concrete Science (Ed.).

Freyssinet Ph., Piantone P., Azaroual M., Itard Y., Clozel-Leloup B., Guyonnet D., Baubron J.C. (2002). Chemical changes and leachate mass balance of municipal solid waste bottom ash submitted to weathering. *Waste Management*, 22, 159-172.

Gerdemann S.J., O'Connor W.K., Dahlin D.C., Penner L.R. and Rush H. (2007). Ex situ aqueous mineral carbonation. *Environmental Science and Technology*, 41, 2587-2593.

Geerlings J.J.C., Mesters C.M.A.M. and Oosterbeek H. (2002). *Process for mineral carbonation with carbon dioxide*, patent number WO02085788.

Giampaolo C., Lo Mastro S., Polettini A., Pomi R. and Sirini P. (2002). Acid neutralisation capacity and hydration behaviour of incineration bottom ash-Portland cement mixtures. *Cement and Concrete Research* 32, 769–775.

Goff F., Guthrie G.D., Lipin B., Fite M., Chipera S.J., Counce D., Kluk E. and Ziock H.J. (2000). *Evaluation of Ultramafic Deposits in the Eastern United States and Puerto Rico as Sources of Magnesium for Carbon Dioxide Sequestration*. Technical Report LA -13694-MS, Los Alamos National Laboratory.

Golubev S.V., Pokrovsky O.S. and Schott J. (2005). Experimental determination of the effect of dissolved CO_2 on the dissolution kinetics of Mg and Ca silicates at 25 °C. *Chemical Geology*, 217, 227-238.

Grasshoff K. and Anderson L.G. (1999). *Methods of seawater analysis*, 3rd Edition Wiley-VCH, Weinheim.

Hänchen M., Prigiobbe V., Storti G., Seward T.M. and Mazzotti M. (2006). Dissolution kinetics of forsteritic olivine at 90-150°C including effects of the presence of CO_2, *Geochimica and Cosmochimica Acta*, 70, 4403-4416.

Hänchen M., Krevor, S., Mazzotti, M. and Lackner, K.S. (2007). Validation of a population balance model for olivine dissolution. *Chemical Engineering Science*, 62, 6412-6422.

Hänchen M., Prigiobbe V., Baciocchi R., and Mazzotti M. (2008). Precipitation in the Mg-carbonate system – effects of temperature and CO_2 pressure, *Chemical Engineering Science*, 63, 1012-1028.

Hilley G.E. and Porder S. (2008). A framework for predicting global silicate weathering and CO_2 drawdown rates over geologic time-scales. *Proceedings of the National Academy of Sciences of the U.S.A. (PNAS)*, 105, 16855-16859.

Hjelmar O. (1996). Disposal strategies for municipal solid waste incineration residues. *Journal of Hazardous Materials*, 47, 345-368.

Höglund, L.O., 2001. Project SAFE. *Modelling of long-term concrete degradation processes in the Swedish SFR repository*. SKB Rapport R-01-08. Svensk Kärnbränslehantering AB, Sweden.

Huijgen W.J.J. and Comans R.N.J. (2003). *Carbon dioxide sequestration by mineral carbonation: Literature Review*. ECN-C—03016 (February 2003). Report downloadable from www.ecn.nl.

Huijgen W.J.J., Witkamp G.J. and Comans, R.N.J. (2005). Mineral CO_2 sequestration by steel slag carbonation. *Environmental Science and Technology,* 39, 9676-2682.

Huijgen W.J.J. and Comans R.N.J. (2006). Carbonation of steel slag for CO_2 sequestration: leaching of products and reaction mechanisms. *Environmental Science and Technology,* 40, 2790-2796.

Huijgen W.J.J., Ruijg G.J., Comans R.N.J. and Witkamp G.J. (2006a). Energy consumption and net CO_2 sequestration of aqueous mineral carbonation., *Industrial & Engineering Chemistry Research,* 45, 9184-9194.

Huijgen W.J.J., Witkamp G.J. and Comans R.N.J. (2006b). Mechanisms of aqueous wollastonite carbonation as a possible CO_2 sequestration process. *Chemical Engineering Science,* 61, 4242-4251.

Huijgen W.J.J., Comans R.N.J. and Witkamp G.J. (2007). Cost evaluation of CO_2 sequestration by aqueous mineral carbonation. *Energy Conversion and Management*, 48, 1923-1935.

Huntzinger D.N., Gierke J.S., Kawatra S.K., Eisele T.C. and Sutter L.L. (2009). Carbon dioxide sequestration in cement kiln dust through mineral carbonation. *Environmental Science and Technology*, 43, 1986-1992.

Hyks J., Astrup T. and Christensen T.H. (2007). Influence of test conditions on solubility controlled leaching predictions from air-pollution-control residues. *Waste Management & Research,* 25, 457-466.

Hyks J., Astrup T. and Christensen T.H. (2009). Long-term leaching from MSWI air pollution control residues: leaching characterization and modelling. *Journal of Hazardous Materials,* 162, 80-91.

IAWG (The International Ash Working Group: Chandler, A.J., Eighmy, T.T., Hartlén, J., Hjelmar, O., Kosson, D., Sawell, S.E., van der Sloot, H.A., Vehlow, J.) (1997). *Municipal Solid Waste Incinerator Residues*. Studies in Environmental Sciences 67, Elsevier Science, Amsterdam.

Ibànez R., Andrés A., Viguri J.R., Ortiz, I. and Irabien, J.A. (2000). Characterization and management of incinerator wastes. *Journal of Hazardous Materials*, A79, 215-227.

ICRAM (2001). Ministero dell'Ambiente e della Tutela del Territorio-Servizio Difesa Mare, *ICRAM, Metodiche Analitiche di Riferimento*, 192.

Iizuka A., Fujii M.,Yamasaki A. and Yanagisawa Y. (2004). Development of a new CO_2 sequestration process utilizing the carbonation of waste cement. *Industrial & Engineering Chemistry Research*, 43, 7880-7887.

IPCC (Intergovernmental Panel on Climate Change) (2001a). *Climate Change 2001: Mitigation*. Contribution of Working Group III, Third Assessment Report of the Intergovernmental Panel on Climate Change (IPCC).(Eds.) Cambridge University Press, UK.

IPCC (2001b). *Climate Change 2001: The Scientific Basis*. Contribution of Working Group I, Third Assessment Report of the Intergovernmental Panel on Climate Change (IPCC). Houghton, J.T., Ding, Y., Griggs, D.J., Noguer, M., van der Linden, P.J., Xiaosu, D. (Eds.) Cambridge University Press, UK.

IPCC (2005). *IPCC special report on carbon dioxide capture and storage*. Cambridge University Press, Cambridge, United Kingdom and New York, NY, USA.

IPCC (2007). *Climate Change 2007: The Physical Science Basis*. Contribution of Working Group I to the Fourth Assessment Report of the Intergovernmental Panel on Climate Change. Solomon S., Qin D., Manning M., Chen Z., Marquis M., Averyt K.B. Tignor M. and Miller H.L. (Eds.). Cambridge University Press, Cambridge, United Kingdom and New York, NY, USA.

Izquierdo M., Lopez-Soler A., Vazquez Ramonich E., Barra M. and Querol X. (2002). Characterisation of bottom ash from municipal solid waste incineration in Catalonia. *Journal of Chemical Technology & Biotechnology*, 77, 576-583.

Jia L. and Anthony E.J. (2000). Pacification of FBC ash in a pressurized TGA. *Fuel*, 79, 1109-1114.

Johanneson B. and Utgennant P. (2001). Microstructural changes caused by carbonation of cement mortar. *Cement and Concrete Research*, 31, 925-931.

Johnson C.A., Moench H., Wersin P., Kugler P. and Wenger, C. (2005). Solubility of antimony in samples taken from shooting ranges. *Journal of Environmental Quality,* 34, 248-254.

Johnson D.C. (2000). Accelerated carbonation of waste calcium silicate materials. *SCI Lecture Papers Series*.

Johnson D.C., Macleod C.L. Carey P.J. and Hills C.D. (2003a). Solidification of stainless steel slag by accelerated carbonation. *Environmental Technology*, 24, 671-678.

Johnson D.C., MacLeod C.L., Hills C.D. (2003b). Acid neutralisation capacity testing of accelerated carbonated stainless steel slag. *Environmental Technology*, 24, 545-551.

Jung C.H., Matsuto T., Tanaka N. and Okada T. (2004). Metal distribution in incineration residues of municipal solid waste (MSW) in Japan. *Waste Management*, 24, 381-391.

Kakizawa M., Yamasaki A. and Yanagisawa Y. (2001). A new CO_2 disposal process via artificial weathering of calcium silicate accelerated by acetic acid, *Energy*, 26, 341-354.

Keleman P.B. and Matter J. (2008). In situ carbonation of peridotite for CO_2 storage. *Proceedings of the National Academy of Sciences of the U.S.A. (PNAS)*, 105, 17295-17300.

Kersten M., Moor H.C. and Johnson, C.A. (1997). Speciation of trace metals in leachate from a MSWI bottom ash landfill. *Applied Geochemistry,* 12, 675-683.

Kirby C.S. and Rimstidt J.D. (1993). Mineralogy and surface properties of municipal solid waste ash. *Environmental Science and Technology*, 27, 652-660.

Kirby C.S., Rimstidt J.D., (1994). Interaction of municipal solid waste ash with water, *Environmental Science and Technology* 28, 443-451.

Kodama S., Nishimoto T., Yogo K. and Yamada K. (2006). Design and evaluation of a new CO_2 fixation process using alkaline-earth metal wastes. *Proceedings of the 8th International Conference on Green House Gas Technology*, 19-22 June 2006, Trondheim (Norway).

Kodama S., Nishimoto T., Yamamoto N., Yogo K. and Yamada K. (2008). Development of a new pH-swing CO_2 mineralization process with a recyclable reaction solution. *Energy*, 33, 776-784.

Kojima T., Nagamine A., Ueno N. and Uemiya S. (1997). Absorption and fixation of carbon dioxide by rock weathering. *Energy Conversion and Management*, 38, S461-S466.

Lackner K.S., Wendt C.H., Butt D.P., Joyce E.L. Jr. and Sharp D.H. (1995). Carbon dioxide disposal in carbonate minerals. *Energy*, 20, 1153-1170.

Lackner K.S., Butt D.P. and Wendt C.H. (1997). Progress on binding CO_2 in mineral substrates. *Energy Conversion and Management*, 38, S259-264.

Lackner K.S. (2002). Carbonate chemistry for sequestering fossil carbon. *Annual Review for Energy and the Environment*, 27, 193-232.

Lackner K.S. (2003). Climate change: a guide to CO_2 sequestration. *Science*, 300, 1677-1678.

Lange L.C., Hills C.D., and Poole, A.B. (1996). The effect of accelerated carbonation on the properties of cement-solidified waste forms. *Waste Management*, 16, 757-763.

Lekakh S.N., Rawlins C.H., Robertson D.G.C., Richards V.L. and Peaslee K.D. (2008a). Kinetics of aqueous leaching and carbonization of steelmaking slag. *Metallurgical and Materials Transactions B*, 39, 125-134.

Lekakh S.N., Robertson D.G.C., Rawlins C.H., Richards V.L. and Peaslee K.D. (2008b). Investigation of a two-stage aqueous reactor design for carbon dioxide sequestration using steelmaking slag. *Metallurgical and Materials Transactions B*, 39, 484-492.

Li X., Fernández-Bertos M., Hills C.D., Carey P.J., Simons S. (2007). Accelerated carbonation of municipal solid incineration fly ashes. *Waste Management*, 27, 1200-1206.

Li X. (2008). Accelerated carbonated municipal solid waste incineration (MSWI) residues. *PhD Thesis*. Department of Pharmaceutical, Chemical & Environmental Sciences, School of Science, University of Greenwich, UK.

Liu J., Xu D., Xiong L., Hills C.D., Carey P.J. and Gardner K.H. (2008). Comparison of properties of traditional and accelerated carbonated solidified/stabilized contaminated soils, *Journal of Environmental Sciences*, 20, 593-598.

Maroto-Valer M.M., Fauth D.J., Kutcha M.E., Zhang Y. and Andrésen, J.M. (2005). Activation of magnesium rich minerals as carbonation feedstock materials for CO_2 sequestration. *Fuel Processing Technology*, 86, 1627-1645.

McKelvy M. J., Chizmeshya A.V.G., Squire, K., Carpenter R. W. and Béarat, H. (2005*). A novel approach to mineral carbonation: enhancing carbonation while avoiding mineral pretreatment process cost*. DOE/DE-FG26-04NT42124, Arizona State University.

Meima J.A. and Comans R.N.J. (1997). Geochemical modeling of weathering reactions in municipal solid waste incinerator bottom ash. *Environmental Science & Technology*, 31, 1269-1276.

Meima J.A. and Comans R.N.J. (1999). The leaching of trace elements from municipal solid waste incinerator bottom ash at different stages of weathering. *Applied Geochemistry*, 14, 159-171.

Meima J.A., van der Weijden R.D., Eighmy T.T. and Comans, R.N.J. (2002). Carbonation processes in municipal solid waste incinerator bottom ash and their effect on the leaching of copper and molybdenum. *Applied Geochemistry*, 17, 1503-1513.

Melton J.S., Tarabadkar K. and Gardner K.H. (2008). Accelerated carbonation of contaminated sediment to immobilize heavy metals. *Proceedings of the 2nd International Conference on Accelerated carbonation for Environmental and Materials Engineering ACEME08*, 1-3 October 2008, Rome, (Italy).

Montes-Hernandez G., Pérez-López R., Renard F., Nieto J.M. and Charlet L. (2009). Mineral sequestration of CO_2 by aqueous carbonation of coal combustion fly-ash. *Journal of Hazardous Materials*, 161, 1346-1354.

Motz H. and Geiseler J. (2001). Products of steel slags an opportunity to save natural resources. *Waste Management*, 21, 285-293.

O'Connor W.K., Dahlin D.C., Rush G.E., Gerdemann S.J., Penner L.R. and Nilsen D.N. (2005). *Aqueous mineral carbonation: mineral availability, pretreatment, reaction parameters, and process studies*. DOE/ARC-TR-04-002. Albany Research Center, Albany OR, USA.

Olsen A.A. (2007). Forsterite dissolution kinetics: applications and implications for chemical weathering. *PhD Thesis*, Blacksburg, Virginia. Available at: http://scholar.lib.vt.edu/theses/available/etd-07052007-135551/unrestricted/olsen.pdf.

OECD (Organization for Economic Cooperation and Development) (2002). *Iron and steel industry report 2000*, Paris.

Papadakis V.G., Vayenas C.G. and Fardis M.N. (1991). Experimental investigation and mathematical modeling of the concrete carbonation problem. *Chemical Engineering Science*, 46, 1333-1338.

Park A., Jadhav R. and Fan L.S. (2003). CO_2 mineral sequestration: chemically enhanced aqueous carbonation of serpentine. *The Canadian Journal of Chemical Engineering*, 81, 885-890.

Park A. and Fan L.S. (2004). CO_2 mineral sequestration: physically activated dissolution of serpentine and pH swing process. *Chemical Engineering Science,* 59, 5241-5247.

Pérez-López R., Montes-Hernandez G., Nieto J.M., Renard F., and Charlet L. (2008). Carbonation of alkaline paper mill waste to reduce CO_2 greenhouse gas emissions into the atmosphere. *Applied Geochemistry*, 23, 2292-2300.

Petterson C., Ephraim J. and Allard B. (2004). On the composition and properties of humic substances isolated from deep groundwater and surface waters. *Organic Geochemistry*, 21, 443-451.

Piantone P., Bodénan F. and Chatelet-Snidaro L. (2004). Mineralogical study of secondary mineral phases from weathered MSWI bottom ash: implications for the modelling and trapping of heavy metals. *Applied Geochemistry*, 19, 1891-1904.

Pokrovsky O.S. and Schott J. (2000). Kinetics and mechanism of forsterite dissolution at 25 °C and pH from 1 to 12. *Geochimica et Cosmochima Acta*, 64, 19, 3313-3325.

Polettini A. and Pomi R. (2004). The leaching behaviour of incineration bottom ash as affected by accelerated ageing. *Journal of Hazardous Materials*, B113 (1-3), 209-215.

Polettini A., Pomi R. and Ragaglia M. (2005). *Accelerated ageing as a tool for sustainable disposal of incinerator bottom ash*, Proc. Sardinia 2005, Tenth International Waste Management and Landfill Symposium, S. Margherita di Pula (CA), October 3-7 2005, Cossu, R., Stegmann, R. (Eds.) (on CD ROM).

Polettini A., Astrup T., Cappai G., Lechner P., Muntoni A., Pomi R., Van Gerven T. and Van Zomeren A. (2007). State-of-the-art and outlook on management of waste-to-energy bottom ashes, part 1- treatment, *Proc. Sardinia 2007, Eleventh International Waste Management and Landfill Symposium*, S. Margherita di Pula (CA), October 1-5 2007, Cossu, R., Stegmann, R. (Eds.) (on CD ROM).

Prigiobbe V., Polettini A. and Baciocchi, R. (2009a). Gas–solid carbonation kinetics of air pollution control residues for CO_2 storage. *Chemical Engineering Journal*, 148, 270-278.

Prigiobbe V., Costa G., Baciocchi R., Hänchen M. and Mazzotti M. (2009b).The effect of CO_2 and salinity on olivine dissolution kinetics at 120 °C, accepted for publication *Chemical Engineering Science*, doi: 10.1016/j.ces.2009.04.035.

Proctor D.M., Fehling K.A., Shay E.C. et al. (2000). Physical and chemical characteristics of blast furnace, basic oxygen furnace, and electric arc furnace steel industry slags. *Environmental Science and Technology*, 34, 1576-1582.

Quina M.J., Bordado J.C., Quinta-Ferreira R.M. (2008). Treatment and use of air pollution control residues from MSW incineration: an overview. *Waste Management,* 28, 2097-2121.

Reddy K.J., Drever J.I. and Hausfurther V.R. (1991). Effects of a CO_2 pressure process on the solubilities of major and trace elements in oil shale solid wastes. *Environmental Science and Technology*, 25, 1466-1469.

Reddy K.J., Gloss S.P. and Wang L. (1994). Reaction of CO_2 with alkaline solid wastes to contaminant mobility. *Water Research*, 28, 1377-1382.

Rendek E., Ducom G. and Germain P. (2006a). Carbon dioxide sequestration in municipal solid waste incinerator (MSWI) bottom ash, *Journal of Hazardous Materials*, B128, 73-79.

Rendek E., Ducom G. and Germain P. (2006b). Influence of organic matter on municipal solid waste incinerator bottom ash carbonation. *Chemosphere*, 64, 1212-1218.

Rendek E., Ducom G. and Germain P. (2007). Influence of waste input and combustion technology on MSWI bottom ash quality. *Waste Management*, 27, 1403-1407.

Rosso J.J. and Rimstidt J.D. (2000). A high resolution study of forsterite dissolution rates. *Geochimica et Cosmochimica Acta*, 64, 797-811.

Roy S.K., Poh K.B. and Northwood D.O. (1999). Durability of concrete-accelerated carbonation and weathering studies, *Building and Environment*, 34, 597-606.

Rynikiewicz C. (2008). The climate change challenge and transitions for radical changes in the European steel industry. *Journal for Cleaner Production*, 16, 781-789.

Sabbas T., Polettini A., Pomi R., Astrup T., Hjelmar O., Mostbauer P., Cappai G., Magel G., Salhofer S., Speiser C., Heuss-Assbichler S., Klein R., and Lechner P. (2003). Management of municipal solid waste incineration residues. *Waste Management*, 23, 61-88.

Sakita S., Shimaoka T., Nishigaki M. and Tanaka T. (2006). Carbonation treatment of lead in municipal solid waste incineration bottom ash for beneficial use. *Extended abstracts of the First international conference on accelerated carbonation for environmental and materials engineering*, June 12-14, London UK, Cement and Concrete Science (Ed.).

Seifritz W., (1990). CO_2 disposal by means of silicates, *Nature*, 345, 486.

Shen H. and Forssberg E. (2003). An overview of recovery of metals from slags. *Waste Management*, 23, 933-949.

Shi C. (2004). Steel slag- its production, processing, characteristics, and cementitious properties. *Journal of Materials in Civil Engineering*, 16, 230-236.

Shi C. and Wu Y. (2008). Studies on some factors affecting CO_2 curing of lightweight concrete products. *Resources, Conservation and Recycling*, 52, 1087-1092.

Shih S.M., Ho C.S., Song Y.S. and Lin J.P. (1999). Kinetics of the reaction of $Ca(OH)_2$ with CO_2 at low temperature. *Industrial & Engineering Chemistry Research*, 38, 1316-1322.

Short N.R., Purnell P. and Page C.L. (2001). Preliminary investigations into the supercritical carbonation of cement pastes. *Journal of Material Science*, 36, 35-41.

Shtepenko O.L., Hills C.D., Coleman N.J. and Brough A. (2005). Characterization and preliminary assessment of a sorbent produced by accelerated mineral carbonation. *Environmental Science and Technology*, 39,345-354.

Shtepenko O.L., Hills C.D., Brough A. and Thomas M. (2006). The effect of carbon dioxide on β-dicalcium silicate and Portland cement. *Chemical Engineering Journal*, 118, 107-118.

Sipilä J., Teir S. and Zevenhoven R. (2008). Carbon dioxide sequestration by mineral carbonation, literature review update 2005-2007, *Åbo Akademi University Faculty of Technology Heat Engineering Laboratory*, report VT 2008-1.

Sorochkin M.A., Shchrov A.F. and Safonov I.A. (1975). Study of the possibility of using carbon dioxide for accelerating the hardening of products made from Portland cement. *Journal of Applied Chemistry*, 48, 1211.

Speiser C., Baumann T. and Niessner R. (2000). Morphological and chemical characterization of calcium-hydrate phases formed in alteration processes of deposited municipal solid waste incinerator bottom ash. *Environmental Science and Technology*, 34, 5030-5037.

Spycher, N., Pruess, K. and Ennis-King, J. (2003). CO_2-H_2O mixtures in the geological sequestration of CO_2. I. Assessment and calculation of mutual solubilities from 12 to 100 °C and up to 600 bar. *Geochimica and Cosmochima Acta*, 67, 3015-3031.

Steketee J.J., Rutten S. and de Bode A. (2006). Accelerated carbonation of MSWI bottom ash on a practical scale. *Extended abstracts of the First international conference on accelerated carbonation for environmental and materials engineering*, June 12-14, London UK, Cement and Concrete Science (Ed.).

Stephens J.C. and Keith D.W. (2008). Assessing geochemical carbon management. *Climatic Change*, 90, 217-242.

Stolaroff J.K., Lowry G.V. and Keith D.W. (2005). Using CaO- and MgO-rich industrial waste streams for carbon sequestration. *Energy Conversion and Management*, 46, 687-699.

Teir S., Eloneva S. and Zevenhoven R. (2005). Production of precipitated calcium carbonate from calcium silicates and carbon dioxide. *Energy Conversion and Management*, 46, 2954-2979.

Teir S., Eloneva S., Fogelholm C.J. and Zevenhoven R. (2007). Dissolution of steelmaking slags in acetic acid for precipitated calcium carbonate production. *Energy*, 32, 528-539.

Teir S. (2008). Fixation of carbon dioxide by producing carbonates from minerals and steelmaking slags. *Doctoral dissertation*, Helsinki University of Technology.

Tawfic T.A., Reddy K.J. and Gloss S.P. (1995). Reaction of CO_2 with clean coal technology ash to reduce trace element mobility. *Water, Air and soil pollution*, 84, 385-398.

Todorovic J. and Ecke H. (2006). Demobilization of critical contaminants in four typical waste-to-enery ashes by carbonation. *Waste Management*, 26, 430-441.

Uibu M. (2008). Abatement of CO_2 emissions in Estonian oil shale-based power production. *Doctoral dissertation*, Tallinn University of Technology.

Uibu M., Uus M. and Kuusik R (2009). CO_2 mineral sequestration in oil-shale wastes from Estonian power production. *Journal of Environmental Management*, 90, 1253-1260.

Van Balen K. (2005). Carbonation reaction of lime, kinetics at ambient temperature. *Cement and Concrete Research*, 35, 647-657.

van der Bruggen B., Vogels G., van Herc, P. and Vandecasteele, C. (1998). Simulation of acid washing of municipal solid waste incineration fly ash in order to remove heavy metals. *Journal of Hazardous Materials,* 57, 127-144.

van der Laan S.R., van Hoek C.J.G., van Zomeren A., Comans R.N.J., Kobesen J.B.A. and Broersen P.G.J. (2008). Chemical reduction of CO_2 to carbon at ambient conditions during artificial weathering of converter steel slag while improving environmental properties. *Proceedings of the 2nd International Conference on Accelerated carbonation for Environmental and Materials Engineering ACEME08*, 1-3 October 2008, Rome, (Italy).

Van Gerven T., Geysen D., Stoffels L., Jaspers M., Wauters G., Vandecasteele C. (2005a) Management of incinerators residues in Flanders (Belgium) and in neighbouring countries: a comparison. *Waste Management*, 25, 75–87.

Van Gerven T., Van Keer E., Arickx S., Jaspers M., Wauters G. and Vandecasteele C. (2005b). Carbonation of MSWI-bottom ash to decrease heavy metal leaching, in view of recycling. *Waste Management*, 25, 291-300.

Van Gerven T., Cornelis G., Vandoren E., Garrabrants A.C., Sanchez F., Kosson D.S. and Vandecasteele C. (2006). Effects of progressive carbonation on heavy metal leaching from waste-containing cement matrices. *AIChE Journal*, 52, (2), 826-837.

van Oss H.G. (2007). 2006 minerals yearbook, iron and steel slag. U. S. Department of the Interior and U.S. Geological Survey, December 2007, available at the following website: http://minerals.usgs.gov/minerals/pubs/commodity/iron_&_steel_slag/myb1-2006-fesla.pdf.

Vehlow J., Bergfeldt B., Visser R. and Wilén C. (2007). European Union waste management strategy and the importance of biogenic waste. *Journal of Material Cycles and Waste Management*, 9, 130-139.

Wogelius R.A. and Walter J. V. (1991). Olivine dissolution at 25 °C: Effects of pH, CO_2 and organic acids. *Geochimica Cosmochimica Acta*, 55, 943-954.

Wolery T.W. and Jarek R.L. (2003). *Software user's manual. EQ3/6, Version 8.0.* Sandia National Laboratories – U.S. Dept. of Energy Report.

Young J.F., Berger R.L. and Breese J. (1974). Accelerated curing of compacted calcium silicate mortars on exposure to CO_2. *Journal of the American Ceramics Society*, 57, 394-397.

Zevenbergen C. and Comans R.N.J. (1994). Geochemical factors controlling the mobilization of major elements during weathering of MSWI bottom ash. (In Goumans, J.J.J.M., van der Sloot, H.A. & Aalbers (Eds.), *Environmental Aspects of Construction with waste materials* (pp. 179-194). Amsterdam: Elsevier Science).

Zevenhoven R., Teir S. and Eloneva S. (2006). Chemical fixation of CO_2 in carbonates: routes to valuable products and long-term storage. *Catalysis Today*, 115, 73-79.

Zhang H., He P.J., Shao L.M. and Lee D.J. (2008). Temporary stabilization of air pollution control residues using carbonation. *Waste Management,* 28, 509-517.

Zhang M.(2000). Incorporation of oxyanionic B, Cr, Mo and Se into hydrocalumite and ettringite: application to cementitious systems. *PhD thesis*, Unversity of Waterloo, Canada.

Ziegler F. and Johnson C.A. (2001). The solubility of calcium zincate ($CaZn_2(OH)_6{\cdot}2H_2O$), *Cement and Concrete Research,* 31, 1327–1332.

Ziock H.J., Lackner K.S. and Harrison D.P (2000). Zero emission coal power, a new concept. *Proceedings of the 1st US National Conference on Carbon Dioxide Sequestration*, Washington D.C., U.S.A., May 14th – 17th, DOE publications.

Publications

Baciocchi R. and. Costa G (2007). Tecnologie per la cattura di anidride carbonica da impianti di recupero energetico. *Nuova Gea- quaderni per l'ambiente* 4, 2, 136-148.

Costa G., Baciocchi R., Polettini A., Pomi R., Hills C. D., Carey P. J. (2007). Current status and perspectives of accelerated carbonation processes on municipal waste combustion residues. *Environmental Monitoring and Assessment* 135, 1-3, 55-75.

Sirini P., Costa G., Lategano E. (2007). I rifiuti solidi dei processi di valorizzazione energetica: tecnologie di smaltimento e/o recupero. *Nuova Gea-quaderni per l'ambiente* 4, 2, 121-135.

Baciocchi R., Costa G., Di Bartolomeo E., Polettini A. and Pomi R. (2009). The effects of accelerated carbonation on CO_2 uptake and metal release from incineration APC residues, submitted to *Waste Management.*

Baciocchi R., Costa G., Polettini A., Pomi R. and Prigiobbe V. (2009). Comparison of different reaction routes for carbonation of APC residues, *Energy Procedia*, 1, 4851–4858.

Baciocchi R., Costa G., Polettini A. and Pomi R. (2009). Influence of particle size on the carbonation of stainless steel slag for CO_2 storage, *Energy Procedia*, 1, 4859–4866.

Prigiobbe V., Costa G., Baciocchi R., Hänchen M. and Mazzotti M. (2009). Analysis of the effect of temperature, pH, CO_2 pressure and salinity on the olivine dissolution kinetics, *Energy Procedia*, 1, 4881–4884.

Prigiobbe V., Costa G., Baciocchi R., Hänchen M. and Mazzotti M. (2009).The effect of CO_2 and salinity on olivine dissolution kinetics at 120 °C, accepted for publication *Chemical Engineering Science*, doi: 10.1016/j.ces.2009.04.035.

Conference proceedings

Gavasci R., Baciocchi R., Costa G. and Lombardi F. (2006). Tecnologie per la riduzione delle emissioni di anidride carbonica. Proceedings of *VIII SIBESA* "*Simposio Italo-Brasiliano di Ingegneria Sanitaria e Ambientale*" Fortaleza, Brasil 17-22/09/2006. on CD-ROM.

Prigiobbe V., Costa G., Baciocchi R., Mazzotti M. and Steinfeld A. (2007). Dry vs. wet route carbonation of incineration residues for CO_2 capture and storage (CCS) in waste to energy plants. Proceedings of *Latsis Symposium 2007 – Research frontiers in Environment and Sustainability*. Zurich, Switzerland 17-19/09/2007.

Baciocchi R., Costa G., Polettini A., Pomi R., Di Bartolomeo E. and Traversa E. (2007). Leaching behaviour and CO_2 sequestration capacity of accelerated carbonated MSWI APC residues. *Proceedings of Sardinia 2007 Eleventh International Waste Management and Landfill Symposium*. Santa Margherita di Pula (Ca) Italy 1-5/10/2007, on CD-ROM.

Lategano E., Costa G., Lombardi F., Baciocchi R. (2007). Characterization of the bottom ash produced in a sanitary waste incineration facility and influence of the operating conditions aimed at material recovery or safe disposal. *Proceedings of Sardinia 2007 Eleventh International Waste Management and Landfill Symposium*. Santa Margherita di Pula (Ca) Italy 1-5/10/2007, on CD-ROM.

Gavasci R., Lombardi F. and Costa G. (2008). Current waste management strategies in the EU. Proceedings of the 6th "*Congreso International de Educatión Superior, Universidad 2008*", La Habana, Cuba, 11-15/2/2008.

Costa G, Lategano E, Lombardi F and Gavasci R (2008). Experimental study on the influence of particle size on the reuse potential of bottom ash from a sanitary waste incinerator facility. Proceedings of the *2nd Int. Conf. on Engineering for Waste Valorization*, Patras, Grece, 3-5/6/2008, on CD-ROM.

Baciocchi R., Costa G., Polettini A., Pomi R. and Prigiobbe V. (2008). Accelerated carbonation of APC residues for CO_2 storage: comparison between dry and wet route. Proceedings of the *2nd Int. Conf. on Engineering for Waste Valorization*, Patras, Grece, 3-5/6/2008, on CD-ROM.

Baciocchi R., Costa G., Polettini A. and Pomi R. (2008) CO_2 sequestration through accelerated carbonation of MSWI ash and effects on metal leaching, *Proceedings of SIDISA08 Simposio Internazionale di Ingegneria Sanitaria e Ambientale*, Florence, Italy, 24-27/6/2008, on CD-ROM.

Baciocchi R., Costa G., Polettini A. and Pomi R. (2008). An insight into the effect of accelerated carbonation on metal release from incinerator ash. Proceedings of the *2nd Int. Conf. on Accelerated carbonation for Environmental and Materials Eng. ACEME08*, Rome, Italy, 1-3/10/2008.

Prigiobbe V., Costa G., Baciocchi R., Costa, Hänchen M. and Mazzotti M. (2008) Experimental study on olivine dissolution kinetics. Proceedings of the *2nd Int. Conf. on Accelerated carbonation for Environmental and Materials Eng. ACEME08*, Rome, Italy, 1-3/10/2008.

Baciocchi R., Costa G., Marini C., Polettini A., Pomi R., Postorino P. and Rocca S. (2008) Accelerated carbonation of RDF incineration bottom ash: CO_2 storage potential and environmental behaviour. Proceedings of the *2nd Int. Conf. on Accelerated carbonation for Environmental and Materials Eng. ACEME08*, Rome, Italy, 1-3/10/2008.

Baciocchi R., Costa G., Di Bartolomeo E., Di Camillo V., Polettini A. and Pomi R. (2008) Accelerated carbonation of different size fractions of stainless steel slag. Proceedings of the *2nd Int. Conf. on Accelerated carbonation for Environmental and Materials Eng. ACEME08*, Rome, Italy 1-3/10/2008.

Baciocchi R., Costa G., Lategano E., Polettini A., Pomi R., Postorino P. and Rocca S. (2008). Accelerated carbonation of different size fractions of bottom ash from RDF incineration. Proceedings of the *2nd Int. Symposium on Energy from Biomass and Waste, VENICE08*, Venice, Italy, 17-20/11/2008, on CD ROM.